A Mean Value Internal Combustion Engine Model in MapleSim

by

Mohammadreza Saeedi

A thesis
presented to the University of Waterloo
in fulfillment of the
thesis requirement for the degree of
Master of Applied Science
in
Mechanical Engineering

Waterloo, Ontario, Canada, 2010

AUTHOR'S DECLARATION

I hereby declare that I am the sole author of this thesis. This is a true copy of the thesis, including any required final revisions, as accepted by my examiners.

I understand that my thesis may be made electronically available to the public.

Abstract

The mean value engine model (MVEM) is a mathematical model derived from basic physical principles such as conservation of mass and energy equations. Although the MVEM is based on some simplified assumptions and time averaged combustion engine parameters, it models the engine with a reasonable approximation and gives a satisfactory amount of information about the physics of the fluid energy passing through an engine system. MVEM can predict an engine's main external variables such as crankshaft speed and manifold pressure, and important internal variables, such as volumetric and thermal efficiencies. Usually, the differential equations used in MVEM will predict fuel film flow, manifold pressure, and crankshaft speed. Because of its simplicity and short simulation time, the MVEM is widely used for engine control development.

A mean value engine based on mathematical and parametric equations has recently been developed in the new MapleSim software. The model consists of three main components: the throttle body, the manifold, and the engine. The new MVEM uses combinations of causal and acausal components along with lookup tables and parametric equations. Adjusting the parameters allows the model to be used for new engines of interest. The model is forward-looking and so benefits from both Maple's powerful mathematical tool and Modelica's modern equation-based language. A set of throttle angle and mass flow data is used to find the throttle angle function, and to validate the throttle mass flow rates obtained from the model and the experiment.

Acknowledgements

This work has involved help from many people. I would like first of all to thank Professor John McPhee and Professor Roydon Fraser, my supervisors, who provided a great opportunity to work with them and their excellent teams. It was mainly their idea that I have expanded on in this work. Their patience, support, willingness to help, and enthusiasm made this work possible.

I am also grateful to Paul Goossens of Maple Inc. for his creative advice and mentoring in the process of creating a new engine model in MapleSim. Most of the mean value engine components were built during our exciting and fruitful bi-weekly sessions by bringing up a new idea and then implementing it inside the model. I would like to thank Wilson Wong and other MapleSoft staff members for supporting this project.

I want to express my extreme gratitude to Dr. Nasser Lashgarian Azad and Dr. Chad Schmitke for their many helpful discussions that we have had, and for their guidance during the validation and development of the model stages. As well, I would like to thank Chris Haliburton for his help with PSAT software and answering software-related questions.

In addition, I want to thank to Joseph Lomonaco from Harley-Davidson Motor Co. for his support and the useful data he provided.

I would also like to thank Mary McPherson of the grad Writing Centre for her editing advice on my thesis.

Finally, I would like to thank my wife Mehranz for all her effort, time, and support as she has helped me prepare this work, and my parents for all their long term and never-failing support.

Table of Contents

List of Figures

List of Tables

Nomenclature

A_p [m^2]	Piston area
A_{thr} [m^2]	Throttle area
AF	Air-fuel ratio
B [m]	Cylinder bore
C_d	Discharge coefficient
C_{dVMax}	Maximum discharge coefficient
D [m]	Throttle bore diameter
d [m]	Throttle pin diameter
Eng_{On_Off}	Engine On-Off Switch
F_{aero} [N]	Aerodynamic resistance force
F_{iner} [N]	Inertia resistance force
F_{roll} [N]	Rolling resistance force
F_p [N]	Piston force
$gear\_index$	Gear index: 0 for neutral gear, and 1,2,3, and 4 for related gears
H_f [kJ/kg]	Fuel heating value
H_l [kJ/kg]	Lower fuel heating value
J_e [kg.m^2]	Engine inertia
l_{conrod} [m]	Connecting rod length
l_{crank} [m]	Crankshaft length
l_p [m]	Displaced length of a piston
L_v [mm]	Valve lift
L_{VMax} [mm]	Maximum valve lift
K_i	Integral gain
K_p	Proportional gain
$\dot{m}_e$ [kg/s]	Engine air mass flow rate

$\dot{m}_f$ [kg/s]	Fuel mass flow rate
$\dot{m}_{fHot}$ [kg/s]	Fuel mass flow rate in hot-engine working condition
$\dot{m}_{fCold}$ [kg/s]	Fuel mass flow rate in cold-engine working condition
$\dot{m}_{thr}$ [kg/s]	Throttle air mass flow rate
$\dot{m}_{fi}$ [kg/s]	Injected fuel mass flow rate
$\dot{m}_{fv}$ [kg/s]	Evaporated fuel mass flow rate
$\dot{m}_{fw}$ [kg/s]	Wall fuel mass flow rate
$m_{inertia}$ [kg/s]	Inertia mass of powertrain
n_e [RPM] or ω_e [rad/s]	Engine speed
P [Pa]	Cylinder pressure
P_{cc} [Pa]	Crank case pressure
P_m [Pa]	Manifold air pressure
P_0 [Pa]	Ambient pressure
P_f [W]	Fuel heat power
P_{ind} [W]	Indicated power
P_b [W]	Brake power
P_{loss} [W]	Engine loss power
$P_{friction}$ [W]	Engine friction power
$P_{pumping}$ [W]	Engine pumping power
PW_{Brake}	Brake command, varying from 0 to1
PW_{cmd}	Powertrain Command, varying from 0 to1
PW_{temp}	Engine warm-up coefficient, varying from 0 to 1
$\dot{Q}$ [W]	Crank-angle-dependant heat release

$\dot{Q}_{Max}$ [W]	Maximum crank-angle-dependant heat release
q_f [W]	Heat energy released by fuel
q_{fCold}	Heat-released-cold index
$\dot{q}_H$ [W]	Heat power rejected from cylinders wall
r	Compression ratio
r_w [N/m]	Wheel Radius
S [m]	Piston stroke
t_s [s]	Combustion starting time
t_e [s]	Combustion ending time
T_{dmd} [N.m]	Demand torque
T_{loss_veh} [N.m]	Loss torque
T_m [^{o}C]	Manifold temperature
T_o [^{o}C]	Ambient temperature
T_{cmd} [N.m]	Normalized command torque
$T_{\max br}$ [N.m]	Maximum available brake torque
T_{in} [N.m]	Gearbox input torque
T_{lossbr} [N.m]	Torque lost by wheels
T_{losstr} [N.m]	Vehicle loss torque
T_{out} [N.m]	Gearbox output torque
$T_{variation}$ [N.m]	Variation torque
T_w [N.m]	Wheel torque
T_{wot_cold} [^{o}C]	Hot wide-open throttle torque value,
T_{wot_cold} [^{o}C]	Cold wide-open throttle torque curve value
V_c [m^3]	Clearance volume of a cylinder
V_m [m^3]	Manifold Volume
V_d [m^3]	Displaced Volume

α_e [rad/s^2]	Engine shaft rotational acceleration
γ	The specific heat ratio
λ	Normalized air-fuel ratio
η_{vol}	Volumetric efficiency
η_{th}	Thermal efficiency
$\varphi_\circ$ [Deg]	Throttle valve closed angle
ω_{wheel} [rad/s]	Wheel Speed

Chapter 1 Introduction

In the last three decades, much progress has been made to improve automotive engine efficiency, fuel economy, and exhaust emissions. This progress is, in part, due to researchers' ability to model engines and thus examine and test possible innovations. Modelling of an internal combustion engine is a complicated process and includes air gas dynamics, fuel dynamics, and thermodynamic and chemical phenomena of combustion. Even in a steady-state condition, in which an engine is hot and runs at a constant load and speed, the pressure inside each cylinder changes rapidly in each revolution, and the heat released by ignited fuel varies during the combustion period.

The main focus in engine modelling is to clarify an engine's phenomena by establishing cause and effect dynamic relations between its main inputs and outputs. The dynamic relations are differential equations obtained from conservation of mass and energy laws. The input variables in engine modelling are usually throttle angle, spark advance angle (SA), exhaust gas recirculation (EGR), and air-fuel ratio (A/F). The output variables are engine speed, torque, fuel consumption, exhaust emissions, and drivability. The challenge in engine modelling is to find the relations between the engine input and output variables that best describe the model and predict the output variables in different working conditions of the engine [1].

A four-stroke spark-ignition (SI) or diesel engine has four main thermodynamic processes - intake, compression, power and exhaust strokes- that occur in every two crankshaft revolutions of an engine in its operating condition. Each stroke refers to a half revolution of the crankshaft or full displacement of a piston from its top-dead-centre (TDC), the closest point of the piston top to the cylinder head, to its bottom-dead-centre (BDC), the closest point of the piston top to the crankshaft or, in reverse, from BDC to TDC. During the intake stroke, the intake valve is open and the piston moves from TDC to BDC. The pressure inside the cylinder drops below the

atmospheric pressure and forces the fuel and air mixture into the cylinder. Sometimes, instead of mixing fresh air with fuel, a percentage of EGR is mixed with the air in the intake manifold to control the exhaust emissions. The compression stroke starts at angles close to the BDC, when both intake and exhaust valves are closed. The piston travels from BDC to TDC, and gas in the cylinder is compressed. The ratio of cylinder volume before and after compression stroke is called the compression ratio, and is about 8 to 11 for most SI engines. The power stroke starts when a piston is close to TDC, and the spark plug ignites the fuel. While both intake and exhaust valves are closed, the pressure inside the cylinder increases suddenly, forcing the piston downward to BDC and generating power. The exhaust stroke starts when the piston is close to BDC, and the exhaust valve is open, allowing the combusted gas to flow out of the cylinder. Inlet and exhaust valves are usually opened shortly before or after TDC and BDC to allow maximum air into the cylinder or the maximum combusted mixture to be swept out of the cylinder.

Fuel can be directly injected into the cylinders, or it can be injected outside the cylinder into the intake port or throttle body. When it is injected outside of the cylinder, a fraction of the injected fuel strikes the wall, and the rest of the fuel evaporates and mixes with the air flowing into the combustion chamber. This phenomenon is called wall-wetting. For central fuel injection, the injector is located at the top of the throttle valve, creating a film mass that depends on the throttle angle. In simultaneous multipoint injection and sequential fuel injection, the amount of fuel left on the wall is constant, regardless of the throttle angle [2].

The ignition angle is the angle of the crankshaft from TDC at which a spark plug ignites the fuel. This angle is mainly a function of engine load and engine speed. Sometimes a retarded ignition angle is used to compensate for high ambient temperature or engine warm-up conditions [3].

1.1 Different Types of Engine Models

In the literature, engine models are categorized by their complexity, starting from very simple transfer function models to mean value engines, and then on to detailed cylinder-by-cylinder engines. The two latter engine types are discussed in Section 1.1.1. Section 1.1.2 compares two types of physical and experimental models. Section 1.1.3 considers input, output, and variable relations in engine models in causal and acausal models. The types of equations usually used in physical and experimental models are covered in **Error! Reference source not found.** andChapter 4.

1.1.1 Mean value and cylinder-by-cylinder engine models

For the above-mentioned engine events, the two main modelling approaches are the cylinder-by-cylinder engine model (CCEM) and the mean value engine model (MVEM). Cylinder-by-cylinder models are more accurate than the MVEM models and capture the details of instantaneous engine events such as pressure and temperature variations inside individual cylinders. CCEM models can be used for evaluating emissions, engine diagnostics, fuel injection studies, and in-cylinder pressure, temperature, and fuel-consumption variations. Cylinder area, volume, pressure, and temperature, along with valve lift, fuel mass burning rate, and engine output power can be found and related to a specified crankshaft angle.

Mean value engine models are simple mathematical models at an intermediate level between simple transfer function engine models and complex cyclic simulation models. Unlike the cylinder-by-cylinder engine models that use a crank angle domain, mean value engine models use time scale domain. Time scales in MVEM are more than a single engine cycle and less than the time that a cold engine needs to warm up and come in two types: instantaneous and time

developing. Instantaneous scale involves a process that very quickly reaches equilibrium, similar to the way that flow passes through the throttle valve. The instantaneous process is described by algebraic equations. Throttle air mass flow is an example of an instantaneous process. Time developing processes are described by differential equations and reach equilibrium in one to three magnitude orders of engine cycles. An example is the equation for manifold pressure [2].

1.1.2 Physical and Experimental models

Physical models are derived from fundamental physical laws such as conservations of mass, momentum, and energy. The main advantage of physical models is that they are generalized and can be used for different systems. Filling and emptying of the air in a manifold, heat transfer, and crank shaft rotational dynamics are among the physical processes modelled.

In the absence of adequate knowledge to establish physical models, and in some phenomena like combustion that are too complex to be described by physical models, relations between system inputs and outputs are defined by experimental models. These experimental models are usually derived from actual engine test data and thus can accurately predict engine's behaviour within the data range. Applying these models to other types of engines or extrapolation of the data is meaningless. The large amount of data in such empirical models needs to be processed, and polynomials or other types of experimental relations between input and output variables must be introduced as equations. Parameters and coefficients in equations are then fitted to the curves through the use of least square or other fitting methods, and optimal settings of input and output variables are obtained. In this work, both physical and experimental models are used.

1.1.3 Causal and Acausal Models

A causal model is a system of inputs, outputs, and variables, and the relations among them. Inputs are introduced from previous systems, or environments to predict the outputs, using a

relation defined in the system. Information always flows into the system (input) and out of the system (output). Causal models are best suited for explicit computations. To build a simple physical model in a causal system, for example, a mass-spring-damper system, different sets of blocks and connections are needed. However, the final system and its components do not resemble the physical components, and it is hard to modify without detailed knowledge of the system. In an acausal model, each component is connected to other components by connecting nodes and lines. The nodes and lines between the components are very similar to nodes and connections in physical systems. For example, in mechanical components, the nodes can be described as mechanical flanges, and the connecting lines as shafts that carry information such as force and displacement. The direction of flow is not important, and components can be replaced or reused in other models. This work uses both causal and acausal models. The acausal model is used mainly for mechanical components after the engine output shaft and formed using Modelica [4] built-in language in MapleSim software.

1.2 Motivation and Goals

Engine controllers need models that are fast enough to interact with different engine sensors and actuators. The MVEM models satisfy this condition. However adding many events to the model, such as changes in the throttle angle, injection timing, gear shiftings, road grade profiles, changing the fuel ratios, exhaust gas recirculation (EGR) percentage, vehicle acceleration and deceleration, and so on, adds too many details creating overwhelming complexity.

The first goal of this thesis is to introduce a type of MVEM created with the new MapleSim [5] software. MapleSim is a multi-domain modelling and simulation tool from MapleSoft [6] and is ideal for engine phenomena, including combustion, heat transfer, fluid mechanics, and electrical domains. The second goal is to incorporate symbol-based equations into the engine model facilitated by Maple software. This software enables one to write and to solve the equations in ways similar to writing and thinking about mathematical equations. The third goal is to use replaceable engine components, a benefit of the Modelica equation-based language. Using

Modelica enables creation of physical components and equations in an equation-based form and in acausal format. The latter can be used to create and to replace components quickly and easily, or change of components or equations are possible from one model to the next. The new components, then, can be introduced into the software library, and many types of engine configurations and components can be obtained.

1.3 Thesis Outline

Using MVEM, this work develops a model for engine gas dynamics. The model is non-thermal, in that it does not involve details of the combustion process such as the fuel mass burning rate. Instead, it calculates the engine power and speed from the throttle angle changed by a driver command (pushing the accelerator pedal). The model uses lookup tables, and physical and experimental equations. The main components modeled are the throttle, intake manifold, and engine. The engine is considered to be naturally aspirated, which eliminates turbocharger and heat exchanger effects. EGR effect can be considered by introducing a percentage of exhaust gas that is mixed with fresh air in the manifold, but no emission and EGR effects are discussed in this thesis.

1.4 Contributions

As mentioned, modelling engines is a complex task involving different domains. The first contribution of this thesis is to create an engine model in the newly introduced MapleSim software in which model components interact together in different domains. To model such complicated phenomena, an engine model is broken down into three systems: physical, input-output model, and causal and acausal. Physical models are used for the parts of the components such as intake manifold pressure calculation and crankshaft rotational dynamics that are based on basic laws of mechanics. The input-output models are used for the parts of the components such as power loss and thermal efficiency that are too complicated to model with a physical model.

The second contribution is to use both lookup tables and parametric equations inside the model. Lookup tables can be replaced by parametric equations, or the reverse, in this model. Although parameters of the input-output equations are defined for the engine of interest, they can be easily redefined inside the model for new engines. The equations are defined inside each component in a symbolic manner by embedded Maple inside the software. The symbolic equations can be changed and customized for new components.

The third contribution is the work's use of both causal and acausal models. Although the acausal models are used only in rotational dynamics, the introduction of gas connectors in future work should make it possible to replace the causal throttle, intake, and engine components with acausal models, which will help to replace and connect the model components faster and more easily.

Finally, the thesis compares different throttle experimental equations by fitting curves to the engine data. For example, throttle angle function is obtained by reviewing similar work in the literature, analyzing the actual data, and fitting the curve to the data.

1.5 Document Structure

The engine model in this thesis is discussed in following chapters:

Chapter 2 provides background on engine models, including physical and experimental models.

Chapter 3 provides a review for current engine-and powertrain-simulation tools and software.

Chapter 4 gives theoretical and mathematical equations for engine models. Different types of engine models for each component are discussed in this chapter.

Chapter 5 presents the new MapleSim engine components and equations that are used in each component.

Chapter 6 demonstrates the simulation setups and results.

Chapter 7 sums up the conclusions of the thesis and makes recommendations for future work.

Chapter 2

Background and Literature Review

With new anti-exhaust emission legislation and increasing oil prices in the 1970s, the automotive industry adopted the goals of increasing fuel economy and reducing emissions. Introduction of exhaust catalytic converters in 1975 helped to reduce carbon monoxide (CO), hydro-carbons (HC), and nitrogen oxides (NOx) emissions significantly. To increase fuel economy, various strategies were implemented, such as downsizing of vehicle and engine, increasing of engine, powertrain, and accessories efficiencies, and reduction of vehicular aerodynamic drag coefficient and rolling resistances. To achieve these goals required better modelling approaches for engine controllers. Controllers should be able to model main engine components in a fast and approximate way. Better computers in recent years have allowed more complex modelling of engine controllers.

Engine models can be divided into different types, such as physical or empirical, and dynamic or steady-state. However, there is no clear distinction between these types, and usually engine models are a combination. The early models were based on steady-state test conditions and regression models. Later, with advances in computers, dynamic models became popular. Because the early models usually used steady-state models, and newer models used dynamic and physical models, the four engine types mentioned above are combined and discussed in two types: steady-state models and dynamic models.

2.1 Steady-state Models

Engine models, until the 1970s, were mainly obtained from steady-state tests at constant speed and torque conditions. Spark advance (SA), air-fuel ratio (AF), and exhaust gas recirculation (EGR) variables were changed slowly to determine the best fuel efficiency and the lowest possible emission relations. Most of the models were obtained by analyzing the effects of varying input variables on output variables, so they were called input-output models [7]. Input-output models were empirical and usually used either mapping techniques or statistical correlations such as regression methods to establish relations between input and output.

2.1.1 Regression Models

In a regression analysis method, empirical functions are approximated by mathematical relations such as a Taylor series. A third order expansion of a Taylor series can be written for f as a function of three input variables: SA, AF, and EGR.

$$f(SA, AF, EGR) = f + df + \frac{d^2 f}{2!} + \frac{d^3 f}{3!} \qquad (2.1)$$

The first derivative of the function can be written as

$$df = \frac{\partial f}{\partial (SA)}\Delta(SA) + \frac{\partial f}{\partial (AF)}\Delta(AF) + \frac{\partial f}{\partial (EGR)}\Delta(EGR) \qquad (2.2)$$

By taking the second and third derivatives of the function and replacing them in the first equation

$$\begin{aligned} f(SA, AF, EGR) = {} & k_1 + k_2(SA) + k_3(AF) + + k_4(EGR) + k_5(SA)^2 + k_6(AF)^2 + k_7(EGR)^2 + \\ & + k_8(SA)(AF) + k_9(SA)(EGR) + k_{10}(AF)(EGR) + k_{11}(SA)^3 + k_{12}(AF)^3 + k_{13}(EGR)^3 + \\ & + k_{14}(SA)^2(AF) + k_{15}(SA)^2(EGR) + k_{16}(AF)^2(SA) + k_{17}(AF)^2(EGR) + k_{18}(EGR)^2(SA) + \end{aligned}$$

$$k_{19}(EGR)^2(AF)+k_{20}(SA)(AF)(EGR) \quad (2.\ 3)$$

Obviously, the above equation has many terms and it is hard to use it as an experimental equation. A statistical t-test can determine the significance of each term, and the terms that should be kept or eliminated from the equation. Simplifying, obtains the final form of regression model and the equation coefficients [8].

One of the first attempts to develop engine control optimization by a regression method was done by Prabhakar, et al. [9]. They used optimization methods to find the relations between SA, AF, speed and torque variables with emissions and fuel consumption at steady-state conditions. However, the model was not validated for a driving cycle. Mencik and Blumberg [8] used regression methods for exhaust emissions. They concluded that the degree of a fitting polynomial depends on experimental data scatter. They also showed that the emission mass flows can be best presented by logarithmic functions in that emissions can vary with the same magnitude of order to the control variables. Delosh et al. [10] used a mixed regression and physical model for total vehicle modelling. The model was able to receive throttle and brake commands from a driver, and thus followed a driving cycle.

2.1.2 Speed-Torque Time Matrix

Blumberg [11] was able to reduce the time and the costs of emission and fuel economy tests over a driving cycle. His method involved using a time distribution matrix of speed and torque over a driving cycle period. The driving cycle was divided into a few regions and representative points (8 to 13 points). The total time spent in each region was considered as a weight factor for the representative point. Figure 2.1 shows an example of a time matrix. Using this method, a driving cycle could be represented by a few points that could handle the drivetrain changes by adjusting the weight factors [12].

Rishavy et al. [13] used a speed-torque matrix method involving a linear programming method to reduce engine emissions. Cassidy [14] implemented an on-line optimization method at selected points in a speed-torque matrix for engine calibrations. Auiler et al. [15] used dynamic programming to allocate emission contributions at selected points. The method combined the steady-state emissions with fuel flow data to minimize the fuel emissions.

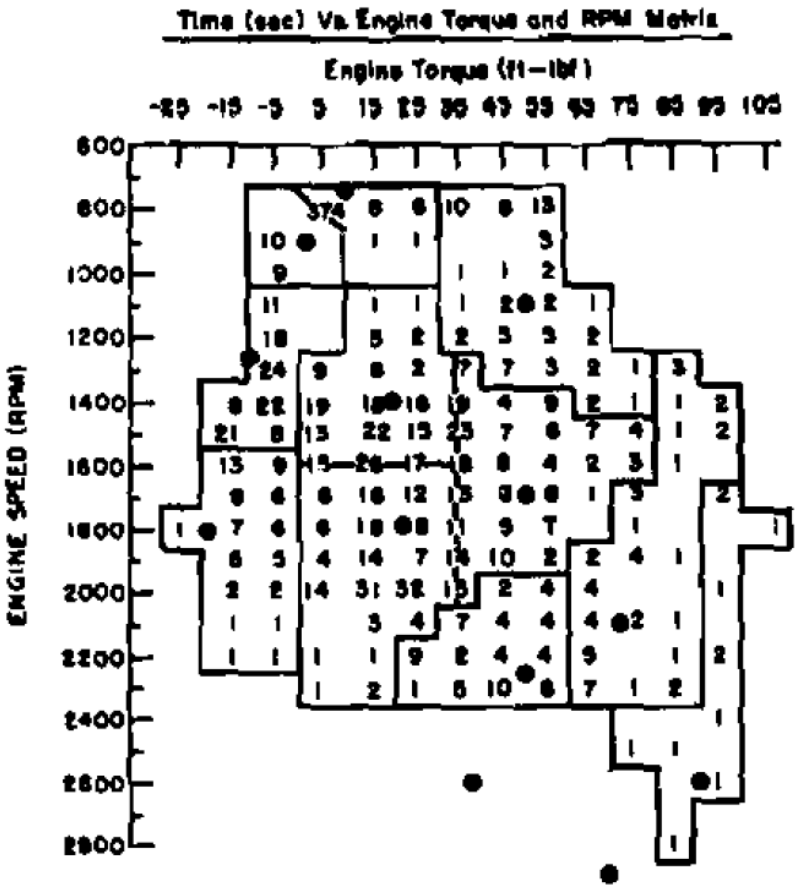

Figure 2.1 An Example of a Speed-Torque Time Density Matrix [12].

2.2 Dynamic Models

In a driving cycle, many transients such as shifting gears and changing the throttle angle can not be captured by steady-state tests. Advances in computer technology and more restrictions for fuel emissions led to dynamic models becoming a general method for engine modelling.

Dobner [16, and17] introduced a dynamic mathematical model for an engine with a carburetor. The model could be used for other engines with only a few changes in input parameters. The control engine variables were SA, AF, EGR, throttle angle, and load torque, and the main output variables were manifold pressure, engine net torque, and engine speed. The dynamics of the model was presented by time delays and integration of dynamic equations. The model was a simple discrete model in which computations were done per each engine firing. The engine system in the model consisted of carburetor, intake manifold, combustion, and engine rotational dynamics.

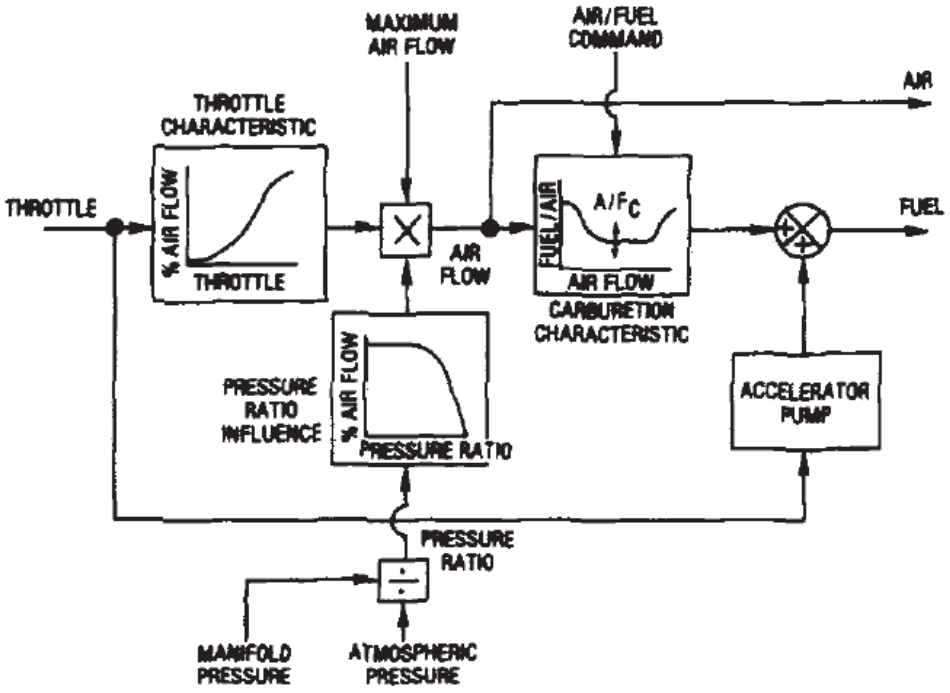

Figure 2.2 Carburetor in Dobner's Engine Model [17]

In the carburetor model (Figure 2.2), the fuel mass flow was calculated by using two individual lookup tables for normalized pressure ratio and throttle angle characteristic. The method of normalizing pressure and throttle angle function is still widely used in mass calculations of engines as lookup tables, or equation-based forms. The fuel flowing out of the manifold was calculated from mass flow rate into the manifold and volumetric efficiency characteristics. By considering fuel delays as drops, wall, and gas contributions, the total fuel mass calculated, and air-fuel ratio was obtained. In the combustion model, the effects of SA, AF, and air charge density were performed as functions of normalized torque in the lookup tables. The output values of these lookup tables were used to obtain the indicated torque. The model used another lookup table for the friction added to the load torque and results were used in engine rotational dynamic to obtain engine speed.

Using volumetric efficiency and engine speed, Aquino [18] presented an equation form of manifold pressure calculations based on continuity law. Unlike Dobner's, this model was a continuous flow model. The model also gave a new set of equations for fuel dynamics. The model tracked the fuel mass in the intake manifold by assuming that, for fuel injected into ports, a fraction of the fuel would evaporate and a fraction of it would be left on the port walls. After a delay, the fuel mass on the port wall is mixed with air and flows into cylinders. The fuel dynamic model defined by Aquino can be easily used for other engines if the time constant (τ) and fraction of injected fuel (X) parameters are adjusted.

Powell [19] introduced a nonlinear dynamic engine model that included induction and an engine power system. Figure 2.3 shows the configuration of the engine model. The model also considered EGR, fuel injection, and throttle valve dynamics. For intake manifold mass calculations, instead of using volumetric efficiency, which has an important role in transient conditions, he directly used a regression model for mass flow changes as a function of engine speed and manifold pressure. The throttle mass flow was obtained from an equation for pressure at choked and non-choked conditions, and a second degree polynomial was fitted for the throttle

angle function. The engine output torque was obtained by another regression equation as a function of engine speed, AF, and intake mass flow. Reference [7] gives more information about similar models for intake mass flow calculation for various engine operation ranges. The paper also included information about induction-power and spark-power delays.

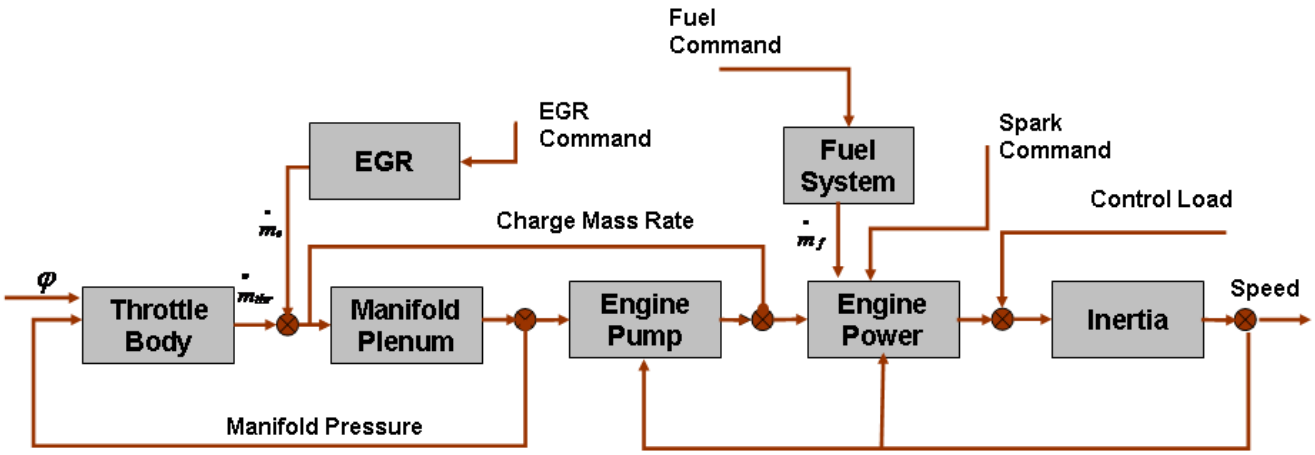

Figure 2.3 The Engine System and its Components [19]

Crossley and Cook [20] used an approach similar to the Powell's but replaced the throttle angle approximate function with a third degree polynomial and used engine output torque as a function of SA, AF, engine speed, throttle mass flow, and engine mass flow variables.

Yuen and Servati [21] presented a dynamic engine model similar to the approach used in reference [16], replacing the throttle body with a carburetor in the engine model. To generalize the model for other engine applications for future, they did not use the throttle area characteristic term, but instead used a normalized function for pressure and another normalized function by using Harington and Bolt's [22] approximation method. Unlike Dobner's, this model considered intake manifold temperature changes and their effect on fuel evaporation and manifold pressure during the transient conditions. Engine emissions were obtained from experimental tables as functions of combustion parameters. The model could predict the mass generations of different pollutants as a function of the throttle mass flow and air-fuel ratio.

In actual engine operating condition, the air mass flow is closely related to throttle area geometry and characteristics. Moskwa [23] introduced throttle area as a function of throttle angle, throttle pin diameter, and throttle bore. The model used friction, AF, and SA lookup tables for output torque calculation. Thermal efficiency in the model was a function of manifold pressure, compression ratio, and engine cylinder geometries.

A model for the first time called the mean value engine model (MVEM), was introduced by Hendricks and Sorenson [24] and then described in more detail in [25]. The idea was to capture engine dynamics in time scales larger than an engine cycle. As shown in Figure 2.4, the model included main components of engine gas flow dynamics, from the intake manifold to the exhaust system. Hendricks and Sorenson introduced new equations for volumetric efficiency, thermal efficiency, and pressure function. For fuel dynamics, they introduced a new model that became a competitor to the Aquino model. Unlike Aquino's fuel-mass-based calculations, the newer model is based on fuel flow in the intake manifold. One of the advantages of Hendricks and Sorenson's model is that most of its parametric equations, such as volumetric efficiency, thermal efficiency, load, and loss power, are presented as functions of manifold pressure and engine speed that are obtained directly from solution of differential equations in the manifold and engine. The engine parameters can be easily adjusted and reused for other engines.

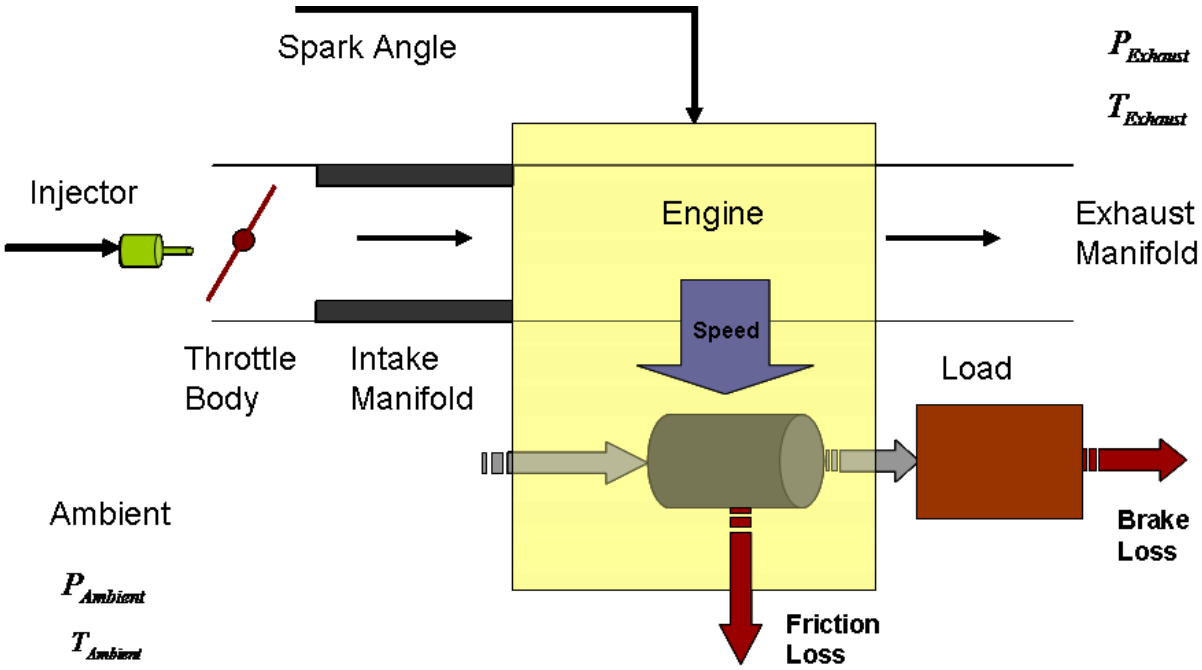

Figure 2.4 Schematic of a Mean Value Engine [24]

Chapter 3

Powertrain Simulation Tools and Strategies

Powertrain modelling and simulation software products are developed for various purposes and can be used for drivetrain analysis, vehicle performance evaluation, or new powertrain development. Powertrain simulation tools generally model the components' interactions on each other by computing torque and speed values in each component. The powertrain strategies define the method and the direction of the power or torque, and speed flows in a simulation relative to the calculations.

3.1 Powertrain Strategies

The power or torque flow in a powertrain starts from the engine (upstream), and ends with the wheels (downstream). The flow of calculations can be either in the same direction as the power flow, or in the reverse. Based on the direction of the power flow and direction of the calculations, vehicle simulation strategies are categorized as one of three types: backward, forward, or combined backward-forward facing, all of which are described in following sections.

3.1.1 Backward Approach

In a backward approach, calculations start from wheels and end with the engine. In a powertrain, wheels are assumed to be the "front" of the powertrain, and the engine "end" of the system, leading to the terms backward or front-to-end, or wheel-to-engine approaches. In the backward method, the power required at the wheels is calculated back to the engine, and the related engine power is calculated. Calculations at the wheels start from the time-speed data from a drive-cycle.

Drive-cycles, standard vehicle speed data regulated by different countries, are prepared to evaluate fuel efficiency and emissions of new vehicles, and used for various accelerating, decelerating, and stop conditions for different highway or in-city driving conditions. The vehicle is assumed to follow the driving cycle with the same speed at the wheels. Vehicle acceleration and travelled distance can be directly obtained by differentiating and integrating the velocity in each instant of time of the driving cycle. The velocity and acceleration values are used to calculate tire roll losses, brake losses, and aerodynamic losses of the vehicle. The reactive force of the vehicle is assumed to be equal to the sum of these three losses. Tire radius, resistance forces, and vehicle velocity are used to calculate tire torque and rotational speed. Torque and speed in the final drive, driveshaft, gearbox, and torque converter (or clutch) are calculated from the torque and speed of the previous downstream components (closer to the wheels). The calculations are continued backward until the required power is obtained from an efficiency lookup table. The calculations for vehicle losses and component efficiencies are simple; results have a simple integration and a fast simulation execution time. One of the drawbacks of the backward approach is the assumption that the vehicle follows the drive-cycle with the same speed at any instant of time. In actual driving condition, the actual speeds of the tires are different from the desired speed due to tire slip.

3.1.2 Forward Approach

In the forward approach, the flow of calculation is in the same direction as the power flow. The process starts when a driver pushes the acceleration pedal or brake. The controller receives this command and translates it into throttle or brake commands, which are then translated to a required torque by calculating an error. The error that is the difference between the vehicle's desired and actual values is used to calculate the total demand torque. In the next step, the computed torque is passed forward through powertrain components to the wheels.

The forward approach is constructed in cause-and-effect form so it is desirable for detailed simulation. In each component instead of assuming required values, real torque and speed are

calculated. This approach gives very realistic results in particular for engine maximum output power calculations at wide open throttle conditions.

The disadvantage of the forward approach is its long running time for simulations. The calculations are based on integration of throttle manifold and powertrain speed state equations, resulting in high order integrations.

3.1.3 Combined Backward-Forward Approach

All components encounter limitations when they are working at their fully loaded conditions. Thus at some levels, when power demand is increased upstream of the component (i.e., components closer to the engine), the components reach a condition that can use only a part of the power or torque. In a forward-backward approach, simulation starts like a forward system until the power or torque in the component reaches its maximum available limit. At this level maximum power or torque is fed back toward the engine, and simulation continues from the engine to the wheels under new limitations [26].

3.2 Simulation Tools

Many tools are available for engine and powertrain modelling, both open source or commercial software. As examples, advanced vehicle simulator (ADVISOR), powertrain system analysis tool kit (PSAT), QSS toolbox, Matlab/Simulink, and Modelica are discussed in this chapter. The focus of the discussion is on how the models work and which types of equations they use. The models include different thermal or non-thermal, input-output or physical, forward or backward, and causal or acausal approaches. Depending on the level of details, the vehicle model can be defined as steady state, quasi steady-state or dynamic. For example, ADVISOR is categorized as a steady-state model, PSAT as quasi steady-state, and the model in this work is a dynamic

model. The main advantage of using steady-state models is their speed of computation. However, they cannot predict dynamic conditions.

3.2.1 Modelling by ADVISOR

Advanced vehicle simulator (ADVISOR) [26,27] is a simulation tool developed at the national renewable energy lab (NREL) in 1994. It was originally designed for hybrid electric vehicles (HEV) to improve fuel economy and vehicle performance, but later on, developed for other configurations of vehicles. ADVISOR can be used for different applications, such as performance and fuel economy analysis, or emission control. The components of ADVISOR are created in Simulink. Using Simulink enables the component orders and their connections to be shown in a graphical way. Figure 3.1 presents an ADVISOR simulation for a conventional vehicle system. The parameters used in each Simulink block are defined in an associated Matlab m-file. The model inside each Simulink block and the Matlab m-file can be redefined or replaced by new models and parameters.

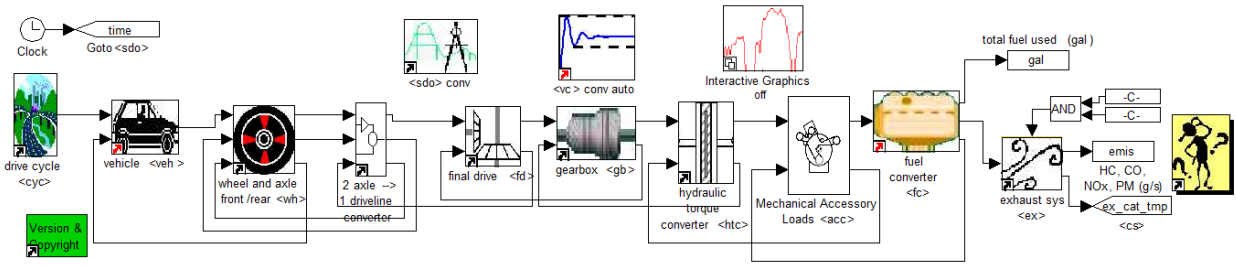

Figure 3.1 Simulation of a Conventional Drivetrain Configuration by ADVISOR [26]

ADVISOR is open source code software. The models inside the components can be scaled to match other types of powertrains. ADVISOR provides three main graphical user interface (GUI) windows: input, setup and result windows. Inside the input window (Figure 3.2), various types of driveline components can be selected from pull down menus.

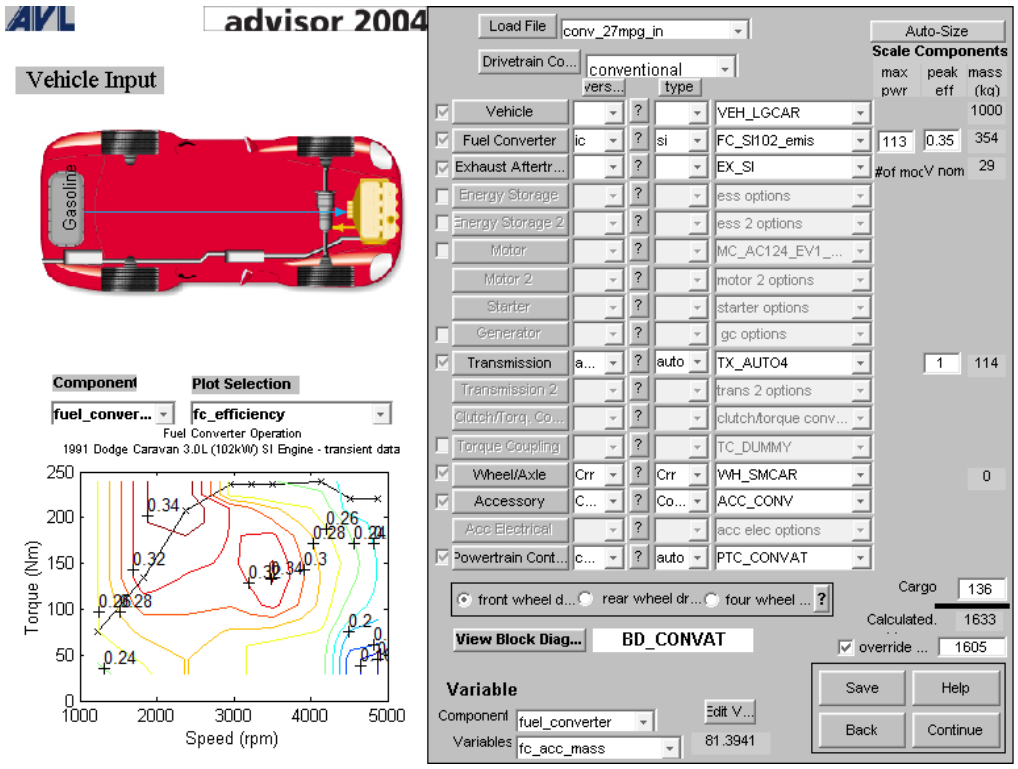

Figure 3.2 ADVISOR Input Window [26]

The values of the components such as engine power and all vehicle configurations can be edited and saved in this window. Upon loading any vehicle configuration, related data are loaded into the Matlab workspace, which are then used during the simulation. The characteristic map of each component can be displayed for the selected configuration at the left side of the window. The value of components can be changed, and the Simulink block diagram of the component can be reached by “Edit Var” and “View Block Diagram” buttons.

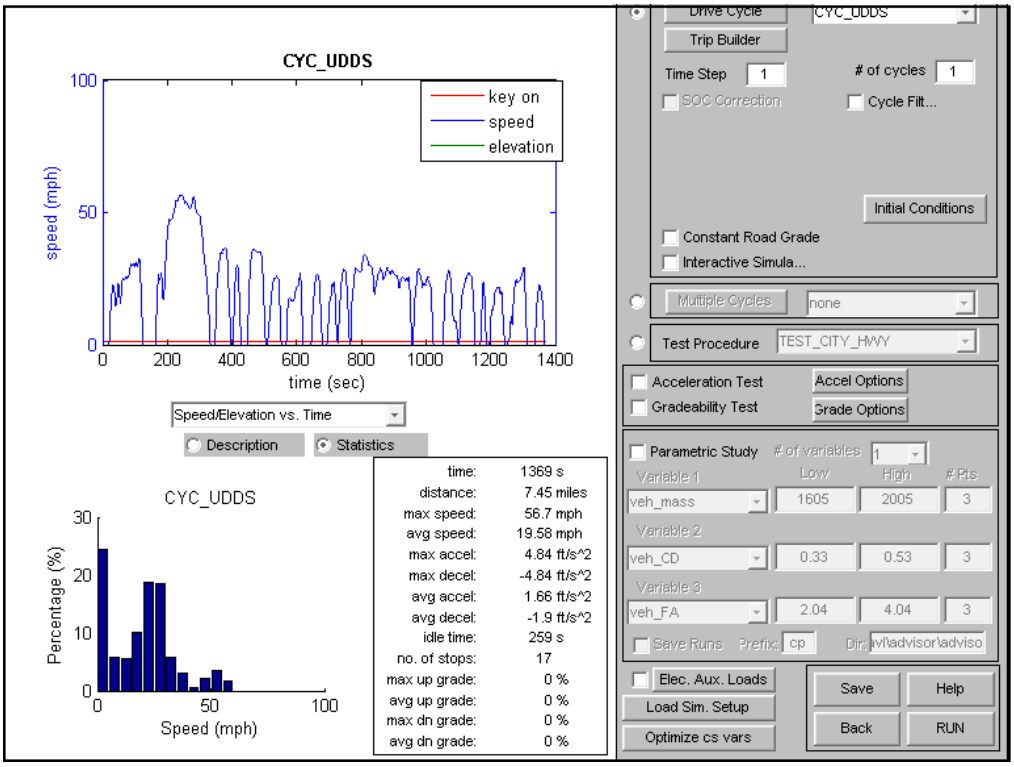

Figure 3.3 ADVISOR Setup Window [26]

The setup window (Figure 3.3) enables one to define different events such as running a simulation as a single or multiple drive-cycles, or including the road grad or acceleration tests. The right side of the window is a portion showing user-defined parameters and the left side window presents related graph information of selected parameters. The result window (Figure 3.4) enables a review of the summary of results about the vehicle and its performance at a specific time or during a driving cycle [28].

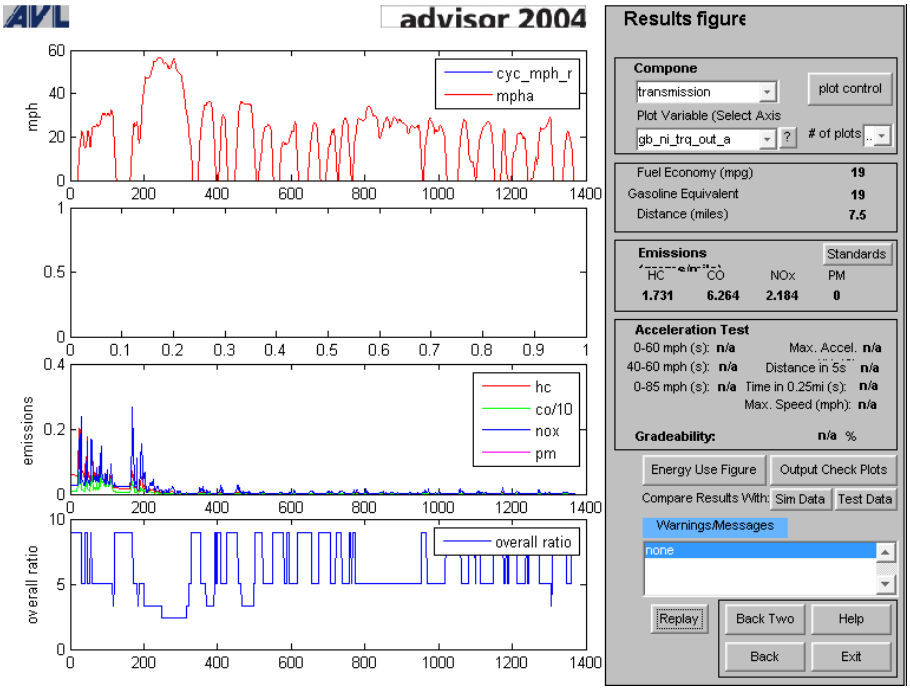

Figure 3.4 ADVISOR Result Window [26]

3.2.2 Modelling by PSAT

The Powertrain System Analysis Tool (PSAT) was developed by the Argonne national lab and the US Department of Energy (DOE) [29, 30, 31 32]. The software is based on Matlab/Simulink modelling environment with a graphical-user interface (GUI). The PSAT library has a large number of predefined mechanical, hydraulic, and electrical components that can be accessed and reused. PSAT also has many predefined vehicle configurations in its library, such as conventional spark ignition (SI) and compression ignition (CI), electric, fuel cell, series hybrid, and parallel hybrid enabling users to simulate complicated systems for different sizes of vehicles. It allows users to import data into the model components, or to define control strategies for the system without needing to write any lines of code. PSAT can be used for various vehicle modelling strategies such as fuel economy, engine performance, drive-cycle studies, parametric modelling, and controller design, but it cannot be used for calibration and drivability studies. Component controllers are controlled by the main controller at the top level of the model.

PSAT is a forward-looking model that starts simulation by receiving brake and acceleration commands from the driver. The controllers then receive these commands and distribute them into the component models. The component controller decides which types of information should be sent to which component, for example, gear information goes to the gearbox, is gear ratio or gear number, or for the clutch is displacement of its plates.

Older versions had three main windows, the same as ADVISOR's, and for any additional tasks, a new window would be added to the model, so it was confusing for the user to follow the process. Newer versions have only one window but with different tabs. In PSAT, the vehicle configurations are fixed, but components inside the configuration can be selected, modified, or replaced. Thus, for example, if a conventional SI engine is selected, the software allows choosing one of the predefined automatic or manual configurations from its subsystem. In all configurations, the order of components and their connection are fixed. In a conventional SI engine the order of the components starts from the starter and engine, and ends with the wheel and the vehicle model. The configuration can be selected from the library list by dragging and dropping it into the work space (Figure 3.5).

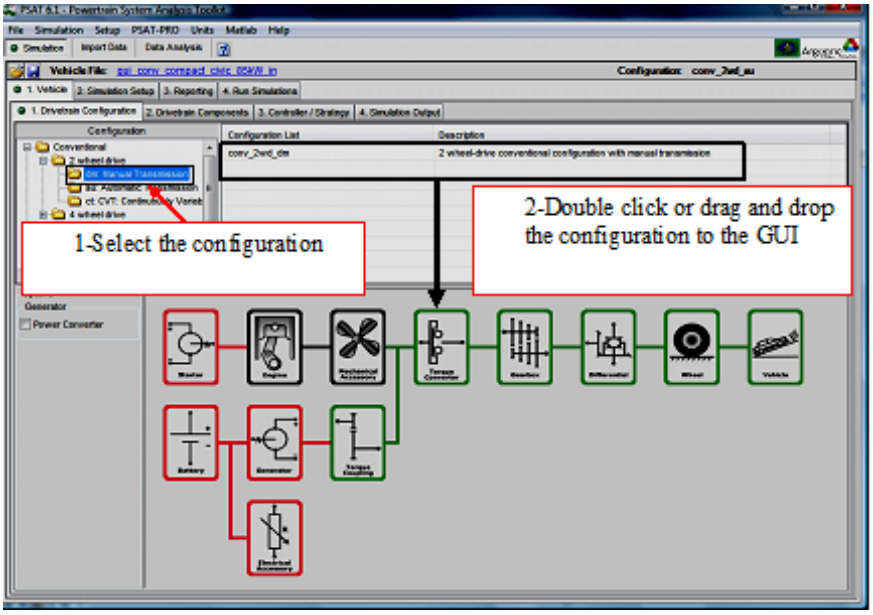

Figure 3.5 Selecting the Configuration in PSAT

In a similar way, components can be selected from the library list, and then its initialization file and related graph can be opened. The software allows access to the component Matlab m-file for any parameters modifications inside the model (Figure 3.6). PSAT allows the choice of different accelerating, decelerating and shifting gear strategies from the predefined strategies in the library. In newer versions, it is possible to model the transient conditions of the components such as the engine or gearbox transition condition.

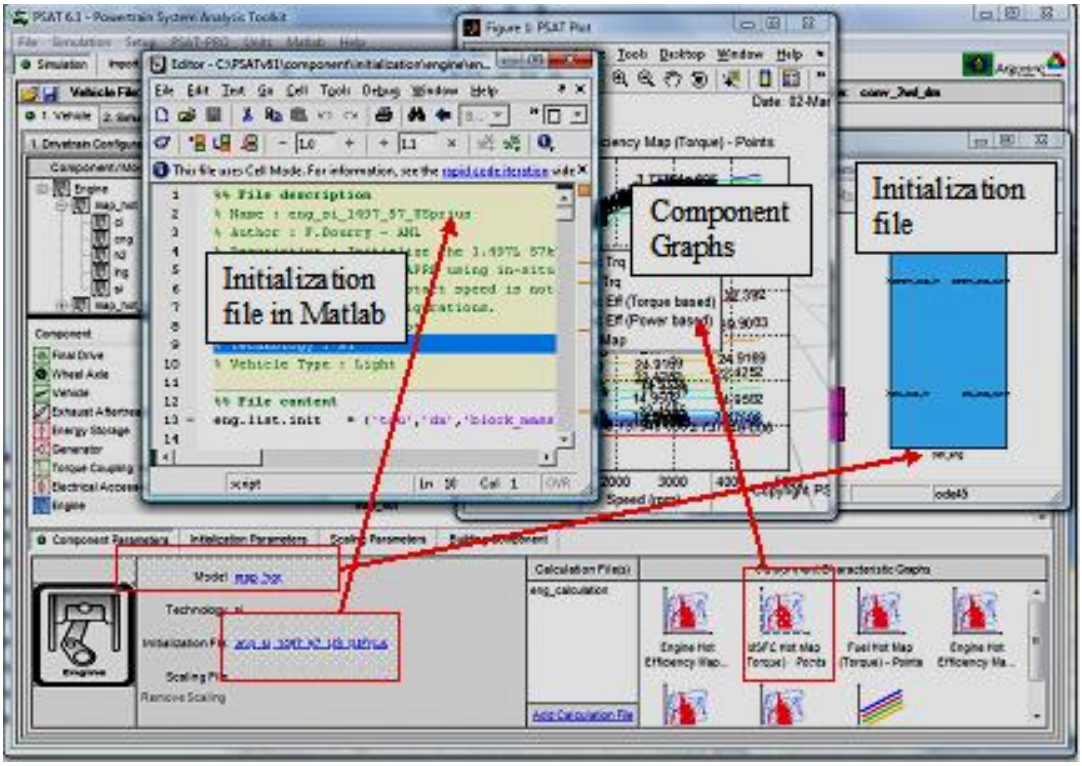

Figure 3.6 A Component and Its Related Files in PSAT

Some of the main components of PSAT and their models are explained in the next sections.

3.2.2.1 Driver Model

The driver model calculates torque demand by converting the error that is the difference between vehicle actual and desired speeds. The vehicle desired speed is obtained directly from a drive-cycle that is used in simulation. Error calculations are shown at the top left corner of Figure 3.7 as

$$V_{Error} = V_{veh\_desired} - V_{veh\_actual} \quad (3.1)$$

Error is used to calculate torque variation (block A).

$$T_{\text{varition}} = K_p V_{Error} + K_i \int V_{Error} dt \quad (3.2)$$

K_p is proportional gain, which is the reaction of the system to current error, and used for the transient portion of the torque demand that helps the vehicle to keep on the signal track during instant speed changes. The integral gain, K_i, is the reaction of the system to the sum of the errors and used to eliminate errors remaining from the steady-state working condition of vehicle.

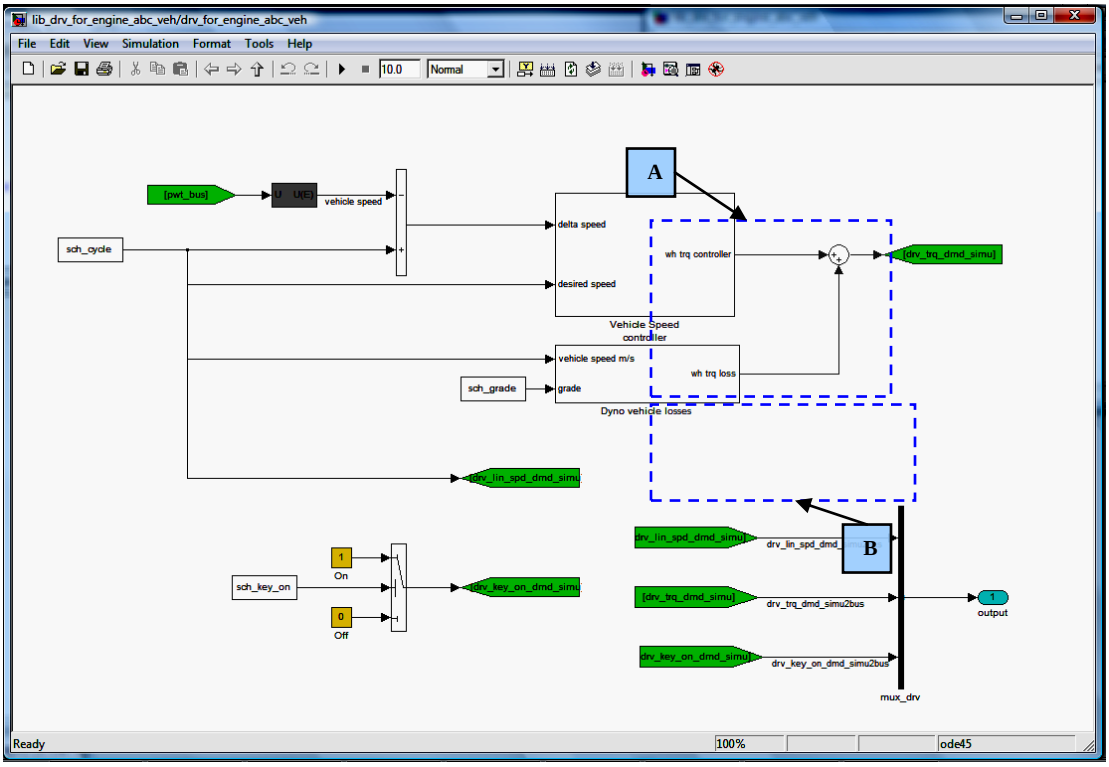

Figure 3.7 Top level of Driver model in PSAT [30]

Vehicle losses, including rolling, aerodynamic, and grade resistance, are calculated by approximating a second degree polynomial obtained from dynamometer experimental data as follows (block B).

$$T_{loss\_veh} = \left(a + bV_{veh\_desired} + cV_{veh\_desired}^{\ 2}\right) r_w \qquad (3.3)$$

where r_w is tire radius, and a, b, and c are experimental coefficients. Demand torque is the sum of variation and vehicle loss torques.

$$T_{dmd} = T_{\text{variation}} + T_{loss\_veh} \qquad (3.4)$$

3.2.2.2 Engine Model

This engine model in PSAT calculates fuel consumption, output torque, and emissions in steady-state (hot) and transient (hot-cold) thermal conditions. Figure 3.8 shows four blocks that calculate engine torque, engine thermal parameters, engine fuel rate, and exhaust emission flows in blocks C, D, E, and F respectively.

Block C, shown in Figure 3.9, calculates engine torque by using a switch. To prevent excess injection of fuel when the engine speed is lower than idling speed (the time when an engine is first switched on with a starter) the cut-off torque is calculated from a lookup table, as shown at the top right of the window. In other conditions, engine torque is calculated from function block as follows (block C1).

$$T_{cmd} = PW_{cmd}\, Eng_{On\_Off}\, \omega_e , \tag{3. 5}$$

where PW_{cmd} is the command coming from the controller, varying from 0 to 1. Eng_{On_Off} is a switch that has values of 0 when the engine ignition switch is off, and 1 when the engine is running. If T_{cmd} is zero, the output torque value calculated by the function block will be zero. If the engine speed is greater than zero and torque command is equal or greater than zero, output torque is calculated in a function block by interpolation of wide open and closed throttle torque values from following equation:

$$T_{out} = (1 - T_{cmd})T_{ctt} + (T_{cmd}\, T_{wot}), \tag{3. 6}$$

where T_{wot} is wide open throttle torque, and T_{ctt} is closed throttle torque.

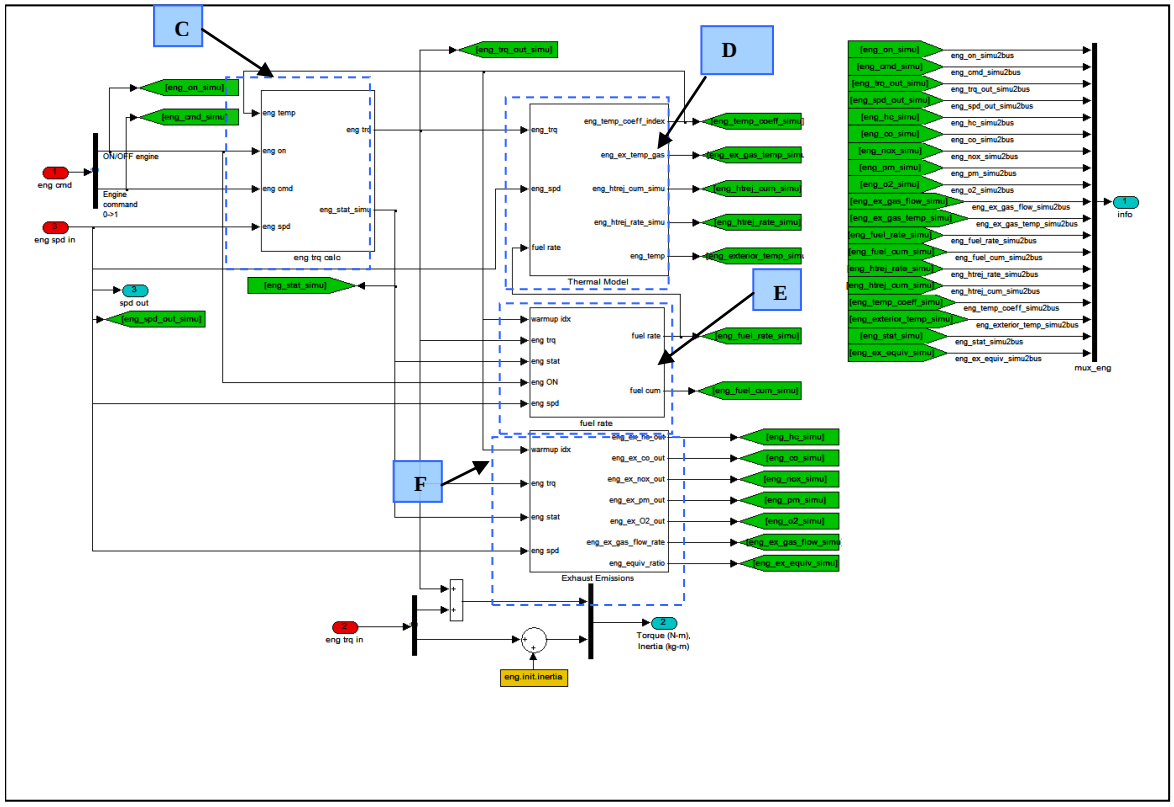

Figure 3.8 Top level of Cold-Hot engine in PSAT [30]

Block C1 (Figure 3.10), illustrates a wide open throttle torque curve (T_{wot}), calculated by interpolation of the cold wide-open throttle curve and the hot wide-open throttle curves:

$$T_{wott} = (1 - PW_{temp})T_{wot\_cold} + PW_{temp}\,T_{wot\_hot}, \qquad (3.7)$$

where T_{wot_cold} is the cold wide-open throttle torque curve value, T_{wot_hot} is the hot wide-open throttle torque value, and PW_{temp} is the engine warm-up coefficient, equal to zero when the engine is cold, to 1 when the engine is hot, and between 0 to 1 during engine warm-up. In a similar way the closed-throttled torque is calculated in the block marked C2.

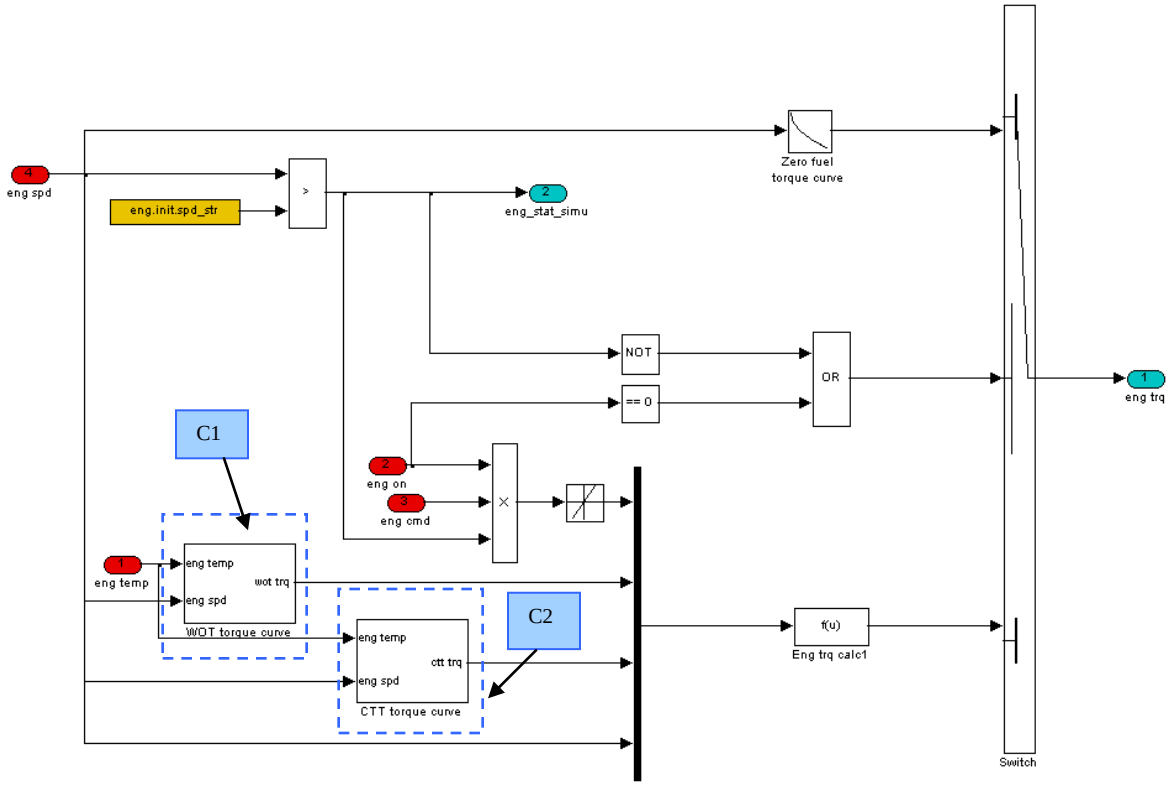

Figure 3.9 Block C: Engine Torque Calculations in PSAT [30]

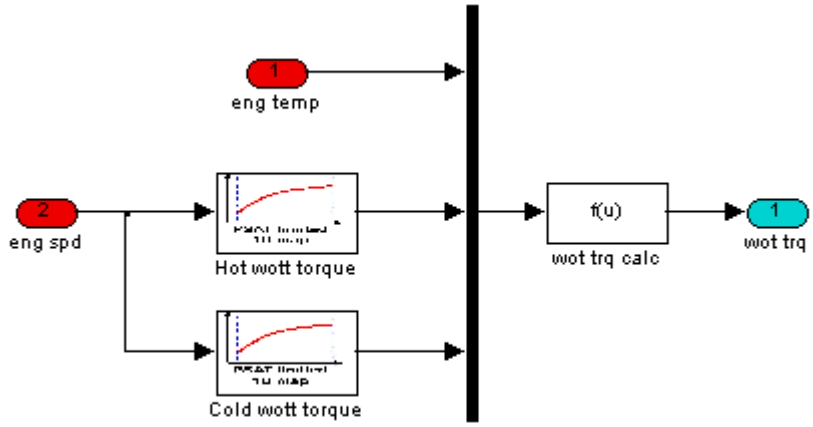

Figure 3.10 Block C1: Wide Open Torque Curve in PSAT [30]

Block D (Figure 3.11) calculates thermal parameters for the engine, including the warm-up index, engine temperature, heat rejected power, and heat rejected energy.

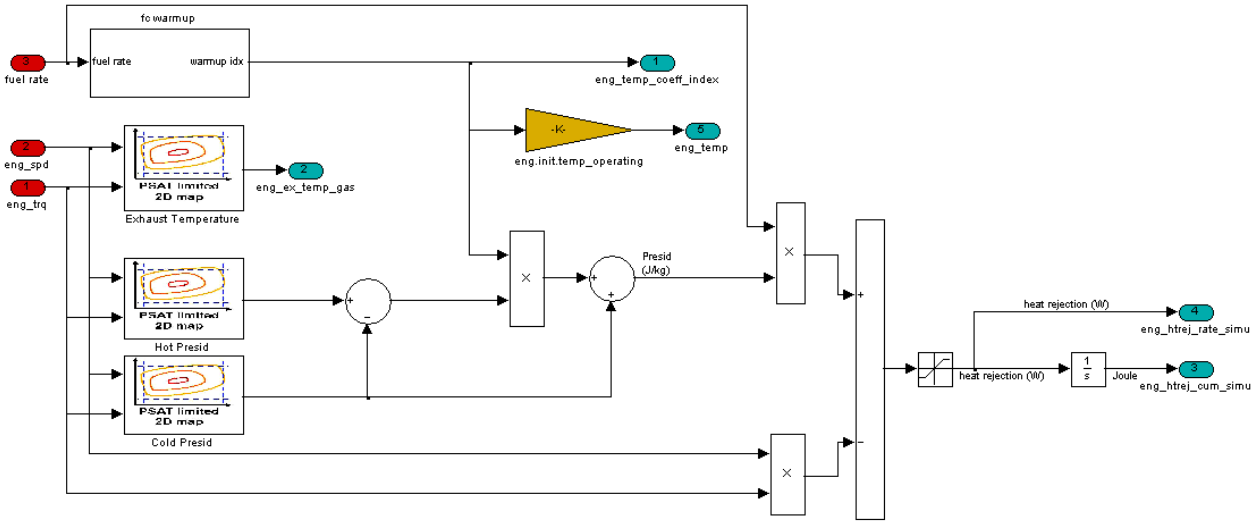

Figure 3.11 Block D: Thermal Model in PSAT [30]

Knowing engine torque and engine speed, and heat power released by fuel per unit mass can be obtained from the heat-released-hot and heat-released-cold indices lookup tables.

$$q_f = PW_{temp}\left(q_{fCold} - q_{fHot}\right) + q_{fCold}, \tag{3. 8}$$

where q_f is the heat power released by fuel per unit mass. Heat power rejected from the cylinder walls or intake and exhaust valves is the power that is generated by fuel minus the power at the engine output shaft.

$$\dot{q_H} = \dot{m}_f q_f - T_e \omega_e \tag{3. 9}$$

The fuel rate is calculated by interpolation of the data from hot and cold fuel rate lookup tables.

$$\dot{m}_f = PW_{temp}\left(\dot{m}_{fHot} - \dot{m}_{fCold}\right) + \dot{m}_{fCold} \tag{3. 10}$$

Engine emissions including particulate matter (PM), hydrocarbons (HC), nitrogen oxides (NOx) and carbon monoxides (CO) are directly obtained from a lookup table as functions of engine speed and torque data.

3.2.2.3 Gearbox Model

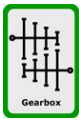

Manual, automatic, and continuous variable (CVT) are three types of transmissions in PSAT. Figure 3.12 shows top level of a CVT gearbox model that calculates speed, torque, and inertia.

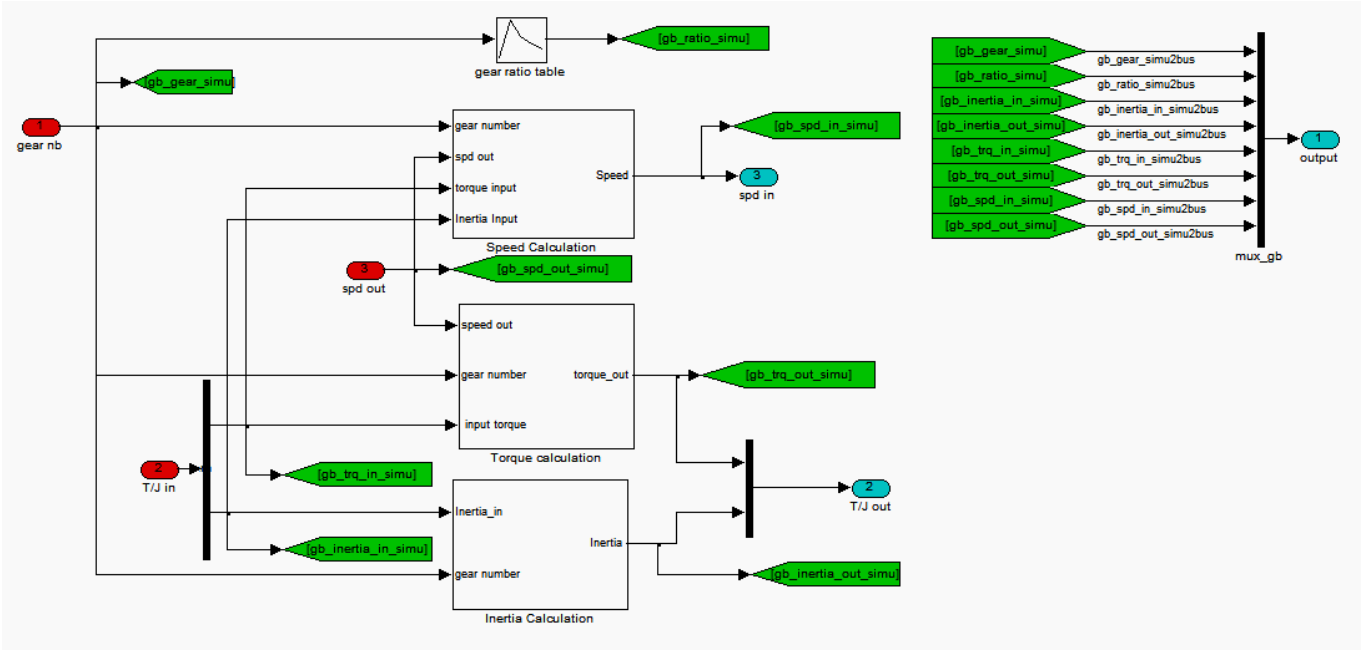

Figure 3.12 Top Level of a CVT Gearbox Model in PSAT [30]

Output torque and speed are calculated by multiplying or dividing input values by a gear ratio. Loss torque is considered in torque calculation by using a 3-D lookup table and three inputs: speed (ω_{in}), input torque (T_{in}), and a gear index. The gear index is calculated from a lookup table

once the gear number is known. It is 0 for neutral gear, and 1,2,3,4 for corresponding gears. A typical torque calculations is shown in Figure 3.13.

$$T_{out} = (T_{in} - T_{loss}) gear\_index \quad (3.\ 11)$$

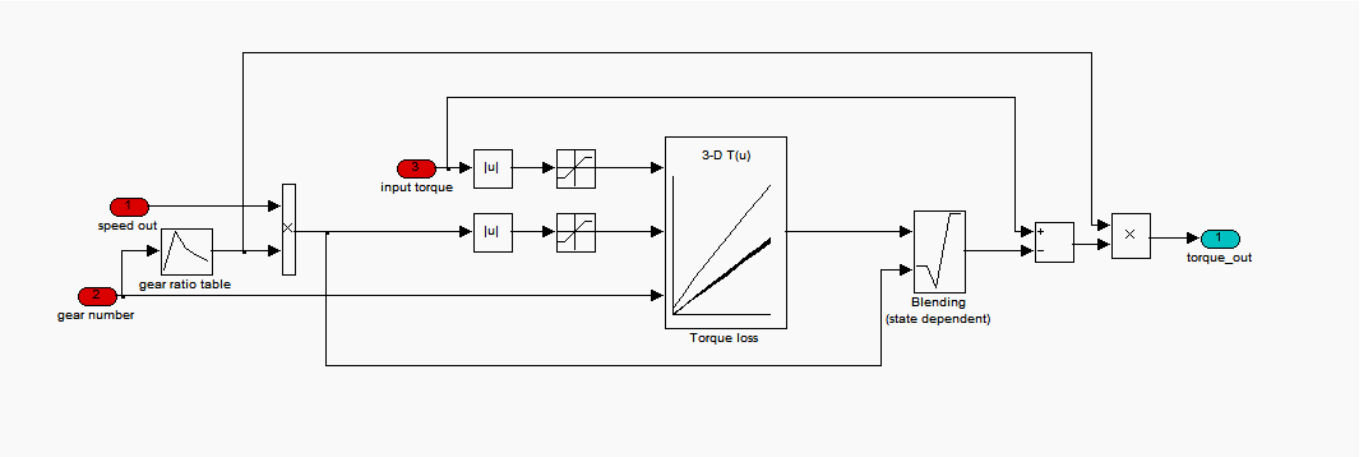

Figure 3.13 Torque Calculations in PSAT [30]

3.2.2.4 Wheel Model

Two types of wheel model exists in PSAT. The first is the Single Wheel model and is based on braking force calculations at each wheel individually, and adding inertias to all wheels. The second model doesn't include the rolling resistance because it is already considered in the driver model and because of three A, B, and C coefficients in the model is called ABC model.

The top corner of the wheel model, displayed in Figure 3.14, includes three types of calculations: speed, force, and mass. The angular velocity of the wheel (ω_{wheel}) is calculated by dividing the speed of the vehicle by the radius of the wheel (r_w).

$$\omega_{wheel} = V_{veh} / r_w \tag{3. 12}$$

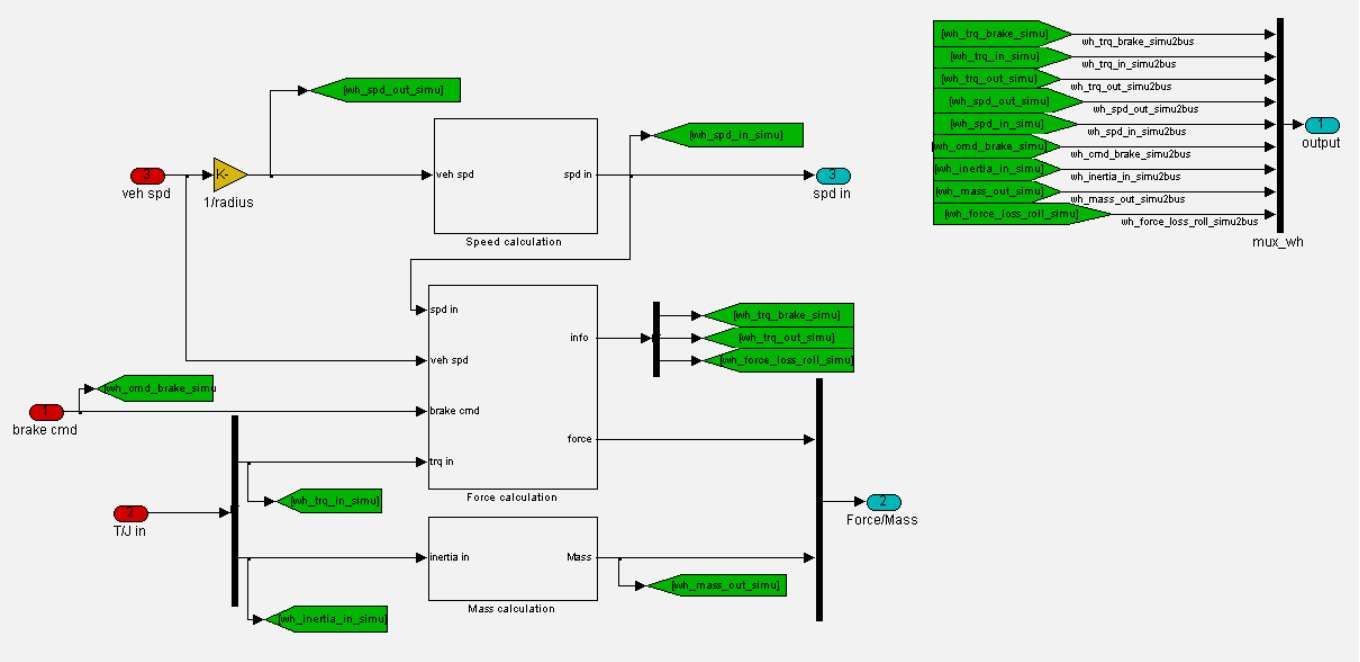

Figure 3.14 Top level of Wheel Model in PSAT [30]

In force calculations block, torque loss for the wheel is calculated by multiplying the brake command value (PW_{Brake}) by the maximum available brake torque.

$$T_{lossbr} = PW_{Brake} T_{\max br} \tag{3. 13}$$

The brake command value varies from -1 to 0, from full brake pedal pushing to no-brake pedal pushing. The wheel losses are calculated in Figure 3.15 by a third-degree polynomial as a function of vehicle speed.

$$T_{losstr} = \left(\left(c_1 + c_2\, V_{veh} + c_3 V_{veh}{}^2 + c_4 V_{veh}{}^3\right) m_{veh}\, g\right) r_w \qquad (3.14)$$

where g is gravity acceleration, r_w is wheel radius, and m_{veh} is mass of the vehicle. The output torque of the vehicle is obtained by subtracting the brake and wheel losses from the input torque coming from the final drive (Tin).

$$T_{out} = T_{in} - T_{lossbr} - T_{losstr} \qquad (3.15)$$

Finally the net force is calculated by dividing the output torque by the wheel radius (r_w).

$$F_{out} = \frac{T_{out}}{r_w} \qquad (3.16)$$

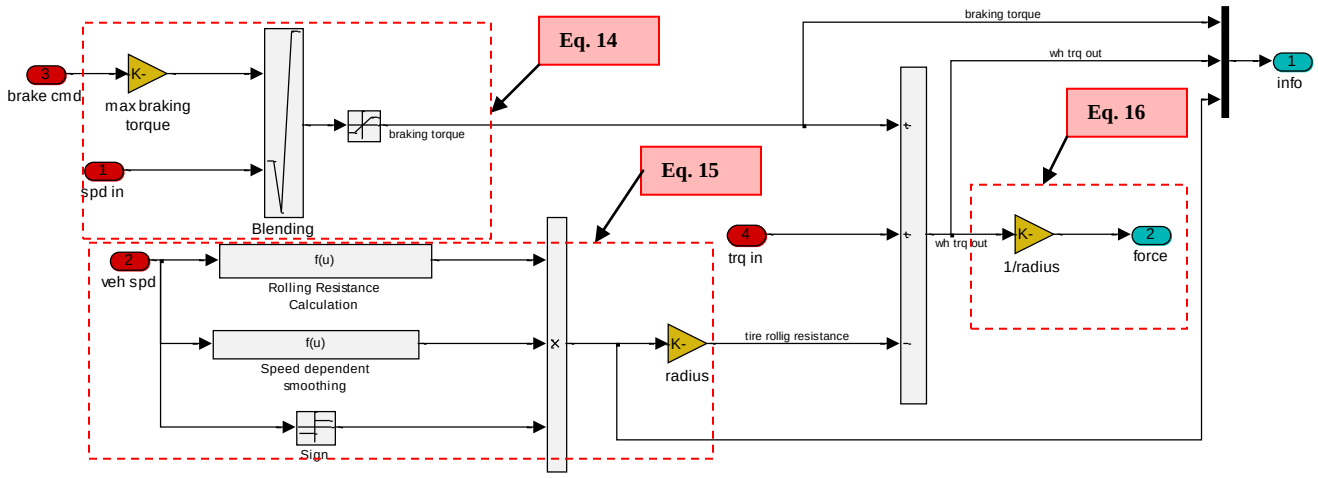

Figure 3.15 Force Calculations in PSAT [30]

Equivalent inertia mass of the powertrain ($m_{inertia}$) is calculated by adding the wheel inertia (J_{wh}) and upstream inertia (J_{in}), and dividing the result by the wheel radius squared.

$$m_{inertia} = \left(J_{in} + J_{wh}\right) / r_w^2 \qquad (3.17)$$

3.2.3 QSS Toolbox

A quasi-static simulation toolbox (QSS) is a discrete backward simulation model that approximates fuel consumption by using a fast and simple calculation algorithm [33, 34]. The calculations start from integration and differentiation of velocity in a driving cycle to obtain approximations of vehicle travelled distance and acceleration. Figure 3.16 depicts the top level of QSS tool box. Various American, European, and Japanese drive-cycles are available in the QSS library. Upon selection of a drive-cycle for a manual gearbox an associated shifting strategy vector file is loaded into the work space. Changing the gears is assumed to be only a function of vehicle speed.

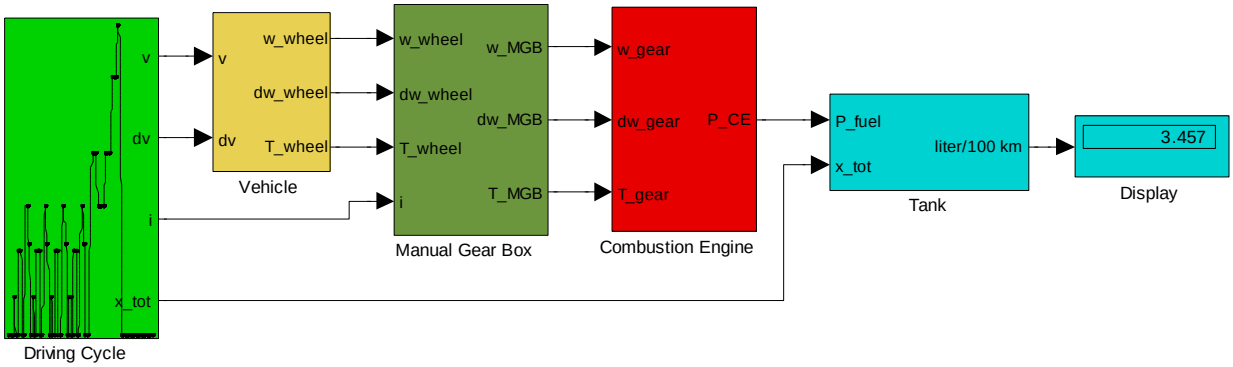

Figure 3.16 Top Level of QSS Toolbox [34]

As depicted in Figure 3.17, wheel rotational speed and torque can be obtained from the following equations

$$V_w = r_w \omega_w \tag{3. 18}$$

$$T_w = \left(F_{aero} + F_{roll} + F_{iner}\right) r_w \tag{3. 19}$$

$$P_w = T_w \omega_w \tag{3. 20}$$

where V_w, r_w, ω_w, T_w, and P_w are vehicle speed, wheel radius, wheel rotational speed, wheel torque, and power. F_{aero}, F_{roll}, and F_{iner} are aerodynamic, tire rolling, and inertia forces. The vehicle is assumed to be moving on a flat road, so grade loss is not considered in this model.

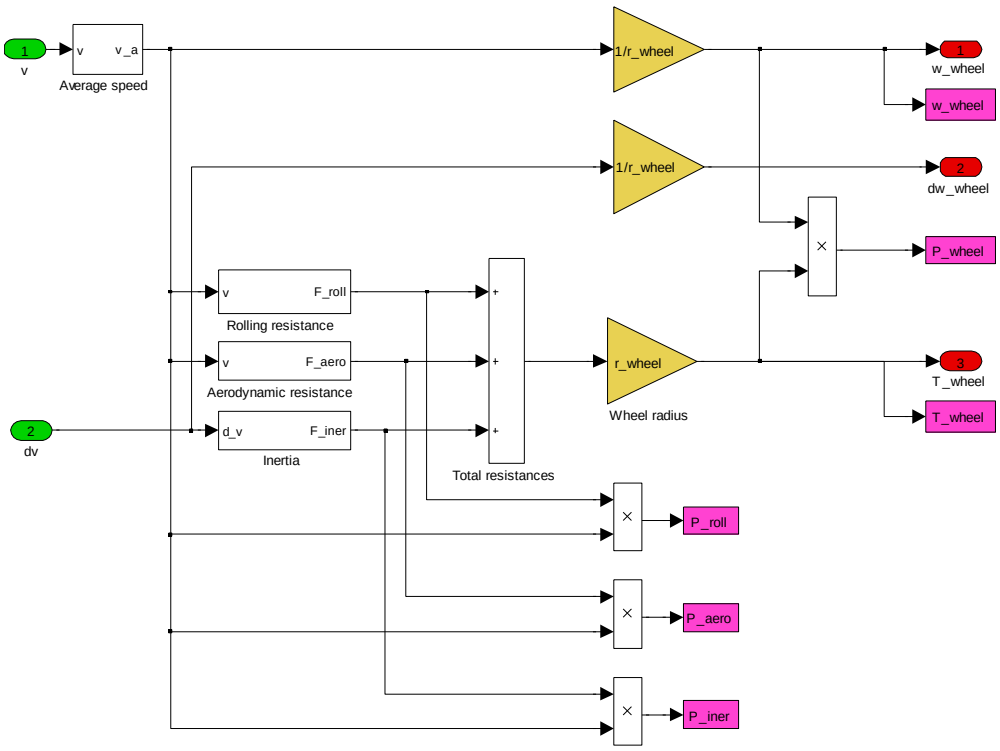

Figure 3.17 Vehicle Calculations in QSS [34]

Gear ratios are used to calculate gearbox input torque and speed in the gearbox block. In the engine block (Figure 3.18), fuel mass flow is obtained by a two-dimensional map and use of gearbox speed and torque inputs. Fuel power is obtained by

$$P_f = \dot{m}_f H_f \qquad (3.\ 21)$$

where H_f is a constant fuel heating value. Finally, the required power level is obtained by adding the auxiliary vehicle equipment (such as air-conditioner) required power to the fuel power.

$$P_e = P_f + P_{aux} \tag{3. 22}$$

The QSS engine model can also detect and control over load, over speed, idle and fuel cut-off conditions.

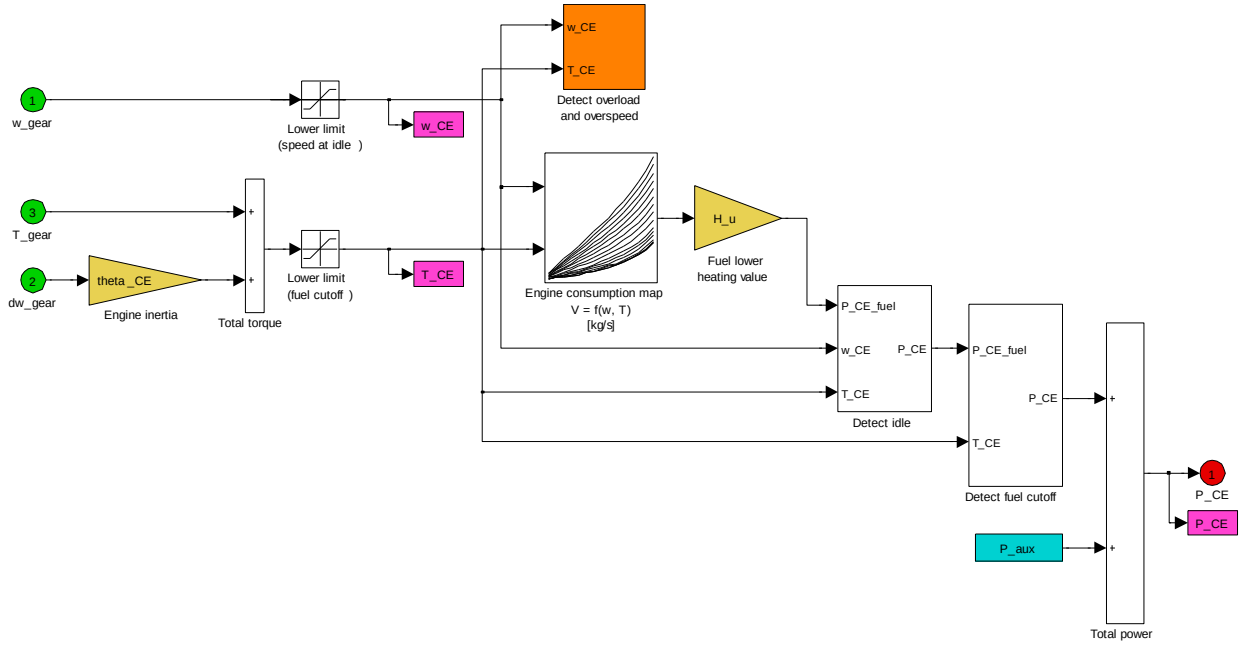

Figure 3.18 Combustion Engine Calculations in QSS [34]

Fuel liter per 100 kilometers is calculated by integrating of fuel mass flow and dividing it by fuel density and distance travelled (Figure 3.19).

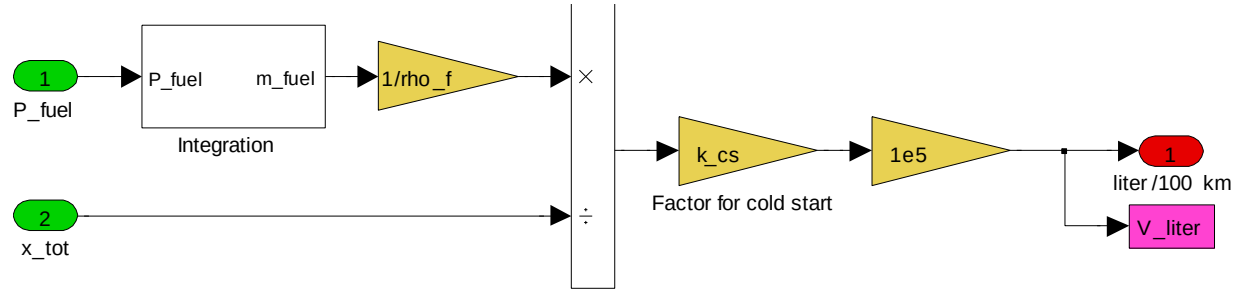

Figure 3.19 Tank Calculations in QSS [34]

3.2.4 Matlab/Simulink and SimDriveline models

Many examples of Matlab [35] software exist in demo models for engine and powertrain modelling. Some of the example models are created in Simulink [36], and others are in a Simulink extended tool called SimDriveline [37, 38] that models the rotating dynamics of a drivetrain. The SimDriveline library contains different types of powertrain components such as transmission, clutch, engine, tire, and vehicle models.

3.2.4.1 A Simulink Engine Model from Matlab

In an internal combustion engine, air continuously flows into the throttle and the intake manifold, but it is discretized by inlet and exhaust valve events. In theory, in a four-cylinder engine, each intake, compression, power, and exhaust stroke can be assumed to happen every 180 degrees of the crankshaft. With this approximation, valve timing occurs at the end of the compression stroke and the beginning of the power stroke at TDC. Figure 3.20 demonstrates such an engine model using a trigger block. For each cylinder, air induction occurs during a 180-degree of a complete cycle (two revolutions of the crankshaft). The intake timings for a four-cylinder, then, can be assumed to be four individual intake processes separated by valve timing events at every 180 degrees of the crankshaft.

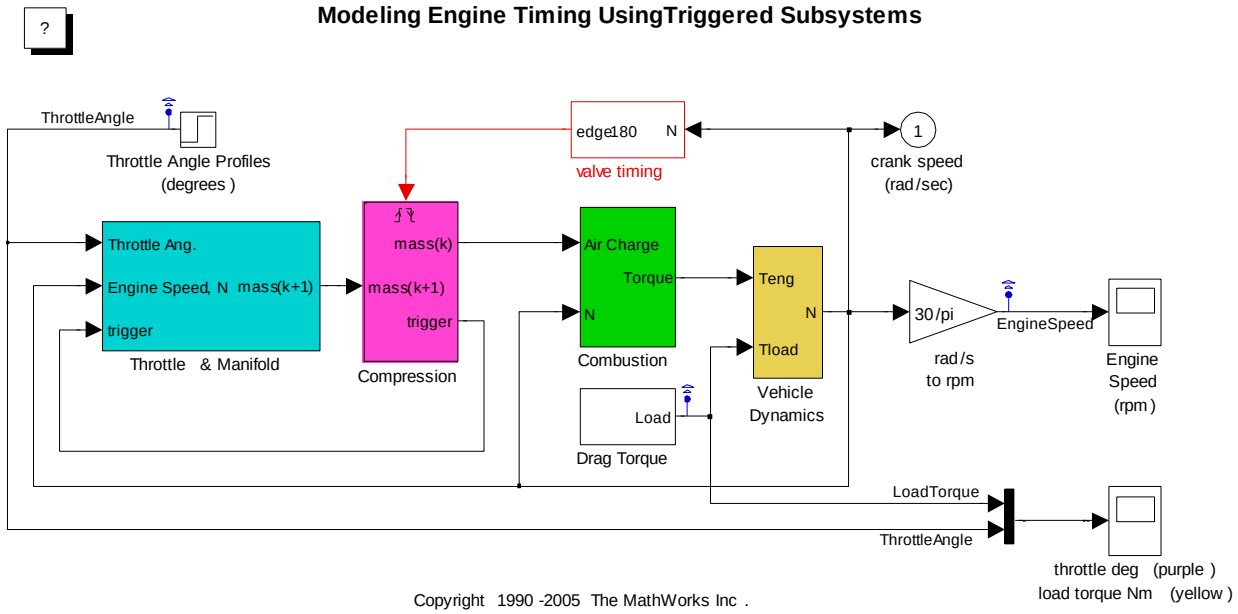

Figure 3.20 An Example from Simulink Models: Top Level of an Engine with a Triggered Subsystem [39]

The Simulink model is based on the Crossley and Cook [20] engine model and the Butts et. al [39] Simulink model. The engine model starts with a throttle valve command. The throttle air mass flow is calculated as a function of the throttle angle and manifold to ambient pressure ratio. As is shown in Figure 3.21, the throttle angle function is approximated by an empirical third-degree polynomial, and pressure function is obtained from the ideal gas flow state in an orifice.

$$\dot{m}_{thr}(\varphi, Pm/P0) = g(\varphi)\, f\left(P_m / P_0\right) \qquad (3.\ 23)$$

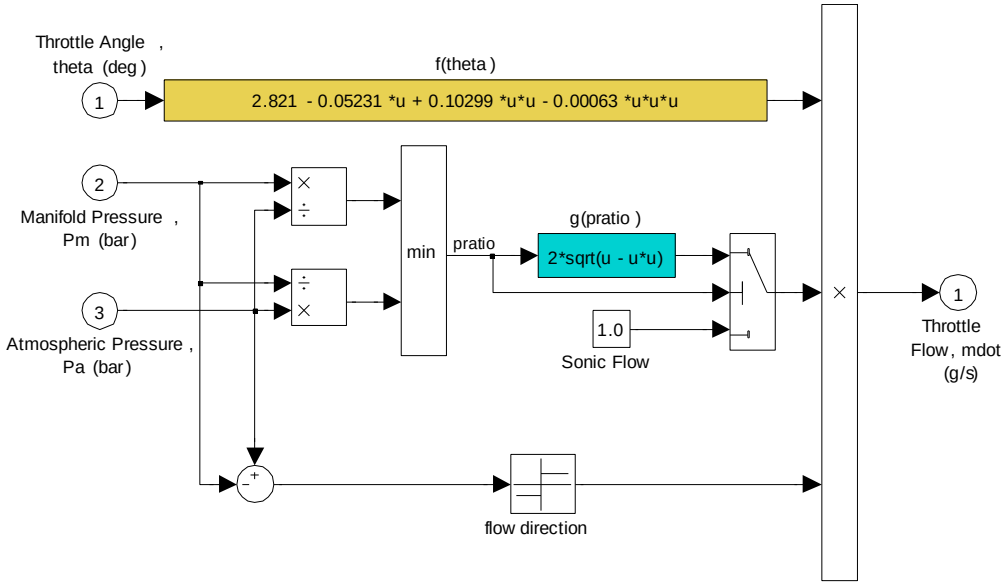

Figure 3.21 An Example from Simulink Models: Throttle Mass Flow Calculations [39]

In an orifice, back flow happens when pressure downstream is higher than that upstream. The block also considers back flow conditions by using a flow direction block. As demonstrated in Figure 3.22, Manifold pressure in the manifold block is calculated from a differential equation as follows:

$$\dot{P}_m = \frac{RT_m}{V_m}\left(\dot{m}_{thr} - \dot{m}_e\right), \tag{3. 24}$$

where P_m, T_m, and V_m are manifold pressure, temperature, and volume, respectively; R is gas constant; and $\dot{m}_e$ is obtained by an empirical equation as a function of manifold pressure and engine speed. The above differential equation obtained from the ideal gas law and will be discussed in more details in chapter 4.

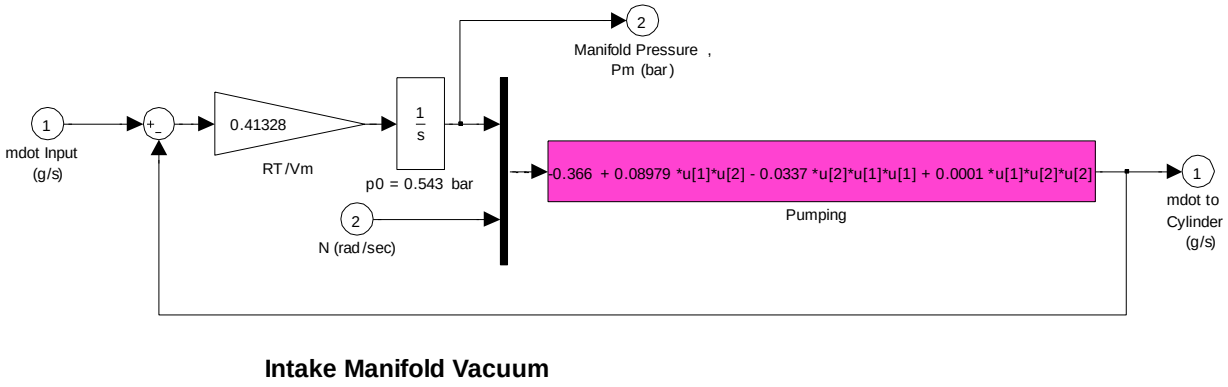

Figure 3.22 An Example from Simulink Models: Intake Manifold Calculations [39]

Engine torque is directly calculated from another empirical equation as a function of spark angle, fuel ratio, engine air mass, and engine speed (Figure 3.23).

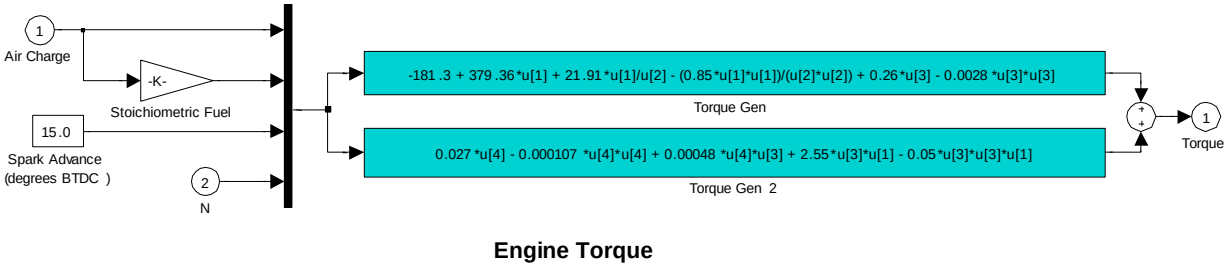

Figure 3.23 An Example from Simulink Models: Engine Torque Calculations [39]

Engine speed is calculated from an equation for engine rotational dynamics as

$$\dot{\omega}_e = \frac{T_e - T_{load}}{J_e} \qquad (3.\ 25)$$

where $\dot{\omega}_e$, T_e, and J_e are engine speed, torque, and rotational moment of inertia, respectively; T_{load} is load torque.

3.2.4.2 A Vehicle SimDriveline Model from Matlab

An example of SimDriveline modelling is presented in Figure 3.24 so called "Full Car Model" [40]. The inputs for the model are gear shifting, throttle command, and brake signals. The output of the system is the vehicle speed. SimDriveline mainly focuses on rotational component modelling. Varieties of transmission models, and advanced tire and vehicle models, are defined and prepared in the library for users. Simulink environment also enables to implement different levels of complexities for controllers. However, the engine model is a very simple model based on a one-dimensional maximum torque lookup table as a function of engine speed.

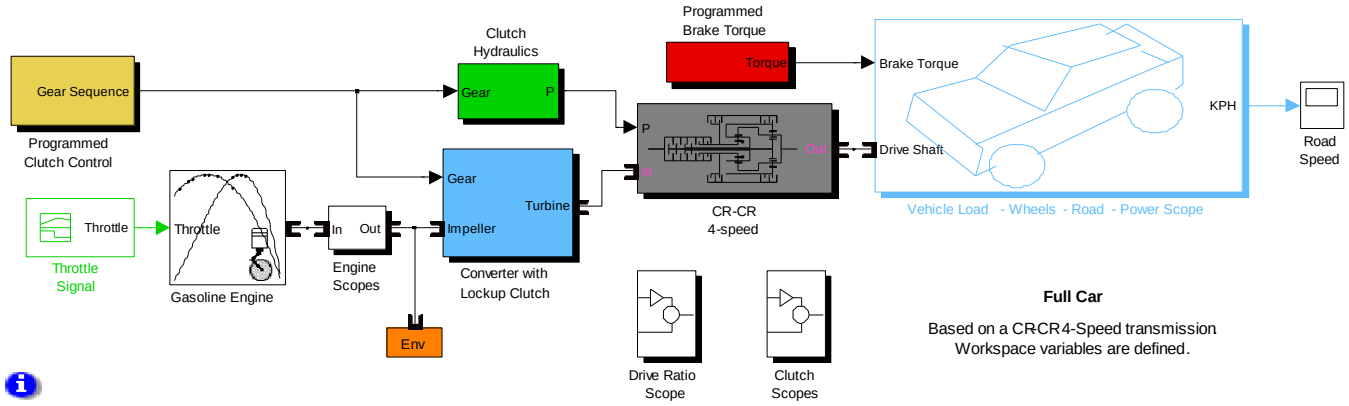

Figure 3.24 An Example from SimDriveline: Top Level of a Full Car Model [40]

The throttle valve opening is a normalized signal varying from 0 to 1, and it is multiplied by the maximum torque value obtained from the lookup table to calculate available torque. Except for signal blocks, components in SimDriveline can be connected to other components by physical connections. The physical connections work as a rotational shaft that can carry torque and speed. Physical connections cannot be connected to signal blocks and vice versa. The intermediate blocks that connect the physical components to the signal blocks are actuators and sensors. Sensors are used to measure shafts speeds and torques, and actuators are used to receive signal

values and convert them into torques or speeds at an output connector that is considered to be a physical shaft. The component right after the engine is the torque converter. A torque converter is a component that couples engine rotational motion to drivetrain rotational components much as a mechanical clutch does. The main difference between a clutch and a torque converter is that in a clutch the engine output shaft, is connected to other powertrain components by pressing the clutch disk together. When the clutch disks are pressed together, friction between the disk surfaces spins the driven shaft. A torque converter has three main parts: the pump impeller, stator, and turbine runner. The pump impeller forces the fluid inside the torque converter to run into the turbine, and the hydrodynamic viscosity causes turbine to rotate. The stator is a part of the casing that directs the fluid from the impeller to the turbine. Figure 3.25 presents the torque converter block calculations.

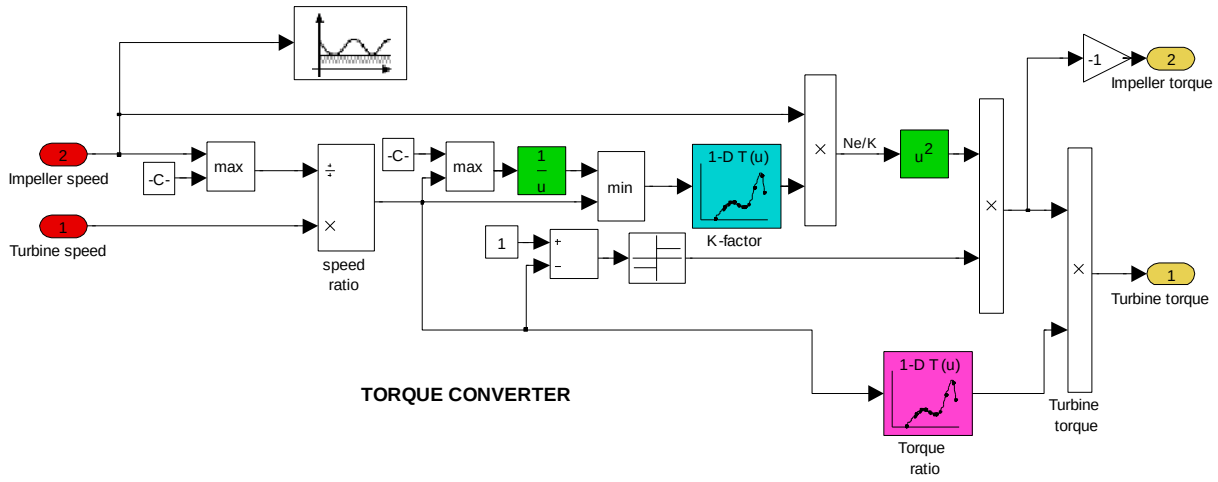

Figure 3.25 An Example from SimDriveline: Torque Converter Block [40]

Speed ratio in a torque converter is calculated as below

$$R_{\omega} = \min\left(\frac{\omega_i}{\omega_t}, \frac{\omega_t}{\omega_i}\right), \tag{3. 26}$$

where R_ω is the speed ratio, ω_i and ω_t are the impeller and the turbine speeds, respectively, and R_ω is used to obtain the torque ratio (R_T), and K-factor from two lookup tables. The impeller and turbine torques are calculated as follows:

$$T_i = \left|1 - \left(\frac{\omega_t}{\omega_i}\right)\right| \cdot \left(\frac{\omega_i}{K}\right)^2 \tag{3. 27}$$

$$T_t = T_i R_t \tag{3. 28}$$

The next powertrain component in the model is the transmission. The transmission as depicted in Figure 3.26 consists of two planetary gears and five clutches.

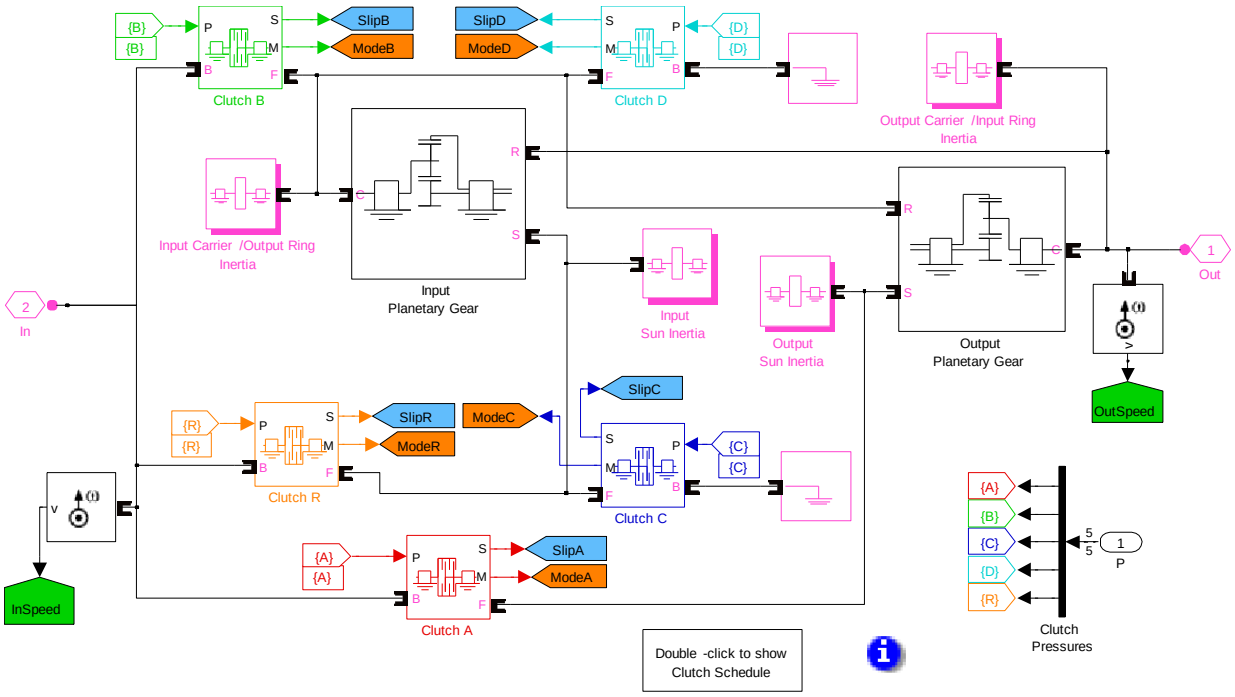

Figure 3.26 An Example from SimDriveline: The Transmission in the Full Car Model [40]

The planetary gear is a set of gears including sun, carrier, planet, and ring gears (Figure 3.27). From the geometry of the planetary gear, the following relations can be obtained:

$$r_c = r_s + r_p \tag{3. 29}$$

$$r_r = r_c + r_p \tag{3. 30}$$

where r_c, r_s, r_p, and r_r are carrier, sun, planet, and ring radii.

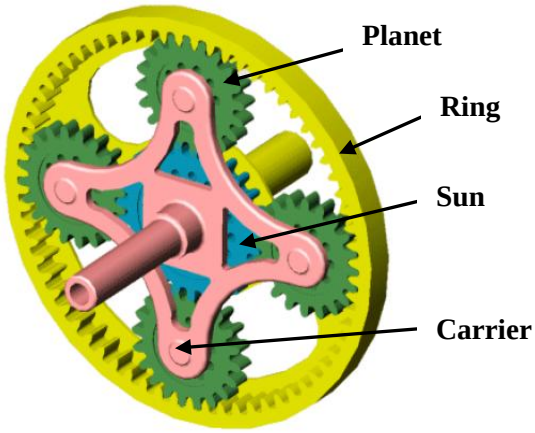

Figure 3.27 A Planetary Gear Set: Ring, Planet, Sun, and Carrier [40]

The kinematics of the gears gives the following relations:

$$r_c \omega_c = r_s \omega_s + r_p \omega_p \tag{3. 31}$$

$$r_r\ \omega_r = r_c\ \omega_c + r_p\ \omega_p \tag{3. 32}$$

.

The gear ratio can be defined as

$$g = \frac{T_{driven}}{T_{drive}} = \frac{\omega_{drive}}{\omega_{driven}} = \frac{N_{driven}}{N_{drive}} = \frac{r_{driven}}{r_{drive}}, \tag{3. 33}$$

where g is the gear ratio, T, ω, r, and N are the gears torque, rotational speed, radius, and number of teeth, respectively. The first planetary gear is the input planetary, and the second planetary gear is called the output planetary. The input planetary gear ratio, g_i, and output planetary gear ratio, g_o, are defined as the ratios of the correspondent ring-to-sun radius or number of teeth ratios.

$$g_i = \left(\frac{r_r}{r_s}\right)_i \tag{3. 34}$$

$$g_o = \left(\frac{r_r}{r_s}\right)_o \tag{3. 35}$$

The two above mentioned planetary gears are used with different combinations of the five clutches in locked and free positions to define the total transmission gear ratio that is the ratio of the output to the input of the transmission. Figure 3.28 shows a shifting gear schedule for a four speed car. The clutches A, B, C, D, R can be set in the locked or the free positions depending on the gear selected. For example, in gear two, the A and C clutches are locked, but B, D, and R clutches are free.

Clutch Schedule

L = Locked
F = Free

Gear	A	B	C	D	R	Ratio
1	L	F	F	L	F	1+go
2	L	F	L	F	F	1+go/(1+gi)
3	L	L	F	F	F	1
4	F	L	L	F	F	gi/(1+gi)
R	F	F	F	L	L	-gi

gi=Input planetary ring /sun gear ratio

go=Output planetary ring /sun gear ratio

Figure 3.28 An Example from SimDriveline: Clutch Schedule [40]

Final drive, wheel, and road calculations are presented in Figure 3.29. Final drive can be considered to be a simple gearbox that changes the gear ratio. By using a torque sensor, the rotational speed at the final drive output (that is, the input of the wheel) is calculated. In the next step, the vehicle longitudinal velocity is obtained by multiplying the wheel rotational speed and radius.

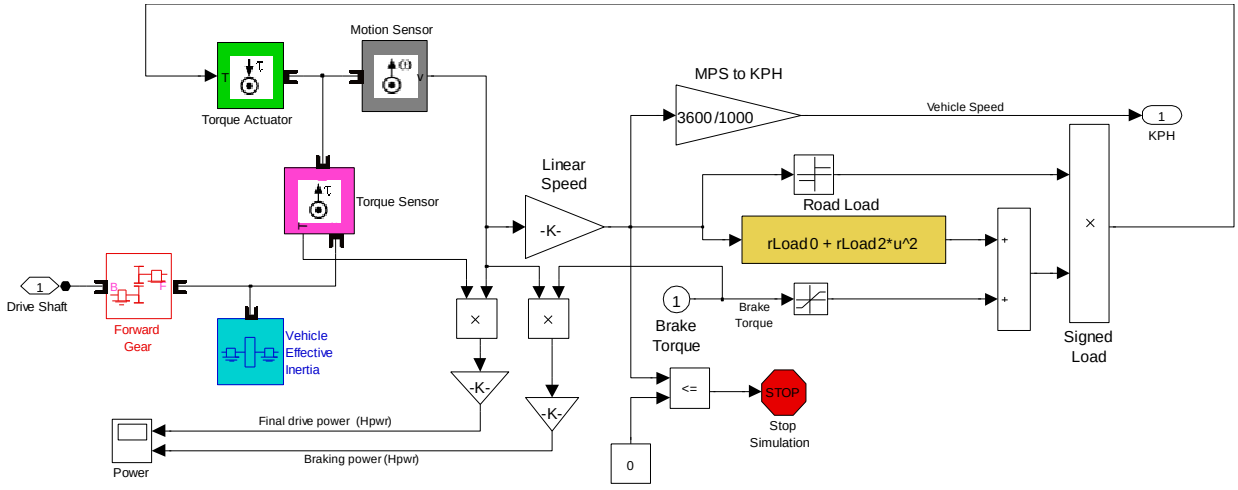

Figure 3.29 An Example from SimDriveline: Final Drive, Wheel, and Road Calculations [40]

The road resistance torque, the sum of the air, roll, and grade resistant forces multiplied by tire radius, is approximated by a second degree polynomial as a function of vehicle speed, and is added to the required torque for braking. The resultant torque is fed back into the system as a negative torque. A more advanced vehicle and wheel models can be found in a SimDriveline example named “Complete Vehicle” [41].

3.2.5 Dymola/Modelica

Modelica is an object-oriented and equation-based modelling language that is suitable for physical modelling. Appendix A provides more details about Modelica. Dymola is one of the simulation tools that uses Modelica language. Different types of domains such as electrical, mechanical, hydraulic, thermal, or control can be modelled in Dymola. It has various libraries of powertrain components, including engine, transmission, drivelines, vehicle dynamics, and other components such as electrical motors, controllers, and hydraulics. Components are demonstrated in the same way as physical models. Each component contains equations inside its model that can be reached and modified easily. Figure 3.30 shows the top level of a conventional vehicle and its components and interfaces [42]. The driver at the top sends acceleration, brake, and gear shifting commands to the driveline components. As shown in Figure 3.31, the engine in this model is a very simple torque generator that is directly proportional to the throttle signal command, and it also includes mounting effects as a component.

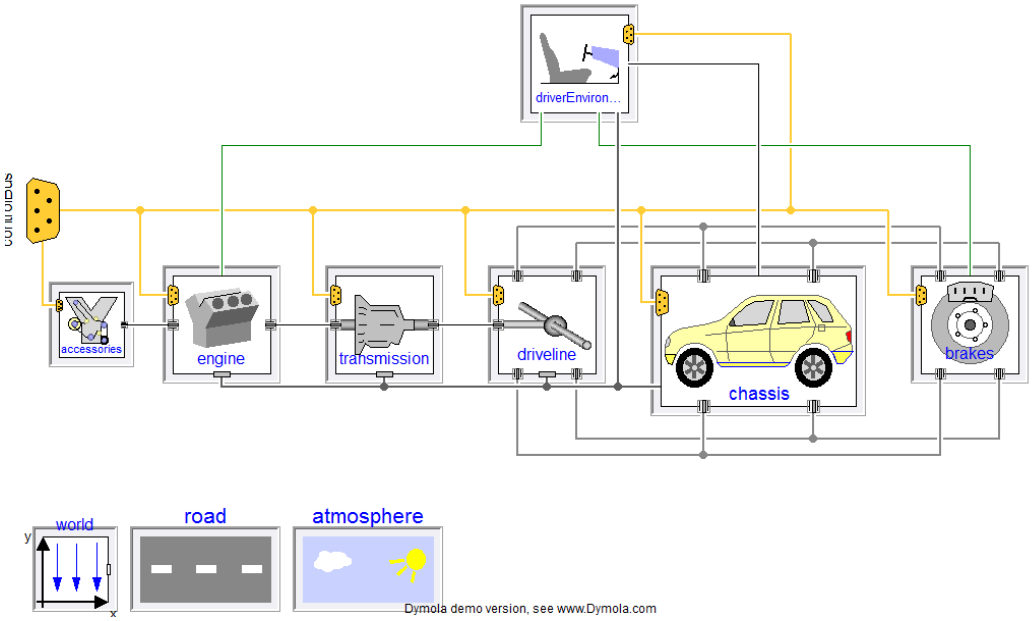

Figure 3.30 Powertrain Components and Interfaces for a Conventional Automatic Vehicle [42]

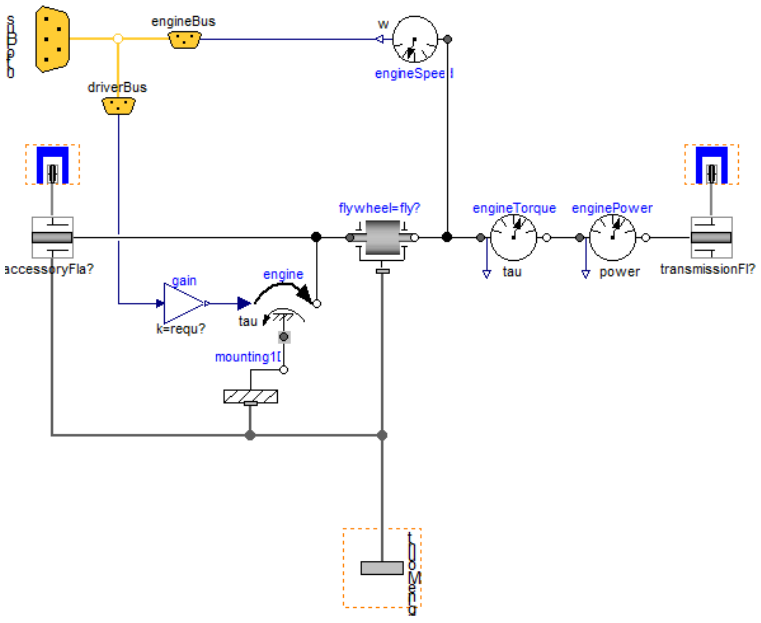

Figure 3.31 Engine Model in a Conventional Automatic Vehicle [42]

An example of a thermal domain is demonstrated in Figure 3.32, with red square shapes as thermal connectors [43]. Heat is transferred from the cylinder gas to the cylinder wall, the piston, the cooling water jacket around the cylinder block, the cylinder head, the vavletrain, the inlet and exhaust valves, and to the lubricant oil. The heat is transferred from the cylinder gas to the engine block in convection form, and from the cylinder block to the coolant water in conductive form of heat transfer.

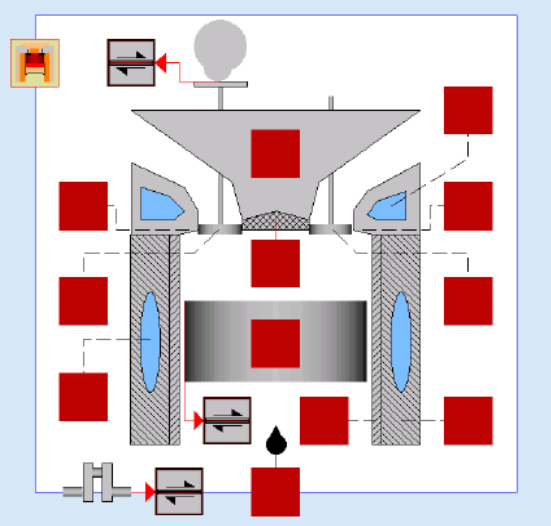

Figure 3.32 Thermal Connectors in a Cylinder [43]

Heat transfer models are generally based on relations for convective heat transfer coefficients found in equations developed by Woschni [44] and Hohenberg [45]. The combustion equation can be defined in different levels of complexity from zero dimensional and single-zone models to complex three dimensional and multi-zone gas burning models. To simulate the mass burning rate in the combustion process, Wiebe [46] or a sigmoid function can be used [47]. The mechanical domain in powertrain modelling generally focuses on one-dimensional dynamics. There are also multi-dimensional mechanical models that are used for vehicle dynamics and engine mounting systems [43]. Most of the engine dynamics such drivetrain rotational dynamics, and piston and valves translational dynamics can be assumed and modelled as 1D dynamics. An example of a one-dimensional rotational dynamics is depicted in Figure 3.33 for a five speed

gear box [48]. A gearbox consists of three planetary wheels and seven switches. The clutches are illustrated as A, B, C, with three D, E, and F brakes, and a freewheel FF. A shifting schedule at the right side of the figure defines which clutches in each gear selection are engaged. A Modelica model of the gearbox is shown in Figure 3.34.

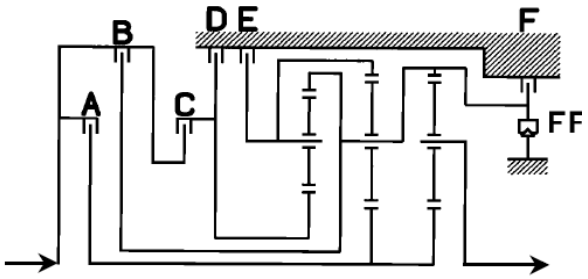

Gear	A	B	C	D	E	F	FF
R			x			x	
N						x	
1	x						x
2	x				x		
3	x			x			
4	x	x					
5		x		x			

Figure 3.33 A Sketch and Shifting Schedule for a Five-Speed Automatic Gearbox [48]

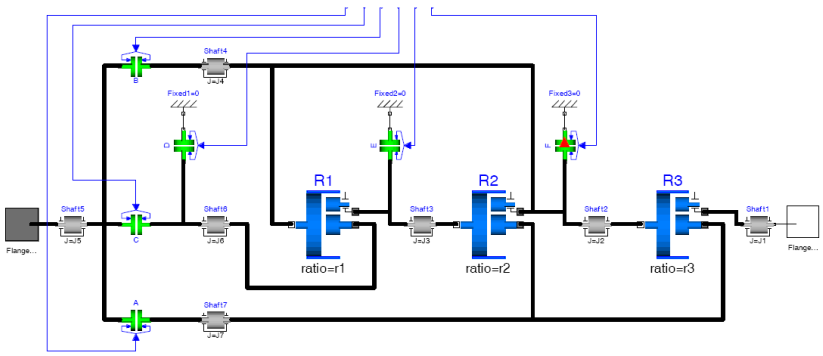

Figure 3.34 Gearbox Simulation for a ZF Automatic Gearbox in Modelica [48]

An example of a multi-domain modelling in Modelica, called “Simple Car”, is shown in Figure 3.35 for a 4-cylinder engine on a dynamometer [49]. The throttle valve is adjusted by a signal command. The manifold inlet and exhaust outlet are connected to ambient air conditions, and both are connected to the engine by gas connections. The throttle valve discharge coefficient is defined by

$$C_d = \sin\left(\frac{\pi}{180}\theta\right) \tag{3. 36}$$

where θ is the throttle angle in degrees.

The engine and the manifold can be considered control volumes in which the air pressure, temperature, and volume inside them are changed based on the ideal gas law. The energy inside the control volume is based on the first law of the thermodynamics. The mass of the gas and the gas species are obtained from the conservation of mass law. Figure 3.36 shows the second level of the engine model with gas connectors for the intake and exhaust valves, and mechanical flange connectors for crankshaft and piston assembly.

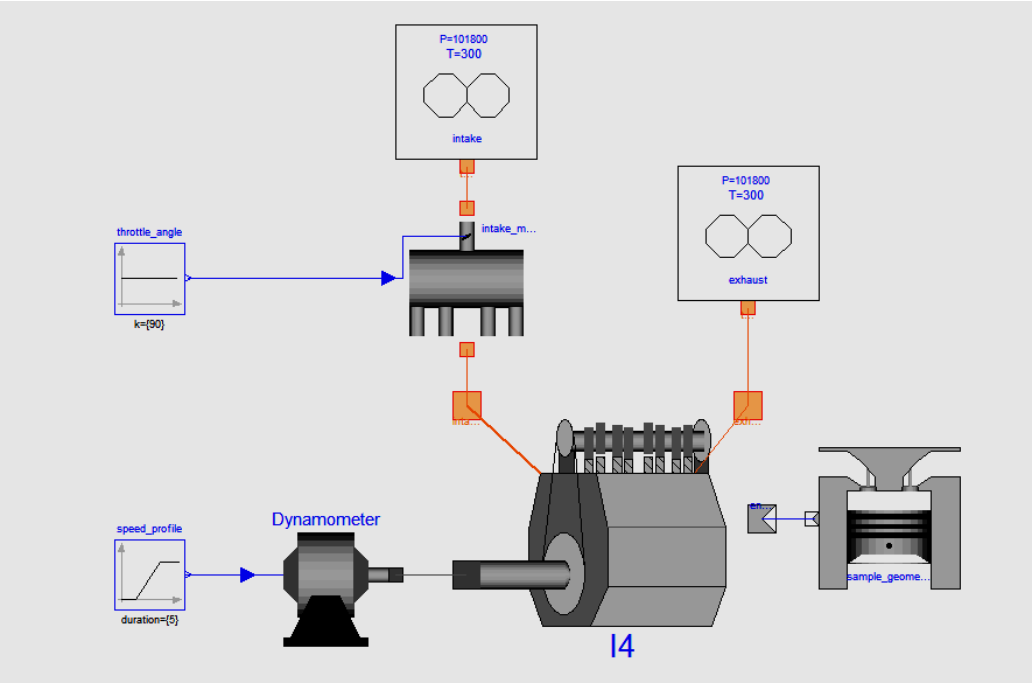

Figure 3.35 Engine on a Dynamometer for a Four Cylinder Engine [49]

The cylinders are identical except than a shift angle in crankshafts by 0, 360, 540, and 180 degrees for cylinder 1 to 4. Intake and exhaust valves opening and closing angles can be set as

parameters. The engine in-cylinder pressure is modelled by a filling and emptying dynamics and relating the pressure changes to the cylinder volume that is changed by the piston movement. Rotating of the camshaft mechanism, cause the valves to open, and to close at predefined angles. The angles between opening and closing of the valves, define the amount of the gas that flows into the cylinder or out of it. The lift profile is calculated from a normalized valve angle function as follows:

$$\begin{cases} L_v = 0 & \theta < \theta_o \; or \; \theta > \theta_c \\ L_v = L_{vMax} \sin\left(\dfrac{\theta - \theta_o}{\theta_c - \theta_o} \cdot \pi \right)^2 & else, \end{cases} \tag{3. 37}$$

where L_v and L_{VMax} are valve lift and maximum valve lifts, and θ_c and θ_o are closed and open valve angles. The valve discharge coefficients are obtained directly from the experimentally obtained maximum discharge coefficient and maximum lift as

$$C_{dV} = \frac{C_{dVMax}}{L_{VMax}} L_v \tag{3. 38}$$

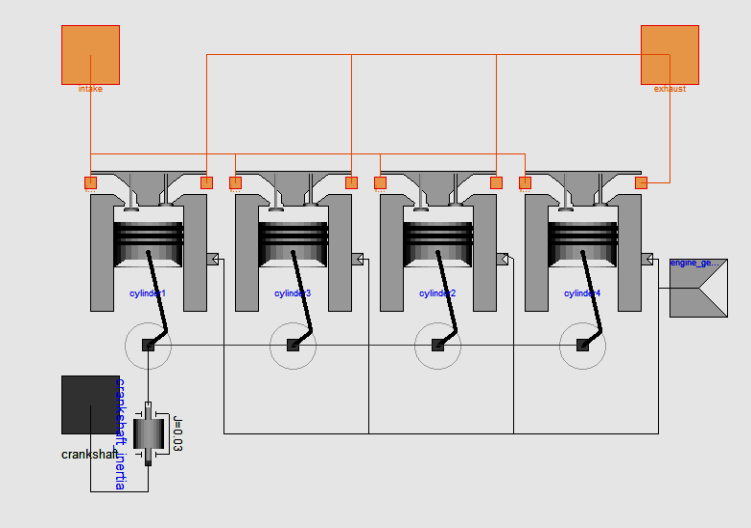

Figure 3.36 Four Cylinders and Their Connections [49]

where C_{dV} and C_{dVMax} are the valve and maximum valve discharge coefficients. The camshaft speed and torque are directionally proportional to the crankshaft speed and torque.

$$2\omega_{cam} = \omega_{crank} \tag{3. 39}$$

$$\tau_{cam} = 2\tau_{crank} \tag{3. 40}$$

The cylinder volume is changed by the up and down piston movement.

$$V = V_c + A_p \cdot l_p \tag{3. 41}$$

where V is the cylinder volume for each position of the crank shaft rotational angle, V_c is the clearance volume, which is the smallest volume of the cylinder when the piston reaches to the TDC, A_p is the piston area, and l_p is the displaced length of the piston in that its minimum is equal to zero at TDC, and its maximum is at BDC and is equal to the stroke $(l_p = S)$. At other angles, l_p is calculated from the following equation:

$$l_p = (l_{conrod} + l_{crank}) - \left(l_{crank}\cos(\theta) + \sqrt{\left({l_{conrod}}^2 - {l_{crank}}^2 \sin(\theta)^2 \right)} \right), \tag{3. 42}$$

where l_{conrod} and l_{crank} are the connecting rod and crank lengths. The force exerted on the piston is calculated from the resultant pressure inside and outside the cylinder.

$$F_p = A_p (P - P_{cc}), \tag{3. 43}$$

where P and P_{cc} are the cylinder and crank case pressures. The generated torque is the torque obtained at the crankshaft.

$$\tau_{crank} = F_p \left(\frac{\sin(\theta) l_{crank} + \cos(\theta)\sin(\theta) {l_{crank}}^2}{\sqrt{{l_{conrod}}^2 - (l_{crank}\sin(\theta))^2}} \right) \tag{3. 44}$$

Combustion is approximated by the following equation

$$\begin{cases} \dot{Q} = 0 & t < t_s \; or \; t > t_e \\ \dot{Q} = -\dot{Q}_{Max} \, Sin\left(\frac{t - t_s}{t_e - t_s} \cdot \pi \right)^2 & else \end{cases} \tag{3. 45}$$

where $\dot{Q}$ and $\dot{Q}_{Max}$ are heat and maximum heat release rates, and t_s, and t_e are start and end times of the combustion period. $\dot{Q}_{Max}$ is obtained by

$$\dot{Q}_{Max} = 2H_l \left(\frac{m_a}{AF + 1} \right) \cdot \frac{\omega_e 180}{\pi (t_e - t_s)}, \tag{3. 46}$$

where H_l is the lower heating value of the fuel, m_a is air mass, and AF is the air-fuel ratio. Figure 3.37 shows a cylinder, its components, and their connections.

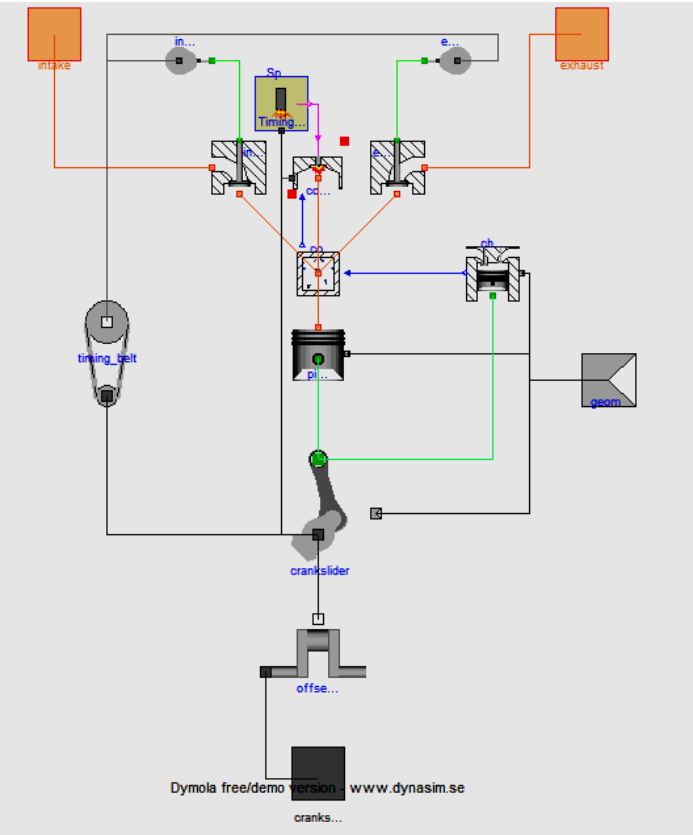

Figure 3.37 The Cylinder Components in "Simple Car" [49]

Chapter 4

Mean Value Engine Model

To estimate intake air flow accurately, one must be able to predict the engine output power and the engine emission. In MVEM, the air mass flow defines the actual air flowing into the engine that is used to calculate the fuel mass flow and air-fuel ratio. The engine output power is proportional to the fuel mass flow rate, and is calculated using the fuel heating value, a constant value for a specified fuel. A throttle valve controls the mass flow, operating as a restriction valve and dictating the amount of air mass flow upstream of the valve. Depending on the engine geometry, manifold pressure, and engine speed, the actual air mass flow into the engine is defined. The difference between the air mass flow into the engine and the air mass flow out of the throttle defines the manifold pressure of a gas state equation. Manifold pressure and engine speed are two main parameters used in most of the mean value engine calculations, including volumetric efficiency, thermal efficiency, throttle air mass flow, and engine load and loss calculations. Engine speed in MVEM is obtained by solving a crankshaft differential equation.

4.1 Model Assumptions

The gas flow system in an actual engine has numerous components. When an engine is working, air is inducted into the air filters at atmospheric pressure and temperature. Air filters reduce the air path, causing the air pressure to drop as it passes through. In the next step, air flows into the throttle body, which is assumed to act as a restriction valve. If an engine is a turbocharged engine, some part of the energy is lost due to the flow resistance in the compressor, intercooler, and turbine. The latter components change the pressure and temperature considerably. The intake manifold has a relatively large volume and can be considered as a gas container. Other pressure

drops occur as flow passes through pipes and connections between components. Intake and exhaust valves, catalytic converters, and mufflers also cause pressure drops. Because such components are not isolated completely from the environment, they lose heat to the environment, changing their temperature. For this model, the following assumptions and simplifications are made:

- ***The air filter effect is neglected***

By this assumption pressure drop in the air filter is neglected; therefore, the pressure and temperature in the throttle inlet are equal to the atmospheric pressure and temperature.

- ***The engine is naturally-aspirated***

In naturally-aspirated engines, there is no turbocharger, thus eliminating compressor, intercooler, and turbine effects from the model. The pressure and the temperature at the output of the throttle body will be the same as those at the intake manifold inlet.

- ***The intake manifold system is isothermal***

The manifold input and output temperatures considered to be constant. This assumption neglects the temperature transition in the manifold. If considerable hot gas from the exhaust system is mixed with fresh air in the manifold, this approximation does not match with the actual temperature in the manifold. More details are given in the discussion of adiabatic and isothermal systems in Section 4.2.2.1in this chapter.

- ***Minor component effects are not modelled***

Intake and exhaust valves, pipes, connections, and the muffler are not modeled individually. Their effects can be lumped together inside volumetric efficiency. The engine pumping effect is modeled separately in engine model.

- ***The system is continuous***

Manifold and engine gas systems can be best described by filling and emptying dynamics. The gas induction process should be considered as a discrete process rather than continuous. As the intake and exhaust valves open in every two revolutions of the crankshaft, a part of air stays in the manifold and a part of it is trapped in cylinders and is cut off from the upstream and downstream flow. In an MVEM, the gas system is approximated by a continuous system. Increasing the number of cylinders makes this approximation more realistic.

4.2 Components of the Engine Model

Three main components affect an MVEM engine and are discussed in this chapter:

- Throttle Body
- Intake Manifold
- Engine

The main dynamics of the model that are discussed in this chapter are

- Air Dynamics
- Fuel Dynamics
- Rotational Dynamics

4.2.1 Throttle Body

A throttle body is a part of engine system that controls the air flow into the engine. Air flow is regulated by a throttle valve, usually an elliptical plate with a pin located at the centre, enabling the valve to rotate around it. When a gas pedal is released, the valve is closed. The plate is always left open in angles between 5 to 10 degrees from the completely closed position to prevent it from binding. In an idle working condition, flow is directed through a bypass path valve. Traditional throttle bodies use a mechanical linkage that transfers pedal input commands to the throttle valve. In newer types, called drive-by-wire, the pedal position is translated to an

electrical signal by a sensor. The electrical control unit (ECU) receives this signal and actuates an electrical motor connected to the valve axis. The drive-by-wire throttle type is more precise than mechanical linkages in terms of positioning of the valve and drivability[1].

Throttle mass flow rate is mainly a function of the discharge coefficient, throttle area, and pressure ratio.

$$\dot{m}_{thr} = C_d \, A_{thr} \, f\left(P_m / P_0\right) \tag{4. 1}$$

where C_d is the discharge coefficient; A_{thr} is the throttle area, P_m is manifold pressure, and P_0 is ambient pressure.

4.2.1.1 Throttle Discharge Coefficient

The throttle discharge coefficient in a restriction is defined as a ratio of the actual mass flow downstream of the restriction to the ideal mass flow at that point. C_d is usually described as a function of pressure and geometry of the restriction. In a throttle valve, the effective area is directly related to the throttle angle. Therefore, C_d can be written as the contributions of throttle angle and pressure

$$C_d(\varphi, P_m / P_0) = C_d(\varphi) C_d(P_m / P_0) \tag{4. 2}$$

Normalizing the geometry and pressure variables provides a map for C_d. Figure 4.1 shows an example of a map for a butterfly valve [50].

[1] Drivability can be defined as the quality of operating of an engine or vehicle driving condition in general.

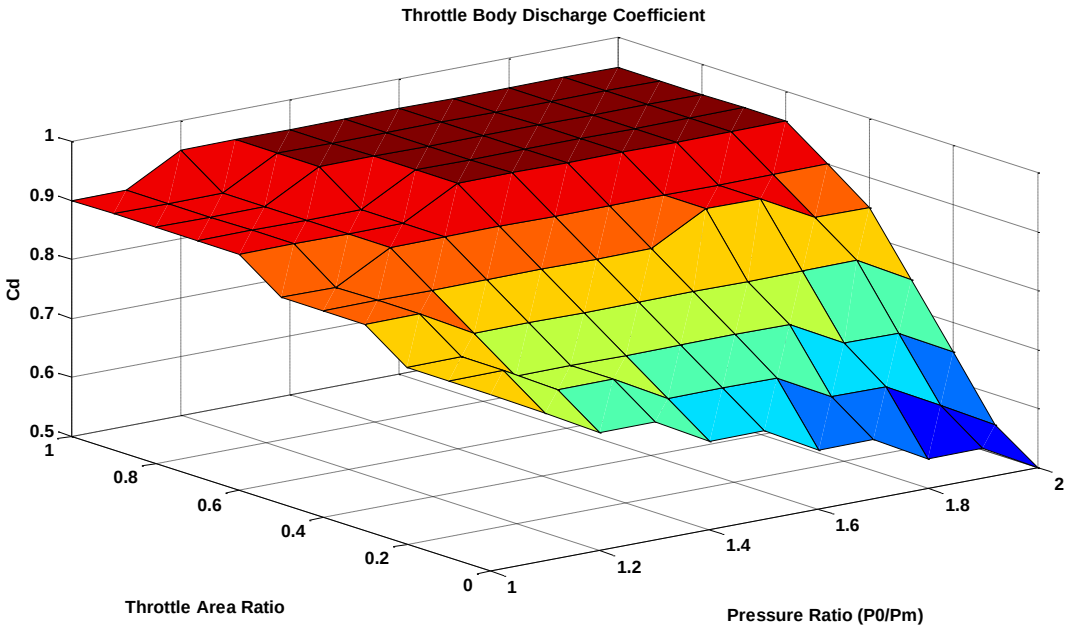

Figure 4.1 Discharge Coefficient in a Butterfly Valve [50]

4.2.1.2 Throttle Area Models

The throttle-effective area is the projected area of the throttle opening in the flow direction. A_{thr} is the function of the throttle bore, D. The throttle pin diameter is d and throttle angle is φ. Harington and Bolt [22] introduced the following equation for A_{thr}

$$A_{thr} = \frac{\pi D^2}{4}\left(1-\frac{\cos\varphi}{\cos\varphi_o}\right)+\frac{d}{2\cos\varphi}\left(D^2\cos^2\varphi-d^2\cos^2\varphi_o\right)^{1/2}+\frac{D^2\cos\varphi}{2\cos\varphi_o}\arcsin\left(\frac{a\cos\varphi_o}{\cos\varphi}\right) \\ -\frac{d}{2}\sqrt{D^2-d^2}+\frac{D^2}{2}\arcsin(a) \qquad (4.3)$$

where $a=\frac{d}{D}$ and φ_o is the throttle angle at closed position. Moskwa [23] presented another equation for A_{thr}:

$$A_{thr} = \frac{-dD}{2}\left[1-a^2\right]^{1/2} + \frac{dD}{2}\left[1-\left(a\frac{\cos\varphi_\circ}{\cos\varphi}\right)^2\right]^{1/2} + \frac{D^2}{2}\arcsin\left[\left(1-a^2\right)^{1/2}\right] - \frac{D^2}{2}\frac{\cos\varphi}{\cos\varphi_\circ}\arcsin\left\{\left[1-\left(a\frac{\cos\varphi_\circ}{\cos\varphi}\right)^2\right]^{1/2}\right\} \quad (4.4)$$

As the throttle angle increases, at a specified angle, A_{thr} reaches to its maximum, and is no longer affected by increases of the throttle angle. This angle is defined as

$$\varphi \geq \arccos\left(\left(\frac{d}{D}\right)\cos\left(\varphi_\circ\right)\right) - \varphi_\circ \quad (4.5)$$

In this condition, A_{thr} is calculated from the following equation

$$A_{thr} = \frac{D^2}{2}\arcsin\left[\left(1-(a)^2\right)^{1/2}\right] - \frac{dD}{2}\left(\left(1-a^2\right)\right)^{1/2} \quad (4.6)$$

Both models use a correction for small throttle angles by introducing $\varphi_\circ^*$ as

$$\varphi_\circ^* = 0.91\varphi_\circ - 2.59 \quad (4.7)$$

Figure 4.2 compares the two models as a function of throttle angle. The effects of throttle pin diameters and bore diameters are shown in Figure 4.3 and Figure 4.4.

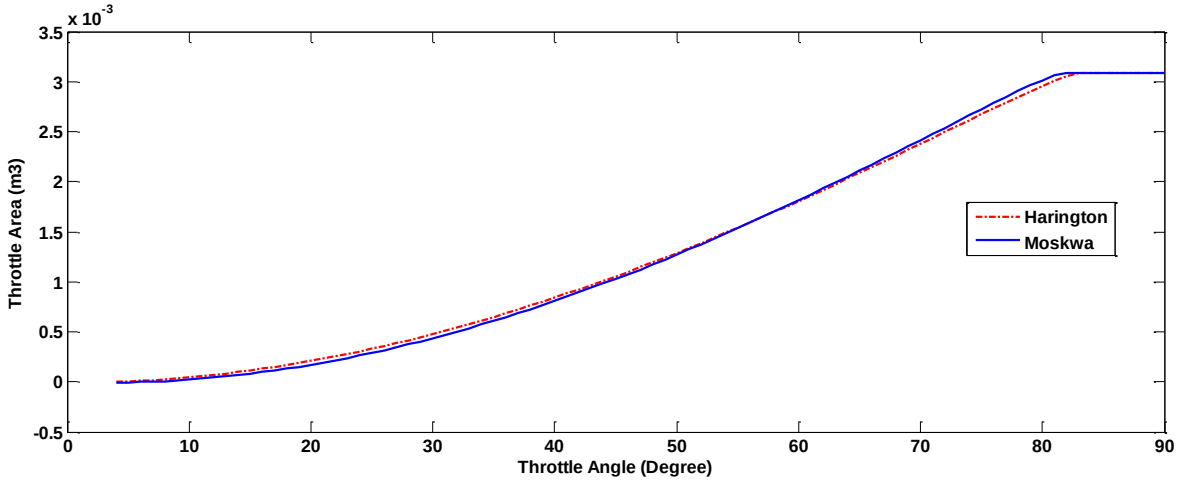

Figure 4.2 Comparing Throttle Effective Areas of Two Models

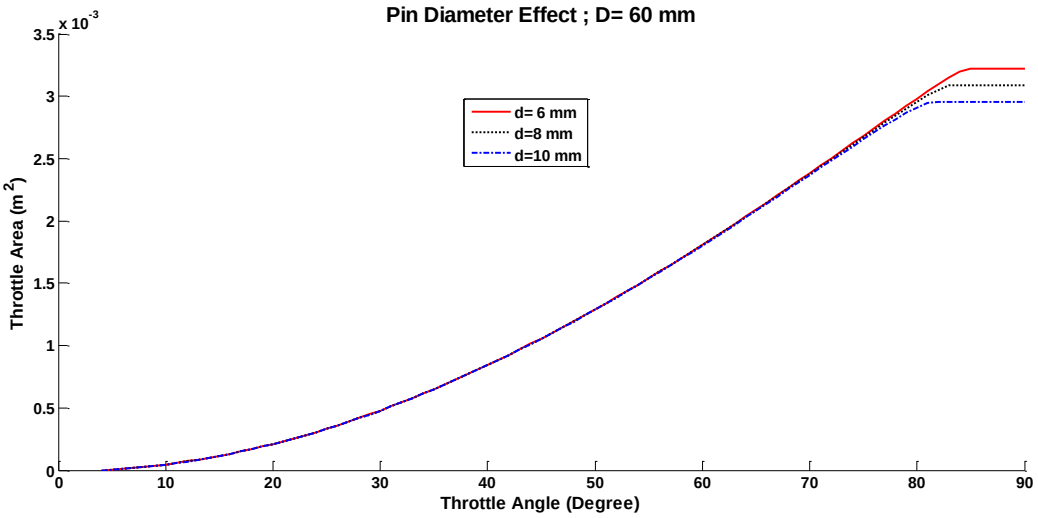

Figure 4.3 Effect of Throttle Pin Diameter on Throttle Area

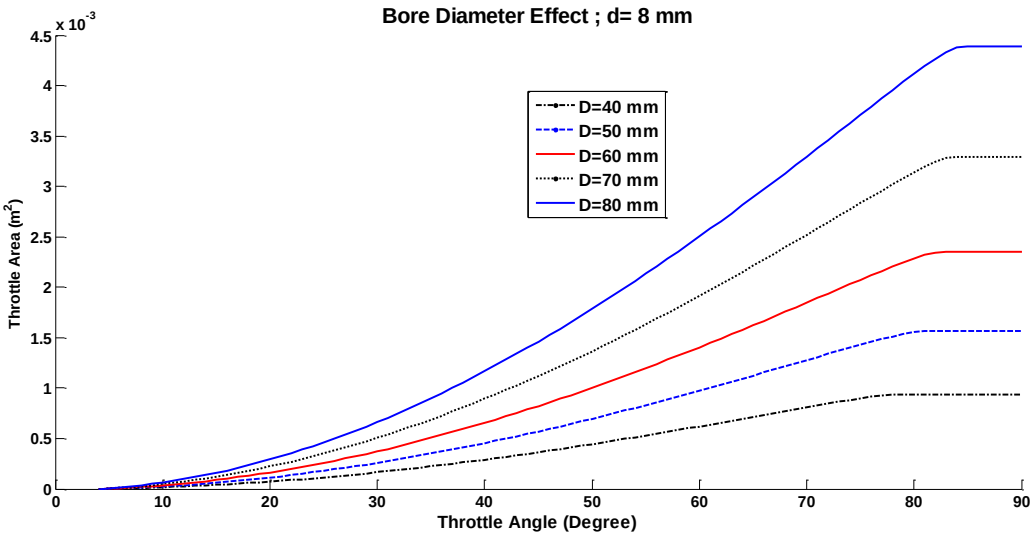

Figure 4.4 Effect of Bore Diameter on throttle Area

4.2.1.3 Pressure Function Models

Based on conservation of mass law for any restrictions such as a nozzle or a throttle valve, if pressure drops on one side of the restriction, velocity increases in the smaller area. By decreasing pressure more, the velocity at a smaller area reaches sonic velocity, and its maximum flow rate. This flow condition is called choked or supersonic flow. In a choked condition, further decreasing pressure will not affect the mass flow. For air, a choked condition occurs at $\frac{P_m}{P_0} = 0.528$.

A standard form of pressure equation for choked and non-choked conditions in a normalized form can be written as

$$f(P_m/P_0)=\begin{cases}\left(\left(\frac{2}{\gamma-1}\right)\left(\frac{\gamma+1}{2}\right)^{\left(\frac{\gamma+1}{\gamma-1}\right)}\right)^{1/2}\left(\frac{P_m}{P_0}\right)^{1/\gamma}\left[1-\left(\frac{P_m}{P_0}\right)^{(\gamma-1)/\gamma}\right]^{1/2} & if \quad \frac{P_m}{P_0}>\left[\frac{2}{\gamma+1}\right]^{\gamma/\gamma-1}\\ 1 & if \quad \frac{P_m}{P_0}\le\left[\frac{2}{\gamma+1}\right]^{\gamma/\gamma-1}\end{cases} \tag{4. 8}$$

where γ is the specific heat ratio. For air γ=1.4. An example of the above equation can be found in [23]. Equation (4.8) is sometimes approximated by the following equation in the literature (for example, Crossley and Cook [20]).

$$f(P_m/P_0)=\begin{cases}2\sqrt{\frac{P_m}{P_0}-\left(\frac{P_m}{P_0}\right)^2} & for\ P_m>\frac{P_o}{2}\\ 1 & for\ P_m\le\frac{P_o}{2}\end{cases} \tag{4. 9}$$

Hendricks [25] introduced another equation for pressure function

$$f(P_m/P_0)=\begin{cases}\frac{1}{p_n}\sqrt{(P_m/P_0)^{p_1}-(P_m/P_0)^{p_2}} & , if \quad (P_m/P_0)\ge p_c\\ 1 & , if \quad (P_m/P_0)<p_c\end{cases} \tag{4. 10}$$

where $p_c=\left(\frac{p_1}{p_2}\right)^{(1/(p_2-p_1))}$, $p_n=\sqrt{{p_c}^{p_1}-{p_c}^{p_2}}$, p_1=0.4404, p_2=2.3143, and p_c=0.4125.

Another equation for pressure function is given by Cho and Hedrick [51]

$$f(P_m/P_0)=1-\exp\left[9\cdot(P_m/P_0)-1\right] \tag{4. 11}$$

All the above mentioned pressure models are compared in Figure 4.5.

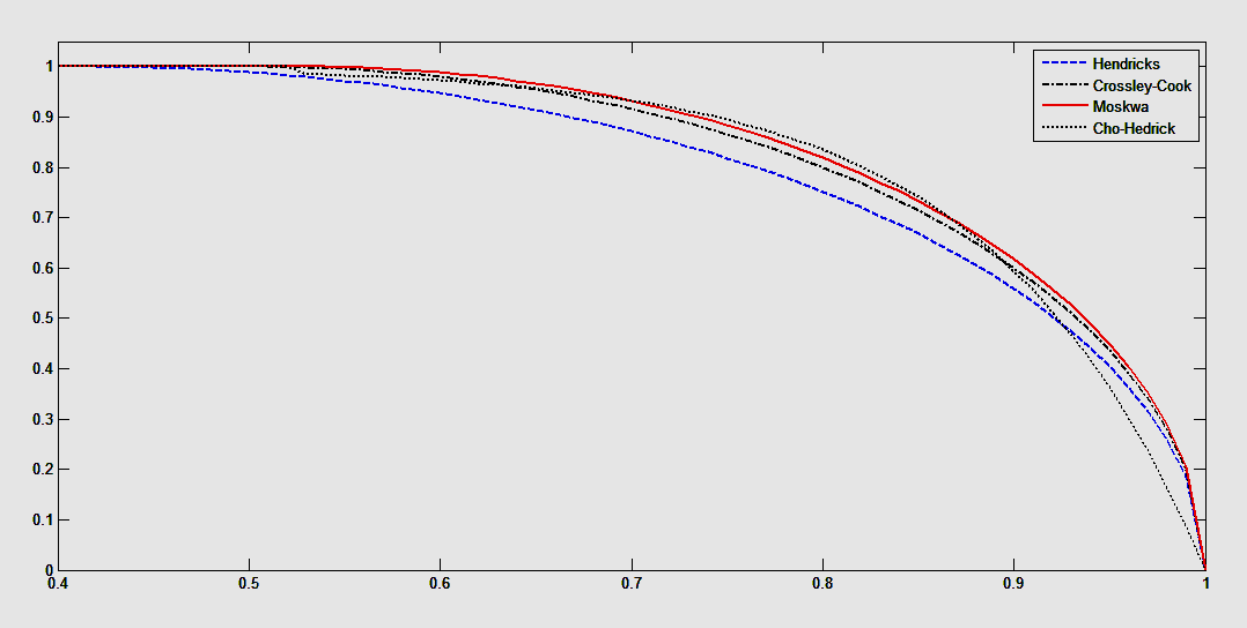

Figure 4.5 Pressure Functions Comparison

Comparing Hendricks, Crossley-Cook, and Cho-Hedrick model with the standard pressure model (Moskwa) reveals that Crossley-Cook model fits very well in the entire range of the pressure. Cho-Hedrick model's error values for pressures lower than 0.9 bar are very low, but the error increases beyond 0.9 bar. The Hendricks model has the highest error relative to the standard model.

4.2.1.4 Throttle Angle Functions

Throttle area, as discussed before, is a function of throttle geometry (D and d) and throttle angle. Therefore, in a specified engine A_{thr} is only a function of throttle angle. Instead of being involving in A_{thr} calculations, throttle angle function can be obtained directly by combining equations (4.1) and (4.2). Mass flow is then obtained by normalizing the angle function:

$$\dot{m}_{thr}(\varphi, Pm/P0) = Cd\ .A_{thr}(\varphi)\ f\left(P_m / P_0\right) = \dot{M}_{thr}\ g(\varphi)\ f\left(P_m / P_0\right) \quad (4.\ 12)$$

where $g(\varphi)$ is the throttle angle function, and $\dot{M}_{thr}$ is the maximum mass flow rate at throttle. $\dot{M}_{thr}$ is characteristic of throttle body geometry obtained at a fully opened throttle angle and choked flow conditions. Two types of throttle angle functions that are widely used in the literature are cosine and polynomial functions. As an example of cosine function, Harington and Bolt [22] introduced a relatively simple function for $g(\varphi)$:

$$g(\varphi) = 1 - \cos(\varphi) \quad (4.\ 13)$$

Hendricks et al. [52] give a slightly different equation as

$$g(\varphi) = 1 - \cos(\varphi) - \frac{\varphi_1^2}{2!} \quad (4.\ 14)$$

where φ_1=0.825 . Reference [25] introduces the following equation

$$g(\varphi) = 1 - \varphi_2 \cos(\varphi) + \varphi_3 \cos^2(\varphi) \quad (4.\ 15)$$

where φ_2=1.4073 and φ_3=0.4087. Cho and Hedrick [53] used a piece-wise function

$$g(\varphi) = \begin{cases} 1 - \cos(\varphi_4(\varphi) - \varphi_5) & for\, \varphi \le \varphi_6 \\ 1 & for\, \varphi > \varphi_6 \end{cases}, \quad (4.16)$$

where φ_4=1.14459, φ_5=1.06, φ_6=79.46.

Another type of equation for throttle angle function involves polynomial functions. Powell and Cook [54], introduced a second degree polynomial function for a 1.26" throttle bore as

$$g(\varphi) = \varphi_7 + \varphi_8 \cdot \varphi + \varphi_9 \cdot \varphi^2 , \quad (4.17)$$

where φ_7=2, φ_8=1.8, and φ_9=0.2. Crossley and Cook [20] used a third-degree polynomial

$$g(\varphi) = \varphi_{10} + \varphi_{11} \cdot \varphi + \varphi_{12} \cdot \varphi^2 + \varphi_{13} \cdot \varphi^3 \quad (4.18)$$

where φ_{10}=2.821, φ_{11}= -0.05231, φ_{12}= 0.10299, φ_{13}=0.00063.

Notice that the latter models are not normalized, and throttle angle functions in both models include the lump effect of the discharge coefficient and normalized throttle angle.

In this work by using a four-stroke test engine data, a third-degree cosine polynomial as follows is found to be the best fit for the throttle air mass flow calculations.

$$g(\varphi) = \varphi_{14} + \varphi_{15}\cos(\varphi) + \varphi_{16}\cos^2(\varphi) + \varphi_{17}\cos^3(\varphi) \quad (4.19)$$

φ_{14}= -1.147, φ_{15}=3.667, φ_{16}=-3.594, and φ_{17}= 1.093. Experimental data and third-degree polynomial are depicted in Figure 4.6.

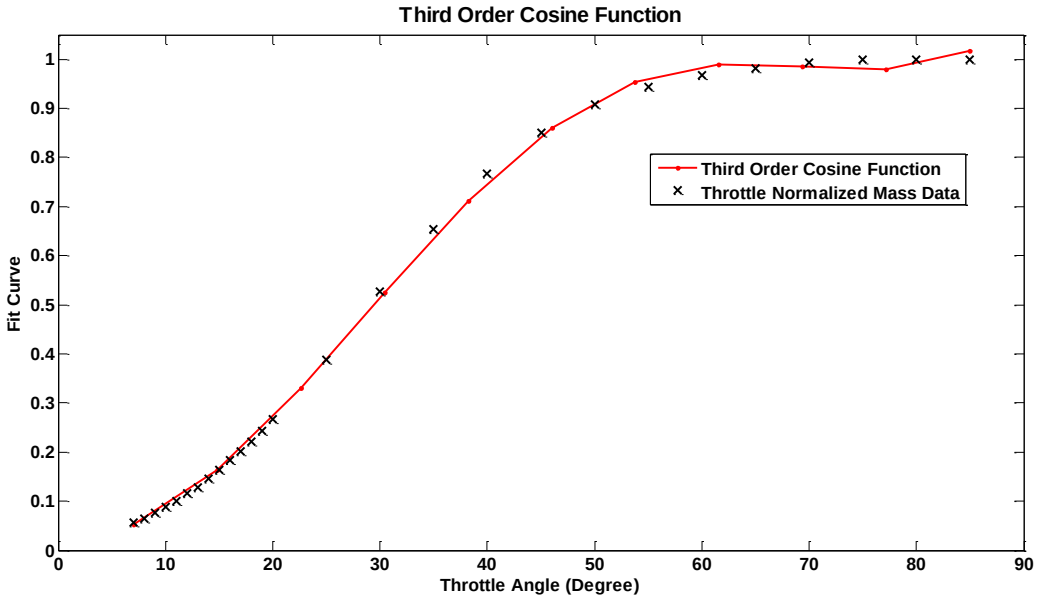

Figure 4.6 The Third- Degree-Cosine Function and Experimental Data

Cosine functions are usually a better fit to the throttle angle data. Polynomial data, especially with higher degrees, diverge very fast out of the data range.

4.2.2 Intake Manifold Models

The intake manifold is a part of an engine system that directs a uniform flow of air to the intake ports. An intake manifold can be considered a control volume for containing inflow coming from the throttle and outflow leaving the engine. Mass and energy conservation laws can be applied to the system. According to the conservation of mass law, the mass change in the system is equal to the net flow into and out of the system.

$$\frac{d m_{cv}}{dt} = \sum_i \dot{m}_i - \sum_o \dot{m}_o \qquad (4.\ 20)$$

where $\frac{dm_{cv}}{dt}$ is the intake mass changes, $\sum_i \dot{m}_i$ are inflows, and $\sum_o \dot{m}_o$ are outflows.

If there is only one inflow from the throttle, and one outflow to the engine, a continuity equation can be written as

$$\frac{dm_{cv}}{dt} = \dot{m}_{thr} - \dot{m}_e \tag{4. 21}$$

If the inflow mass from an EGR valve is considered, above equation becomes

$$\frac{dm_{cv}}{dt} = \dot{m}_{thr} + \dot{m}_{EGR} - \dot{m}_e \tag{4. 22}$$

Based on conservation of energy law, the time rate changes of energy inside a control volume are equal to the net heat transfer into the system minus the work done by the system plus the time rates of the energy flowing into and out of the control volume [55].

$$\frac{dE_{cv}}{dt} = \dot{Q}_{cv} - \dot{W}_{cv} + \sum_i \dot{m}_i \left(h_i + \frac{V_i^2}{2} + gZ_i \right) - \sum_e \dot{m}_e \left(h_e + \frac{V_e^2}{2} + gZ_e \right), \tag{4. 23}$$

where $\frac{dE_{cv}}{dt}$, $\dot{Q}_{cv}$, and $\dot{W}_{cv}$ are time rate of control volume energy changes, net control volume heat transfer, and shaft or any other works done by changing control volume; h, V, and Z are the entering and existing flow enthalpy, velocity, and elevation of the system; g is acceleration gravity. In an intake manifold there is no shaft work, and the volume of the intake is fixed, so the $\dot{W}_{cv}$ term become zero. Velocities and elevations of the fluid entering and existing the intake manifold are considered to be equal. Using the above assumptions, the conservation of energy equation is simplified into the following equation:

$$\frac{dE_{cv}}{dt} = \dot{Q}_{cv} + \sum_i \dot{m}_i (h_i) - \sum_e \dot{m}_e (h_e) \tag{4. 24}$$

Energy changes are in the gas flow mainly due to the internal changes

$$\frac{dE_{cv}}{dt} = \frac{dU_{cv}}{dt} = \frac{d(m_{cv} u_{cv})}{dt} = \frac{m_{cv} d(u_{cv})}{dt} \tag{4. 25}$$

Where u_{cv} is the internal energy of control volume per unit mass. Air flow in an intake manifold is considered to be an ideal gas. By this assumption, internal energy and enthalpy equations are simply proportional to the gas temperature, and the equations become simpler. According to the ideal gas law,

$$PV = mRT\ , \tag{4. 26}$$

where, P, V, m, and T are gas pressure, volume, mass, and temperature, and R is the gas constant equal to $8.314 \frac{J}{K\,mol}$. Volume of the manifold has a constant value. By differentiating the ideal gas equation relative to the time following equation can be obtained:

$$\dot{P}V = RT \frac{dm_{cv}}{dt} + m_{cv} R\dot{T} \tag{4. 27}$$

Internal and enthalpy can be written as

$$u = c_v T \tag{4. 28}$$

$$h = c_p T \tag{4. 29}$$

where c_p and c_v are specific heat ratios at constant pressure and temperature. Substituting equations (4.22) and (4.26) for (4.29) in the equation (4.24) provides the following equation in general form for an intake manifold equipped with EGR valve [56].

$$\dot{P}_m = \frac{R\gamma}{V_m}\left[\dot{m}_{thr}T_{thr} + \dot{m}_{EGR}T_{EGR} - \dot{m}_e T_m + \frac{\dot{q}_m}{c_p T_m}\right] \tag{4. 30}$$

where $\dot{m}_{thr}$, $\dot{m}_{EGR}$, and $\dot{m}_e$ are throttle, EGR, and engine air mass flow rates; γ is a specific heat ratio; T_{thr}, T_{EGR}, and T_m are throttle, EGR, and manifold temperatures; V_m is the manifold volume. Similarly another equation can be obtained for the manifold temperature:

$$\dot{T}_m = \frac{RT_m}{P_m V_m}\left[\dot{m}_{thr}(\gamma T_{thr} - T_m) + \dot{m}_{EGR}(\gamma T_{EGR} - T_m) - \dot{m}_e(\gamma - 1)T_m + \frac{\dot{q}_m}{c_v}\right] \tag{4. 31}$$

The two differential equations above are usually simplified by considering the process to involve adiabatic or isothermal conditions.

4.2.2.1 Adiabatic and Isothermal Systems

In a thermodynamic system, adiabatic system is one that is isolated from its environment and so no heat is transferred from the system to the outside, or from outside to the inside of the system. Adiabatic assumption can be used for large manifolds. In adiabatic systems, the temperature of the flow entering into the manifold does not affect the intake manifold temperature, and temperature exiting the system is assumed to be equal to the control volume temperature, i.e., the intake manifold. Isothermal process is one for which temperature is constant for flow entering, exiting, and inside the system. Isothermal assumptions are used when control volume is small in

size, so the inflow temperature is considered to be the same as the temperature of the control volume. Using these assumptions, Equations (4.29) and (4.30) can be simplified to

Adiabatic Manifold: i.e., $\dot{q}_m = 0$

$$\dot{P} = \frac{R\gamma}{V_m}\left[\dot{m}_{thr}\,T_{thr} + \dot{m}_{EGR}\,T_{EGR} - \dot{m}_e\,T_m\right] \tag{4. 32}$$

$$\dot{T}_m = \frac{RT_m}{P_m V_m}\left[\dot{m}_{thr}\left(\gamma T_{thr} - T_m\right) + \dot{m}_{EGR}\left(\gamma T_{EGR} - T_m\right) - \dot{m}_e\left(\gamma - 1\right)T_m\right] \tag{4. 33}$$

Isothermal Manifold: i.e., $\dot{T}_m = 0$ and $\dot{q}_m = 0$

$$\dot{P} = \frac{RT_m}{V_m}\left[\dot{m}_{thr} + \dot{m}_{EGR} - \dot{m}_e\right] \tag{4. 34}$$

$$T_{thr} = T_m \tag{4. 35}$$

In this work, an isothermal manifold assumption is used for engine modelling. By this assumption for the conditions that an EGR valve does not exist or is not open, the Equation (4.34) becomes

$$\dot{P} = \frac{RT_m}{V_m}\left[\dot{m}_{thr} - \dot{m}_e\right], \tag{4. 36}$$

Pressure transitioning in the manifold can be calculated form the above equation. Since R, T_m, and V_m are all constant, pressure changes in the manifold are only related to the net mass entering and exiting the manifold. $\dot{m}_{thr}$ calculations were discussed in detail earlier. $\dot{m}_e$ can be described as

$$\dot{m_e} = \frac{N_{cyl}\,\eta_{vol}\,V_d\,n_e}{120\,RT_m}P_m, \tag{4. 37}$$

where N_{cyl}, η_{vol}, V_d, and n_e are the number of cylinders, volumetric efficiency, cylinder displaced volume, and engine speed in RPM. P_m is obtained by replacing Equation (4.37) in (4.36).

$$\dot{P} = \frac{RT_m\,\dot{m}_{thr}}{V_m} - \left(\frac{N_{cyl}\,\eta_{vol}\,V_d\,n_e}{120\,V_m}\right)P_m \tag{4. 38}$$

Engine speed calculations are discussed in the "Engine Models" section of this chapter. Volumetric efficiency definition and models are discussed in the following section.

4.2.2.2 Volumetric Efficiency

Volumetric efficiency is the ratio of actual air inducted into the cylinder to the theoretical air that is supposed to be inducted into the cylinder by displacement of the piston from TDC to BDC in an induction stroke. Taylor [57] introduces a simple equation for volumetric efficiency as a function of the pressure ratio and compression ratios.

$$\eta_{vol} = \frac{\gamma - 1}{\gamma} - \frac{r - (P_m / P_0)}{\gamma (r - 1)} \tag{4. 39}$$

where r is the compression ratio, and γ=1.4. Figure 4.7 shows Taylor's model for volumetric efficiency. As can be inferred from the figure, the volumetric efficiency has values higher than unity. However, as Taylor has mentioned in his book, volumetric efficiency is a function of various other variables such as gas temperature, engine geometry, coolant temperature and so on. By dimensional analysis, the reference categorizes the role of each variable set and introduces different correction factors for each set that can be obtain by different graphs. The actual volumetric efficiency is calculated by multiplying the correction factors by the ideal volumetric efficiency.

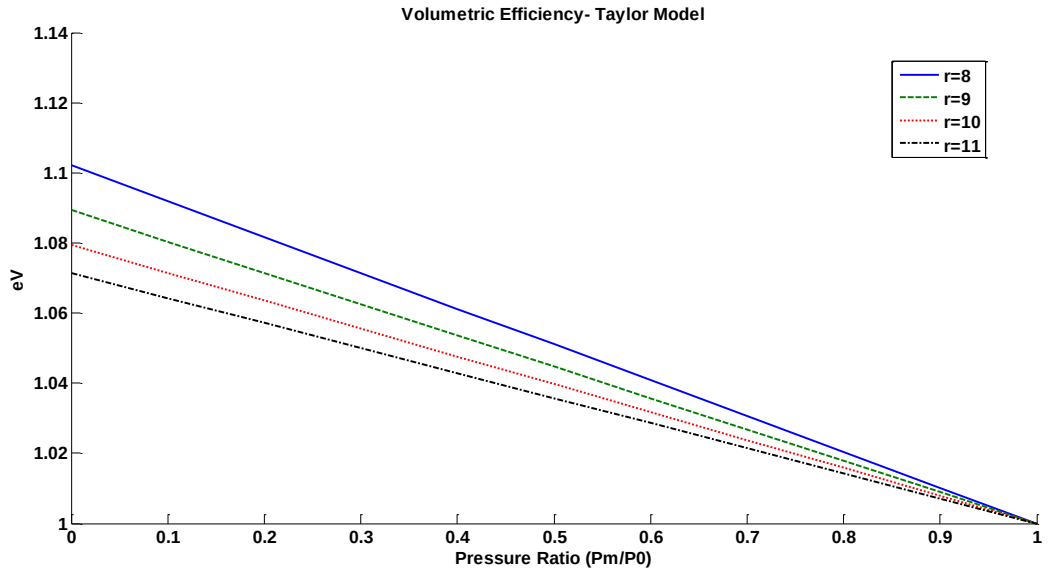

Figure 4.7 Volumetric Efficiency –Taylor's Model [57]

Hendricks et al. [25] introduced a regression-based model for volumetric efficiency as functions of engine speed and manifold pressure

$$\eta_{vol} = e_1 + e_2 P_m + e_3 n_e + e_4 n_e^2 \tag{4. 40}$$

where e_1 =0.696, e_2 =0.16, e_3 =-0.0262, and e_4 = -0.00643. P_m is manifold pressure in bar. The pressure ratio effect in this model is shown in Figure 4.8. In the same paper, Hendricks et al. give a second model for volumetric efficiency by normalizing air charge per stroke as

$$\eta_{vol} = e_5 + \frac{e_6}{P_m}, \tag{4. 41}$$

where e_5 =0.952, and e_6 = -0.0793. This model is presented as a function of manifold pressure in Figure 4.9. It is notable that multiplying both sides of the above equation by P_m should result in a linear function:

$$\eta_{vol} P_m = e_5 P_m + e_6 \tag{4. 42}$$

Hendricks et al. showed that this result agrees well with experimental results for different engines. Equation (4.42) can be used in equation (4.37):

$$\dot{P} = \frac{RT_m \dot{m}_{thr}}{V_m} - \left(\frac{N_{cyl} V_d n_e}{120 V_m} \right) \left(P_m \eta_{vol} \right) = \frac{RT_m \dot{m}_{thr}}{V_m} - \left(\frac{N_{cyl} V_d n_e}{120 V_m} \right) \left(e_5 P_m + e_6 \right) \tag{4. 43}$$

.

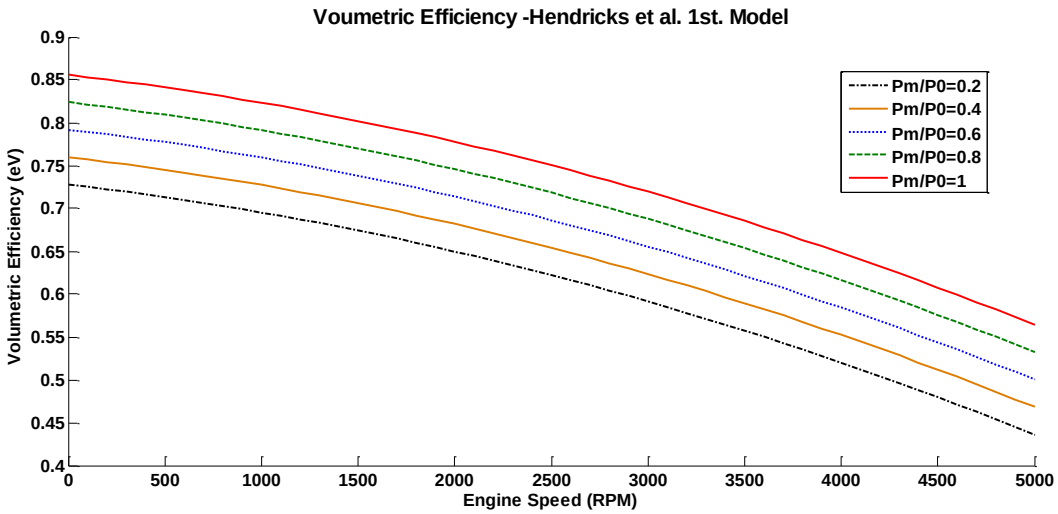

Figure 4.8 Volumetric Efficiency, Hendricks et al., 1st model [25]

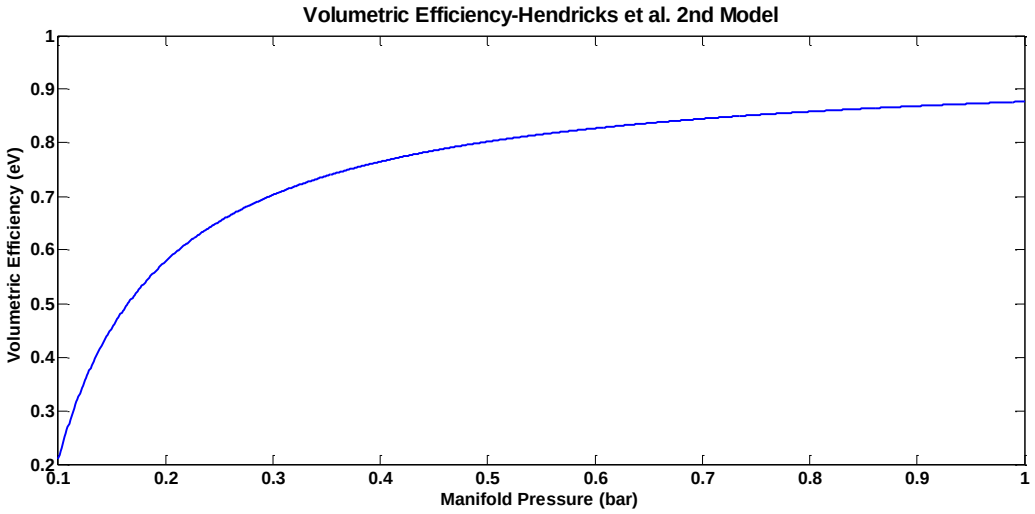

Figure 4.9 Volumetric efficiency, Hendricks et al., 2nd Model [25]

Another method for approximating volumetric efficiency is using lookup tables or maps. Figure 4.10 shows an example of a lookup table map.

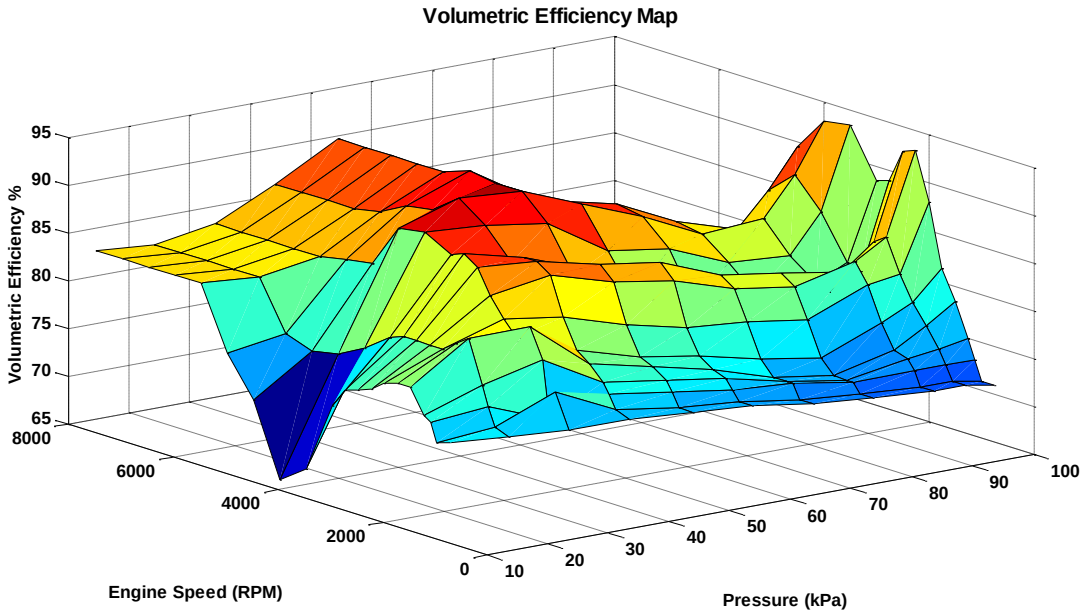

Figure 4.10 Volumetric Efficiency Map [25]

4.2.2.3 Fuel Dynamics

For direct fuel injection systems, fuel is injected inside the cylinders; in other types, fuel is mixed outside of the combustion chamber. A fraction of injected fuel (x) strikes the cylinder wall, and the rest of the fuel (1-x) evaporates and mixes with the air flowing into the combustion chamber. This phenomenon is called wall-wetting. The fuel film on the wall is then heated and evaporated by the manifold after a time constant τ_{fuel}. The two models introduced by Aquino [18], and Hendricks and Sorenson [24] are both very popular in the literature. Aquino's model follows the track of the fuel left on the walls, while Hendricks and Sorenson model follows the track of fuel mass flow. Aquino assumed that injected fuel flow is proportional to the air flow, and the amount of the fuel that leaves the film is proportional to the amount of fuel in the film. He then derived following equations from a continuity equation:

$$\frac{dm_{fw}}{dt} = -\frac{1}{\tau_f} m_{fw} + x\dot{m}_{fi} \tag{4. 44}$$

$$x = \frac{\dot{m}_{fv}}{\dot{m}_{fi}} \tag{4. 45}$$

$$\dot{m}_{fv} = (1-x)\dot{m}_{fi} \tag{4. 46}$$

$$\dot{m}_f = \dot{m}_{fv} + \frac{m_{fw}}{\tau_f} \tag{4. 47}$$

where $\dot{m}_{fi}, \dot{m}_{fv}$, and $\dot{m}_{fw}$ are injected, evaporated, and wall film mass flows respectively. $\ddot{m}_{fv}$ is time derivative of wall film. The time constant in the model was inversely proportional to the manifold temperature that can be approximated by the following function:

$$\tau_f = f_1 \exp(-f_2 T), \tag{4. 48}$$

where $f_1 = 5\times10^6$, and f_2=0.0473; T is manifold temperature in $^\circ K$; x is a linear function of crank angle

$$x = \frac{\theta}{f_3} + f_4, \tag{4. 49}$$

where f_3= 46 , f_4=-0.106. Hendricks and Sorenson obtained the following equations for fuel flow dynamics:

$$\ddot{m}_{fw} = \frac{1}{\tau_f}\left(x\dot{m}_{fi} - \dot{m}_{fw}\right) \tag{4. 50}$$

$$\dot{m}_{fv} = (1-x)\dot{m}_{fi} \tag{4. 51}$$

$$\dot{m}_f = \dot{m}_{fv} + \dot{m}_{fw} \tag{4. 52}$$

Where τ_f and x are modeled as functions of manifold pressure and engine speed.

$$\tau_f = f_5(f_6 n + f_7)(P_m + f_8)^2 + (f_9 n + f_{10}) + f_{11} \tag{4. 53}$$

,

where f_5 = 1.35 , f_6 = -0.672 , f_7 = 1.68 , f_8 =-0.852 , f_9 =-0.06 , f_{10} = 0.15, and f_{11} =0.56.

$$x = f_{11} P_m + f_{12} n + f_{13} \tag{4. 54}$$

where f_{11} = -0.277, f_{12} = -0.055, and f_{13} =0.68.

Time delay due to the wall-wetting has a negative effect on fuel delivery systems that changes the fuel-air ratio in transient conditions. During engine controller design, this effect is eliminated by use of a compensator algorithm. For defining the reverse model, the amount of extra fuel due to the wall-wetting effect is calculated, and the amount of fuel needed to compensate is injected into the system. More details are provided in [52,58].

4.2.3 Engine Models

In an internal combustion engine, power is generated from the conversion of fuel into heat energy. Air is mixed with fuel or fuel is directly injected into the cylinders by a ratio close to the stoichiometric value. The combustion starts with ignition of the fuel by a spark at the end of the compression stroke in certain angles close to TDC. In actual combustion, expansion of the gas in each cylinder is the main source of power and varies as flame progresses and the piston moves downward. Details of the combustion process are not of interest in MVEM; instead an average of

the convertible energy in each cycle is calculated. Since the fuel amount is directly proportional to the supplied air, it is easy to calculate the energy that can be extracted from the fuel in each cycle. The maximum theoretical power that can be extracted from fuel can be described so

$$P_f = \dot{m}_f H_f \quad , \tag{4.55}$$

where P_f is fuel power; H_f is a low heating value that is a constant value for fuels. For gasoline, H_f is about $43 MJ/kg$. The fuel mass flow is $\dot{m}_f$ and is defined by

$$\dot{m}_f = \frac{\dot{m}_e}{\lambda L_{th}} \quad , \tag{4.56}$$

where λ is the normalized air-fuel ratio, that is, a ratio defined by dividing the actual air-fuel ratio to the stoichiometric air-fuel ratio. In modern engines, as it mentioned, is close to stoichiometric fuel (i.e., $\lambda \approx 1$). L_{th} is stoichiometric normalization factor, for air-gasoline is equal to 14.67.

Some part of the fuel power is dissipated by the coolant water flowing around the cylinder. Another part of a fuel's power is lost at the end of the exhaust stroke in the form of hot gas or unburned gas, and flows out of the cylinder. The remaining power is called indicated power and described as

$$P_{ind} = \eta_{th} P_f \, , \tag{4.57}$$

where η_{th} is thermal efficiency, described in detail in the next section; P_{ind} is indicated power, that is the maximum available power in any specific cylinders. However, some part of this power is lost inside the cylinder due to the friction of the engines' rotating components, and some part is used for pumping air into the cylinder. The power that is left is called brake power and is the available power at the engine output shaft.

$$P_b = P_{ind} - P_{loss} = P_{ind} - \left(P_{friction} + P_{pumping} \right) \tag{4.58}$$

In terms of efficiency, the ratio of brake power to indicated power is called brake or mechanical efficiency.

$$\eta_m = \frac{P_b}{P_{ind}} \tag{4.59}$$

In a similar way, the efficiencies of other components of a powertrain, such as the torque converter, gearbox, differential, and wheel, can be defined as

$$\eta_{TC} = \frac{P_{TC}}{P_b}\ ; \qquad \eta_G = \frac{P_G}{P_{TC}}\ ; \qquad \eta_{Dif} = \frac{P_{Dif}}{P_G}\ ; \qquad \eta_w = \frac{P_w}{P_{Dif}}, \tag{4.60}$$

where η_{TC}, η_G, η_{Dif}, and η_w are the torque converter, gearbox, differential, and wheel efficiencies, respectively, and P_{TC}, P_G, P_{Dif}, and P_w are torque converter, gearbox, differential, and wheel output powers. By combining the above equations, the overall efficiency of the powertrain that is the ratio of the available power at the wheels to the fuel power, can be defined in this way

$$\eta_{overall} = \eta_{th}\eta_m\eta_{TC}\eta_G\eta_{Dif}\eta_w = \frac{P_{ind}}{P_f}\frac{P_b}{P_{ind}}\frac{P_{TC}}{P_b}\frac{P_G}{P_{TC}}\frac{P_{Dif}}{P_G}\frac{P_w}{P_{Dif}} = \frac{P_w}{P_f} \tag{4.61}$$

In this work, only thermal efficiency will be discussed in detail.

4.2.3.1 Thermal Efficiency

In an SI engine, ideal thermal efficiency can be calculated from an Otto air standard thermodynamic cycle. An Otto air cycle assumes that compression of the working fluid occurs from BDC to TDC as an isentropic process, i.e., adiabatic and reversible. The combustion process is replaced by an external source of heat that instantaneously adds heat to the air at a constant volume at TDC. The expansion process is considered to be another isentropic process where piston moves from TDC to BDC. When the piston reaches BDC, the heat is rejected instantaneously. Following these assumptions, the ideal thermal efficiency of air cycle can be expressed as

$$\eta_{thi} = 1 - \frac{1}{r^{\gamma-1}}, \tag{4.62}$$

where r is a compression ratio. Heat transfer between the gas and the walls, and friction and pumping effects are examples of deviations of an actual SI cycle from an ideal cycle. On the other hand, combustion is not an instantaneous process, and some part of combustion heat is lost from the cylinder walls, cylinder head, and piston during combustion and expansion strokes. Intake and exhaust valves are opened and closed at different angles from BDC and TDC. Thermal efficiency in general is a function of many parameters such as engine geometry, normalized air-fuel ratio (or equivalence fuel-air $\phi = \frac{1}{\lambda}$), spark angle, and some engine working parameters such as engine speed and manifold pressure.

In the following sections, two types of models for thermal efficiency are discussed. The first model was developed by Chang [59] and the second, by Hendricks et al. [25]. Both models are parametric ones that can be adjusted and reused for other engines.

4.2.3.1.1 Chang's Thermal Efficiency Model

The Chang model considers different parameters affecting engine geometry, such as the cylinder bore and stroke, fuel-air ratio, compression ratio, manifold pressure, and engine speed. Earlier than this work, Nitschke [60] had developed a model for volumetric, thermal efficiency, and engine pumping work. The thermal efficiency in Nitschke's model had most of the above mentioned parameters, but it was limited to a configuration of a special engine. Another shortcoming for Nitschke's model was that the geometry was not included in the model explicitly. The Chang model consists of sub models for each parameter. In order to find the coefficients of the models, a cycle simulation data developed by Poulos [61] was used. Sub models of Chang's thermal efficiency model can be described as follows:

Compression Ratio

$$\eta_{cr} = e_1 \, \eta_{thi} + e_2 \, r \tag{4.63}$$

where $e_1 = 0.729;\ e_2 = -0.226$.

Normalized Air-Fuel

$$\begin{cases} \lambda = 1 & P_m \le 85\,kPa \\ \lambda = \dfrac{1}{1 + \left[e_3 (P_m - 85)\right]^2} & P_m > 85\,kPa \end{cases} \tag{4.64}$$

$$\eta_\lambda = e_4 + e_5 \, \lambda \tag{4.65}$$

where $e_3 = 0.0419;\quad e_4 = 2.230;\quad e_5 = 35.166$.

Manifold Air Pressure

$$\eta_{Pm} = e_6 + e_7 \left(\frac{P_m}{101.3} \right)^{e_8} \tag{4.66}$$

where $e_6 = 42.1; \quad e_7 = -4.36; \quad e_8 = -0.258.$

Engine Speed

$$\eta_n = e_9 + e_{10} n^{e_{11}} \tag{4.67}$$

where $e_9 = 44.6; \quad e_{10} = -15.1; \quad e_{11} = -0.088.$

Bore-to-Stroke Ratio

$$\eta_{B/L} = e_{12} + e_{13} (B/L)^{e_{14}} \tag{4.68}$$

where $e_{12} = -108.6; \quad e_{13} = 145.7; \quad e_{14} = -0.02$

Displaced Volume

$$\eta_{Vd} = e_{15} + e_{16} V_d^{\,e_{17}} \tag{4.69}$$

where $e_{15} = 45.7; \quad e_{16} = -13.8; \quad e_{17} = -0.083.$

The above six independent models can then be integrated based on superposition law, and total thermal efficiency is obtained thus:

$$\eta_{th} = c_1 + c_2 \eta_{cr} + c_3 \eta_\lambda + c_4 \eta_{Pm} + c_5 \eta_n + c_6 \eta_{BL} + c_7 \eta_{Vd} \tag{4.70}$$

where $c_1 = -157.5; \quad c_2 = 0.962; \quad c_3 = 1.016; \quad c_4 = 0.854; c_5 = 0.647; \quad c_6 = 0.647; \quad c_7 = 1.037$

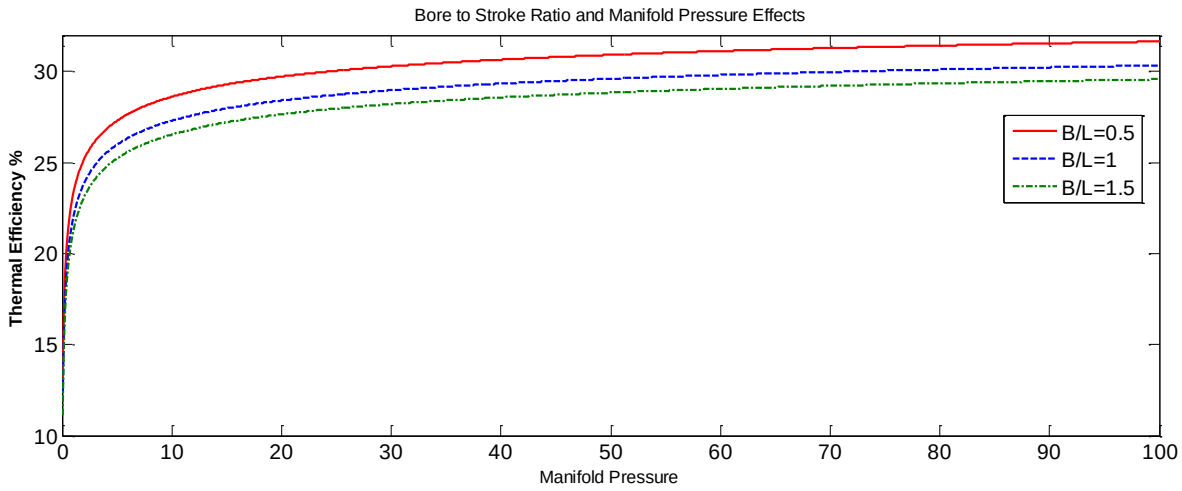

Figure 4.11 Bore-to-Stroke Ratio and Manifold Pressure Effects on Thermal Efficiency [59]

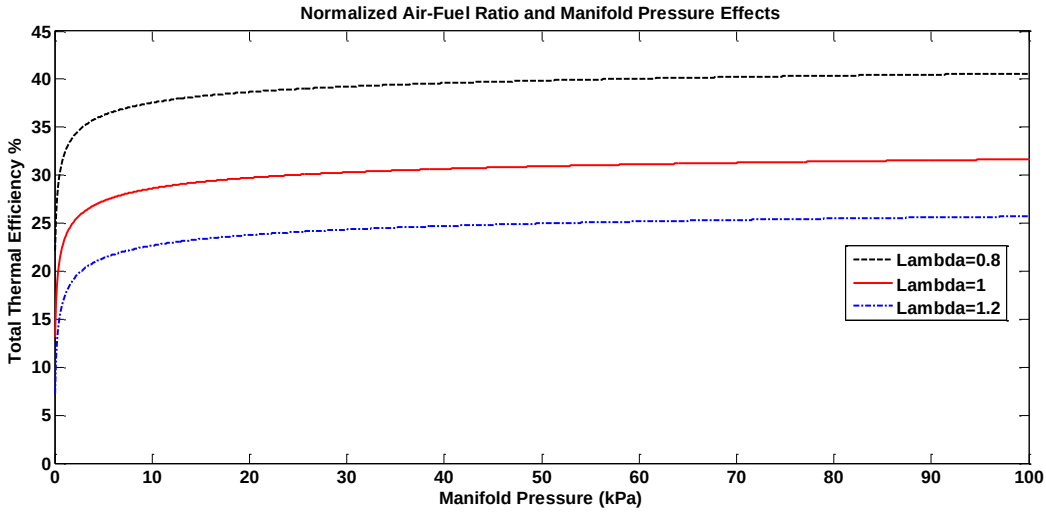

Figure 4.12 Air-Fuel Ratio and Manifold Pressure Effects on Thermal Efficiency [59]

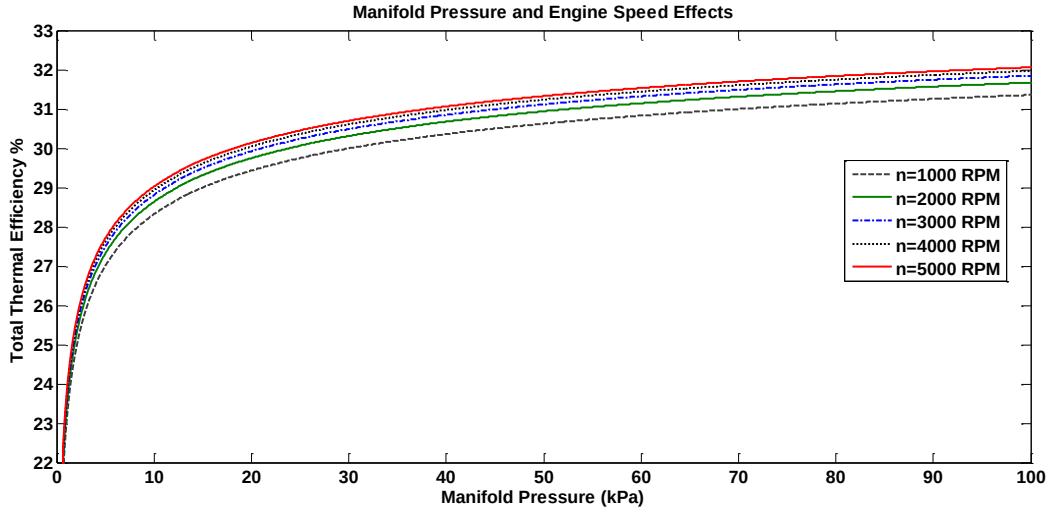

Figure 4.13 Manifold Pressure and Engine Speed Effects on Thermal Efficiency [59]

As shown in Figure 4.11 and Figure 4.12 increasing of bore-to-stroke ratio and normalized air-fuel ration cause to decrease thermal efficiency, but increasing the engine speed has positive effect of it (Figure 4.13 and Figure 4.14).

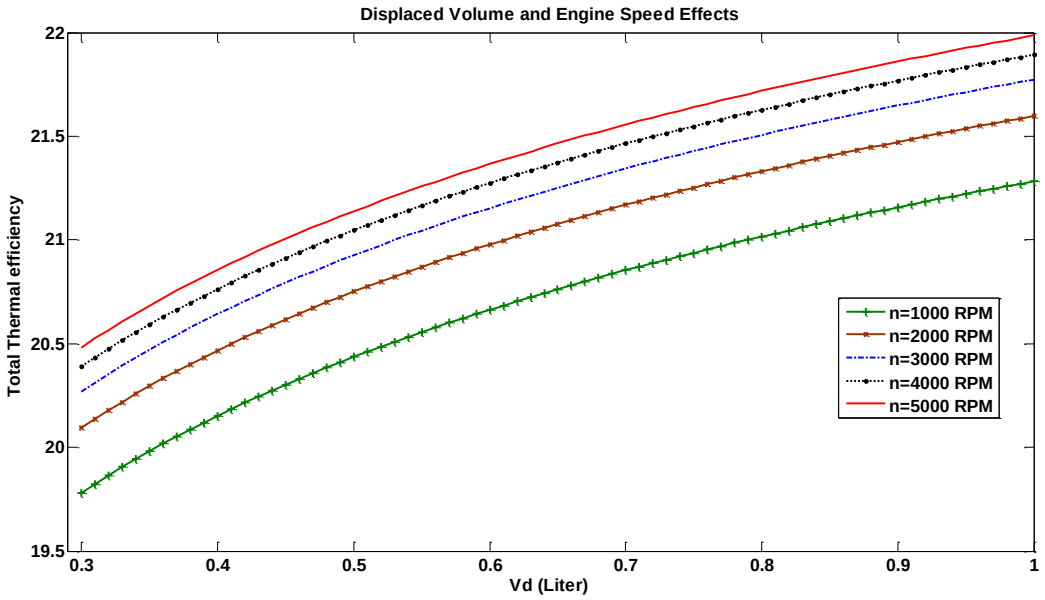

Figure 4.14 Displaced Volume and Engine Speed Effects on Thermal Efficiency [59]

4.2.3.1.2 The Hendricks et al. Model for Thermal Efficiency

The model Hendricks et al. created is more general, and it is not related to engine specifications such as the compression ratio or engine geometry parameters. Thermal efficiency in this model has four contributions: engine speed, manifold pressure, normalized air-fuel ratio, and spark angle.

Engine Speed

$$\eta_{thn} = h_1\left(1 + h_2 n^{h_3}\right) \tag{4.71}$$

where $h_1 = 0.558 \quad ; h_2 = -0.392 \quad ; h_3 = -0.360$

Manifold Pressure

$$\eta_{thPm} = h_4 + h_5 P_m + h_6 P_m^{\ 2} \tag{4.72}$$

where $h_4 = 0.9301; \quad h_5 = 0.2154 \quad ; h_6 = -0.1657.$

Normalized Air-Fuel Ratio

$$\eta_{th\lambda} = \begin{cases} h_7 + h_8\lambda + h_9\lambda^2 \\ h_{10} + h_{11}\lambda + h_{12}\lambda^2 \end{cases} \tag{4.73}$$

$h_7 = -1.299 \quad ; h_8 = 3.599 \quad ; h_9 = -1.332 \quad ; h_{10} = -0.0205 \quad ; h_{11} = 1.741 \quad ; h_{12} = -0.745.$

Spark Angle

$$\eta_{th\theta} = h_{13} + h_{14}\left(\theta - \theta_{mbt}\right) + h_{15}\left(\theta - \theta_{mbt}\right)^2$$

$$n_{47} = \begin{cases} h_{16} \cdot n & n < h_{17} \\ h_{16} \cdot h_{17} & n \geq h_{17} \end{cases}$$

$$\theta_1 = h_{18} P_m + h_{19} + n_{47} \tag{4.74}$$

$$\theta_2 = h_{20} P_m + h_{21} + n_{47}$$

$$\theta_{mbt} = \min(\theta_1, \theta_2)$$

$$h1 = 0.558 \quad ; h2 = -0.392 \quad ; h3 = -0.360 \quad ; h4 = 0.9301 \; ; h5 = 0.2154 \quad ; h6 = -0.1657$$

$$h_7 = -1.299 \quad ; h_8 = 3.599 \quad ; h_9 = -1.332 \quad ; h_{10} = -0.0205 \; h_{11} = 1.741 \quad ; h_{12} = -0.745$$

$$h_{13} = 0.7 \quad ; h_{14} = 0.0240 \quad ; \quad h_{15} = -0.00048 \quad ; h_{16} = 4.7 \quad ; h_{17} = 4.8 \quad ; h_{18} = 47.31$$

$$h_{19} = 2.6214 \quad ; h_{20} = -56.55 \quad ; h_{21} = 57.34 \quad ; h_{22} = 45$$

Total Thermal efficiency in this model can be obtained by the products of sub-model contributions

$$\eta_{th} = \eta_{thn} \eta_{thPm} \eta_{th\lambda} \eta_{th\theta} \tag{4.75}$$

The Hendricks et al. thermal efficiency model is used in this work, and details of simulations are discussed in the next chapters.

4.2.3.2 Rotational Dynamics

Engine speed transitions can be obtained from crankshaft rotational dynamics (the power available at the wheels). Some part of the fuel-generated power is lost as friction, and some part of it is used to pump air into the cylinders. Another part, called the load power, uses the available

power at a shaft to rotate the powertrain components, including the torque converter, gearbox, drive-shafts, final drive, and wheel assembly. The part that remains is considered to accelerate the powertrain.

$$I\omega_e \dot{\omega}_e = P_b - P_{load} = P_f - P_{friction} - P_{pump} - P_{load} \tag{4.76}$$

where I is the powertrain's moment of inertia and ω_e is the angular velocity of the powertrain rotating parts that is related to engine speed by

$$\omega_e = \frac{2\pi}{60} n_e \tag{4.79}$$

Power and torque are connected by angular velocity

$$P_e = T_e \omega_e \tag{4.80}$$

Frictional power occurs as energy is lost during the contacts between engine's moving parts, including the pistons and cylinders, crankshaft bearings, piston assemblies, and vavletrain assembly. At idle speed, all power is directed to overcoming engine frictional power, $P_{friction}$. In reference [25] is given by approximating a second degree polynomial for engine frictional torque and relating to frictional power

$$P_{friction} = n_e \left(p_1 + p_2 n_e + p_3 {n_e}^2 \right) \tag{4.81}$$

where p_1=1.673, p_2=0.272, p_3=0.0135.

Pumping losses are due to the required air induction power during the intake and exhaust strokes. In naturally aspirated engines, the pressure in the induction stroke is less than the exhaust pressure. In turbocharged engines, the pressure in the intake process is more than the exhaust pressure, so extra power is added to the system. Reference [25] introduces the following equation for pumping loss power as a function of manifold pressure

$$P_{pump} = n_e\left(p_4 + p_5 n_e\right)P_m\,, \tag{4.82}$$

where $p_4 = -0.969$, $p_5 = 0.206$.

And the powertrain load power is approximated by

$$P_{load} = p_6\, n_e^{\,3} \tag{4.83}$$

4.3 Powertrain and Vehicle Models

The power required to thrust the vehicle is transmitted from the powertrain components to the wheels. When an engine is engaged, each component of the powertrain rotates with a rotational speed proportional to the engine speed. Torque in each component is obtained from corresponding power and speed. Speed and torque are amplified or reduced when they pass through the transmission and final drive. The transmission, also called gearbox, reduces the engine speed and increases the torque by a ratio called the gear ratio

$$GR = \frac{T_{driven}}{T_{drive}} = \frac{\omega_{drive}}{\omega_{driven}} = \frac{n_{drive}}{n_{driven}} \tag{4.84}$$

where $n = \omega\dfrac{60}{2\pi}$.

A gearbox has different sets of gears that enable it to provide different torques at different working conditions of the vehicle. The power lost in each component reduces the power, and hence the torque in that component, but this loss has no influence on speed reduction. For each component, torque and speed can be obtained as follows [62]:

Torque-converter

$$T_{Tc} = \eta_{Tc}\left(T_e - I_e \alpha_e\right) = \eta_{Tc}\left[T_e - I_e\left(\frac{2\pi}{60}\dot{n}_e\right)\right], \tag{4.85}$$

$$\text{where } \omega_{Tc} = \omega_e \text{ or } n_{Tc} = n_e \quad ; \quad and \quad \alpha_{Tc} = \alpha_e \tag{4.86}$$

where T_e, α_e , n_e and I_e are an engine's torque from dynamometer data at a given speed, rotational acceleration, speed, and moment of inertia. T_{Tc} , η_{Tc}, and n_{Tc} are the torque-converter's torque at gearbox input , efficiency, and speed.

Transmission

$$T_{Gb} = \left(T_{Tc} - I_{Gb}\alpha_e\right)\eta_{Gb} GR_{Gb} \tag{4.87}$$

$$\omega_e = GR_{Gb}\,\omega_{Gb} \quad or \quad n_e = GR_{Gb}\,n_{Gb} \quad ; \quad and \quad \alpha_e = GR_{Gb}\,\alpha_{Gb} \tag{4.88}$$

where T_{Gb} is torque at the gearbox output, or at the driveshaft input . I_{Gb}, η_{Gb}, n_{Gb} , α_{Gb} and GR_{Gb} are the moment of inertia, efficiency, rotational speed, rotational acceleration, and ratio of the gear box.

Final Drive

$$T_{Ax} = \left(T_{Gb} - I_d\,\alpha_d\right)\eta_{Fd}\,GR_{Fd} = F_x\,r_w + I_w\alpha_w \tag{4.89}$$

$$\omega_{Gb} = GR_{Fd}\,\omega_{Ax} \quad or \quad n_{Gb} = GR_{Fd}\,n_{Ax}; \quad and \quad \alpha_{Gb} = GR_{Fd}\,\alpha_{Ax} \tag{4.90}$$

where η_{FD} and GR_{FD} are the final drive efficiency and gear ratio; T_{ax}, n_{ax}, and α_{ax} are the axle torque, speed, and rotational acceleration; I_d and α_d are the driveshaft moment of inertia and rotational acceleration. r_w, I_w, and α_w are the wheel radius, moment of inertia, and rotational

acceleration; F_x is tire traction force at contact point with the ground. Traction force can be obtained by combining the above equations:

$$F_x = \frac{T_e \eta_{Gb} \eta_{Fd} G_{Gb} G_{Fd}}{r_w} - \left[\left(I_e + I_{Gb} \right) \left(G_{Gb} G_{Fd} \right)^2 + I_d G_{Fd}^2 + I_w \right] \frac{a_x}{r_w^2}. \tag{4.91}$$

Chapter 5

MapleSim Implementation

The mean value engine model in this work consists of a throttle body, a manifold, and an engine as main components of the system (Figure 5.1). The powertrain simulation uses a forward-looking strategy starting with a driver speed command and compares it with a calculated engine speed. The engine at this level is considered to be on a dynamometer. Therefore, the load is added to the system as a negative torque to the system.

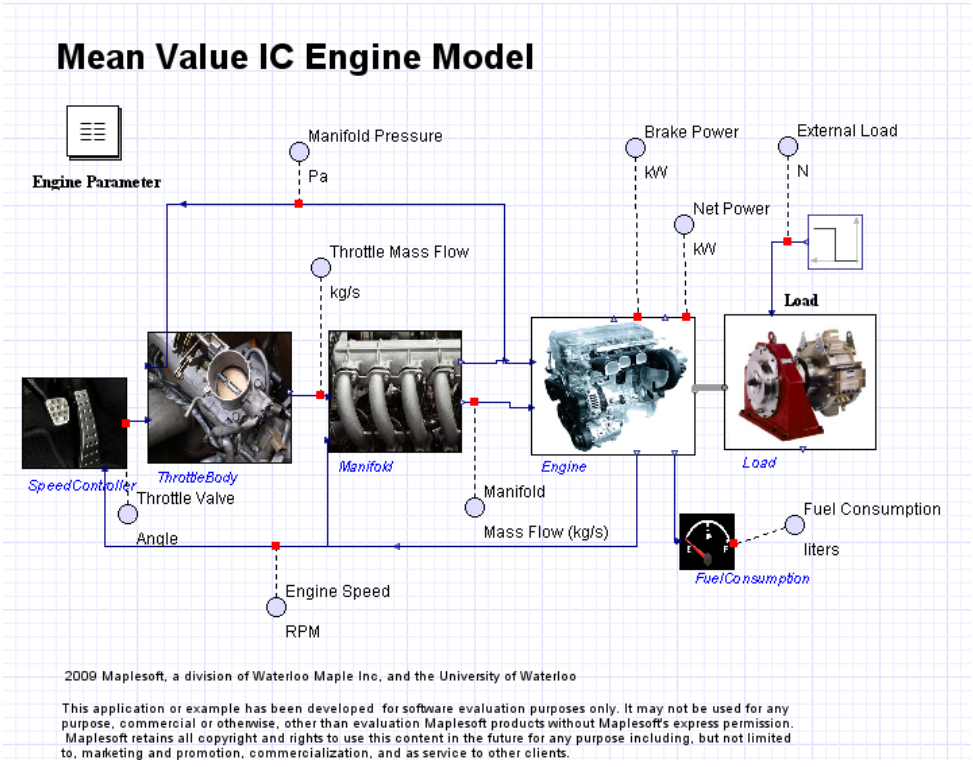

Figure 5.1 Top Level of the MapleSim Mean Value Engine

The MapleSim MVEM is a parametric model. The parameters can be defined by a block, as shown at top left of the window. The parameters at this level are global and accessible from any other subsystem components. Parameters also can be defined inside each sub-model. Probes can easily be attached to any connecting lines to measure the data flowing from one component to another. The PID control in Figure 5.2 outputs throttle angle demand based on an engine's actual speed and driver-required speed.

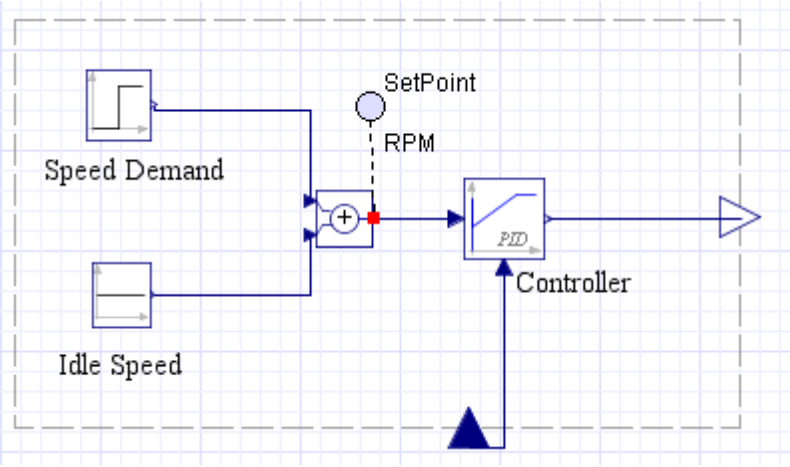

Figure 5.2 Speed Controller in the MapleSim Model

The air mass flow rate in the throttle component (Figure 5.3) is calculated in two blocks: one for the throttle area calculations and the other for the air mass flow calculations. Throttle air mass flow is obtained by

$$\dot{m}_{thr}(\varphi, P_m / P_0) = Cd \,.A_{thr}(\varphi)\, f\left(P_m / P_0\right) \qquad (5.1)$$

where, the throttle effective area is obtained from Equation (4.4), and the pressure function from Equation (4.8). The discharge coefficient is a function of the throttle angle and manifold pressure. For simplicity, both are considered to be constant. These blocks are created by using custom components in Maple, and can be accessed by double-clicking on the components.

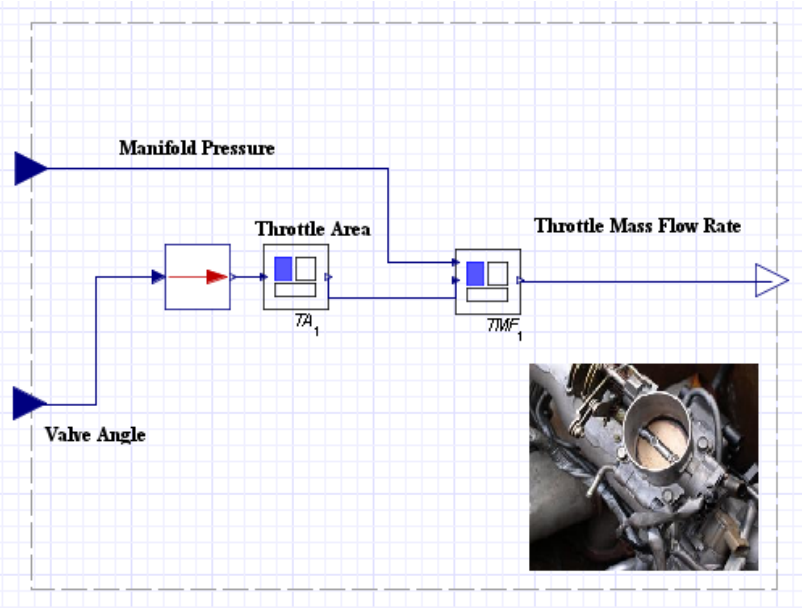

Figure 5.3 Throttle Body Model in MapleSim Engine

Figure 5.4 shows the throttle effective area equation in a MapleSim custom component document. Various types of equation formats are available for use with such algebraic and differential custom components. Depending on the application, each of these components can be opened and replaced with new equations. The input or output connectors can be added to or deleted from the component. It is also possible to introduce parameters to a model of the component, as is shown for throttle bore and pin diameters at the figure's bottom line.

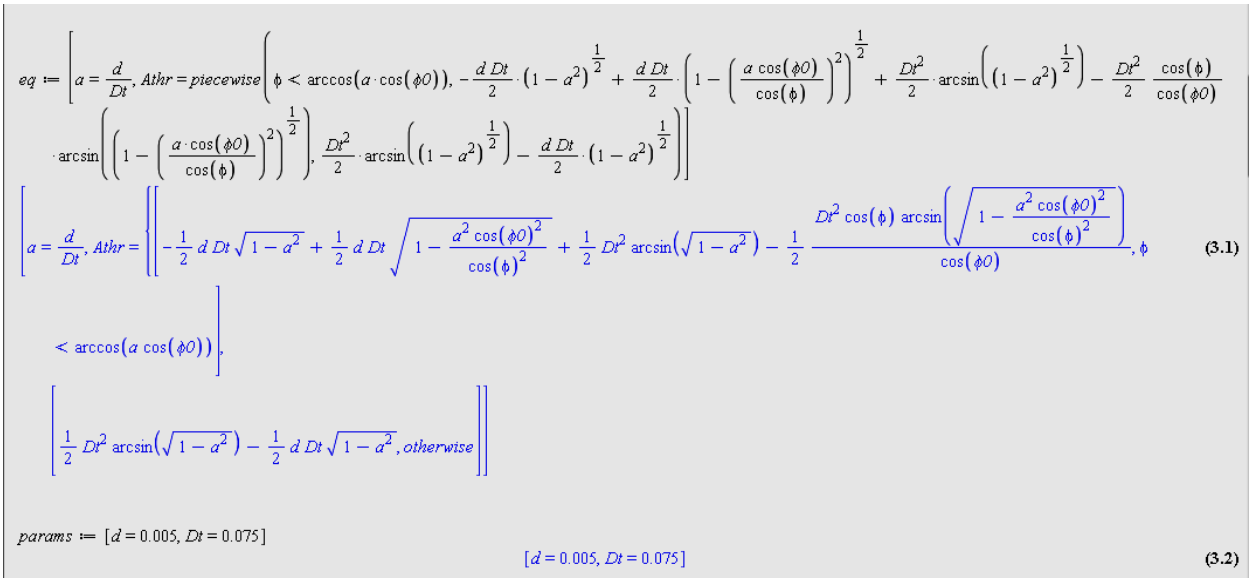

Figure 5.4 Writing Equations in MapleSim

The manifold block calculates air flow into the engine and manifold pressure. The input to the intake manifold block includes the mass inflow that is calculated in the throttle body component, the engine speed that is calculated in the engine block, and the volumetric efficiency (Figure 5.5).

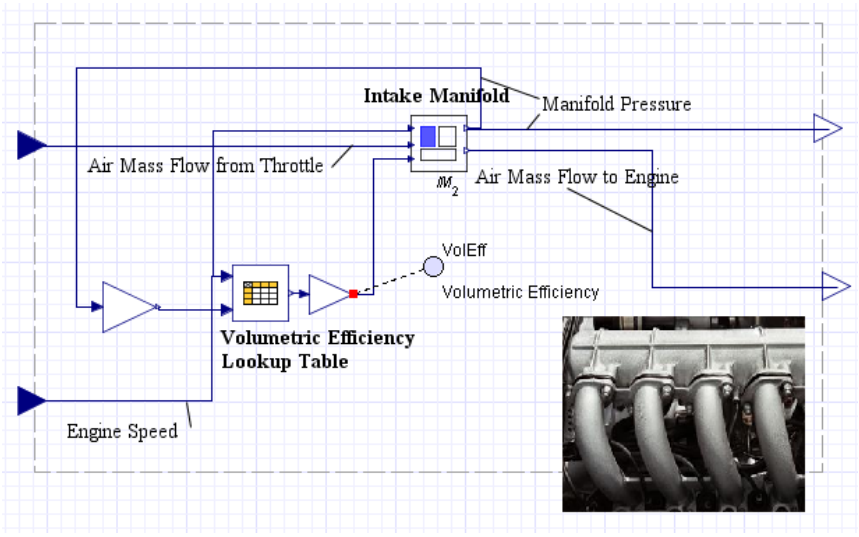

Figure 5.5 Intake Manifold Model in a MapleSim Engine

Manifold pressure is calculated from a differential equation derived from conservation of mass and ideal gas laws.

$$\dot{P}_m = \frac{RT_m}{V_m}\left(\dot{m}_{thr} - \dot{m}_e\right), \tag{5.2}$$

where P_m, T_m, and V_m are manifold pressure, temperature, and volume; R is the gas constant; $\dot{m}_e$ is air mass flow into the engine.

$$\dot{m}_e = \frac{\eta_v N_{cyl} V_d P_m n}{120 R T_m}, \tag{5.3}$$

where, η_v, N_{cyl}, V_d, and n are volumetric efficiency, number of cylinders, displaced volume, and engine speed. Volumetric efficiency is obtained from a lookup table (Figure 5.6).

	10.3	19.9	29.9	39.8	50.2	60.1	70.1	80	90	95.2	100
750	75.5	75	74.5	74.5	74	73.5	72.5	72	71.5	71.5	71
1000	75	75.5	78	75	74	73.5	72.5	72	71.5	71.5	71
1125	77	77.5	75	76.5	75.5	74.5	74	73	73	73	73
1250	77.5	79.5	81	77.5	76.5	75.5	74	73	74	74.5	75
1500	80	84	84	79	77.5	76	74	73	74.5	76.5	78.5
1750	80	83	82.5	80	78	77	75.5	74.5	77	78.5	81.5
2000	79.5	82	84	83							
2250	78.5	82	86	87							
2500	78	82	88.5	88							
2750	77.5	82	89.5	88							
3000	75.5	81.5	89	87							
3500	68	79.5	90.5	90							
4000	66	78	90	92							
4500	73.5	77.5	85.5	90							
5000	77.5	78.5	85	89.5							
5500	84	83.5	84.5	88							
6000	84	83.5	84.5	87.5							
6500	84	83.5	84.5	87.5							
7000	84	83.5	84.5	87.5							
7500	84	83.5	84.5	87.5							

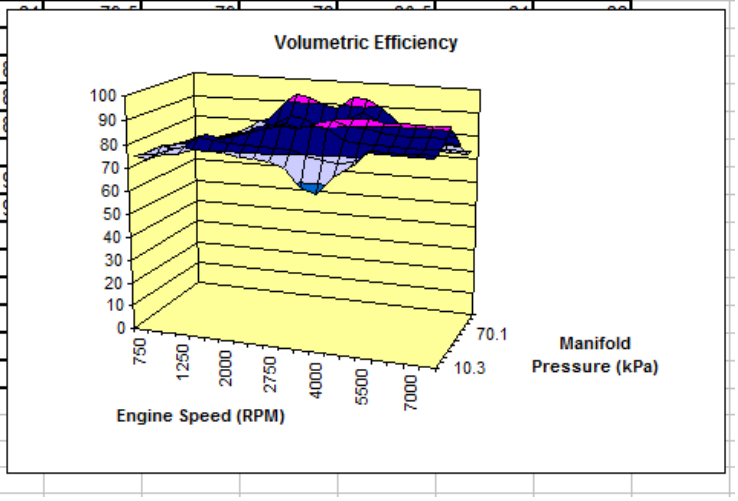

Figure 5.6 The Volumetric Efficiency Lookup Table in the Intake Manifold Model [25]

The engine model (Figure 5.7) calculates indicated, brake, and loss powers. A sensor measures powertrain angular speed and load power. The load power is then fed back into the engine model and is used for power calculations. The engine speed is calculated from a differential equation (Equation 4.76). The losses are the sum of the pump and friction losses, and are obtained from an empirical function for manifold pressure and engine speed variables.

$$P_{loss} = P_{friction} + P_{pump} = n\left(p_1 + p_2 n + p_3 n^2\right) + n\left(p_4 + p_5 n\right)P_m \tag{5.4}$$

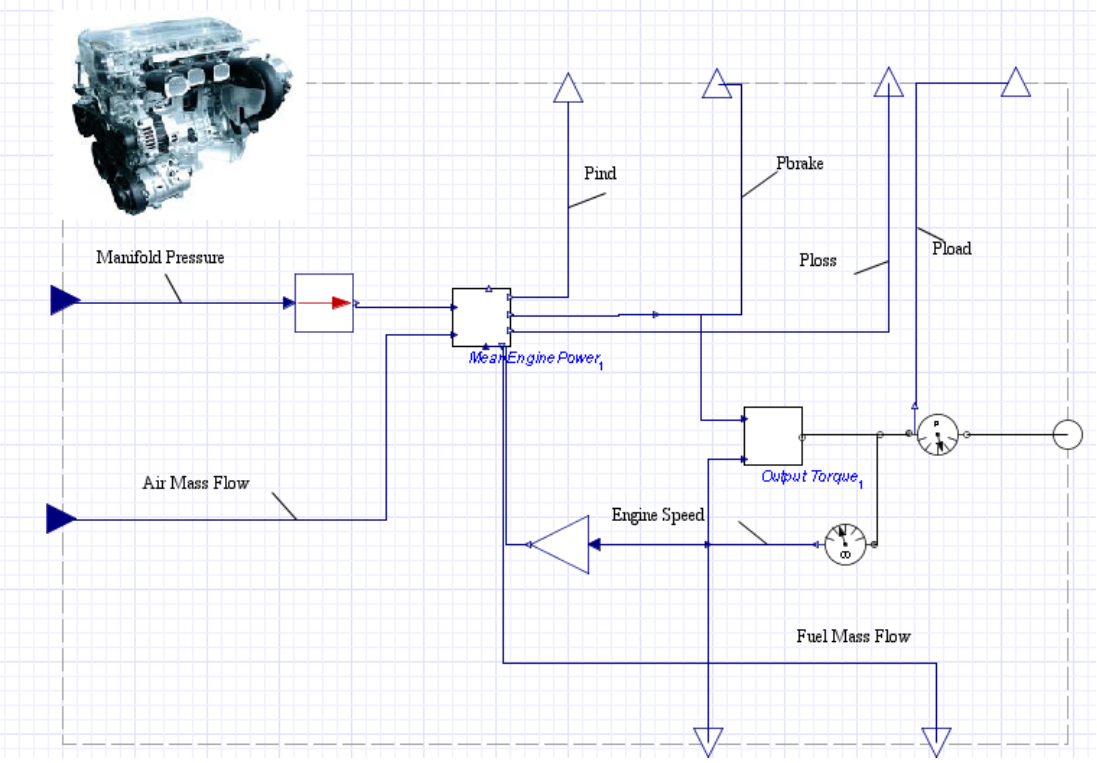

Figure 5.7 Engine Model in the MapleSim Model

The connector at the output of the sensor at the right end of the Figure 5.7 Engine Model in the MapleSim Model is a physical shaft that drives the drivetrain components downstream of the engine, as demonstrated in Figure 5.8. The drivetrain in this model consists of a simple rotational inertia for the driveshaft and differential, and a rotational to translational gear for the wheel model. Roll, grade, and air resistance forces are introduced as a drag force on the system. The

drag force is added to the dynamometer load and result is the total negative power in the vehicle model. The vehicle velocity is measured at the wheels by a translational speed sensor.

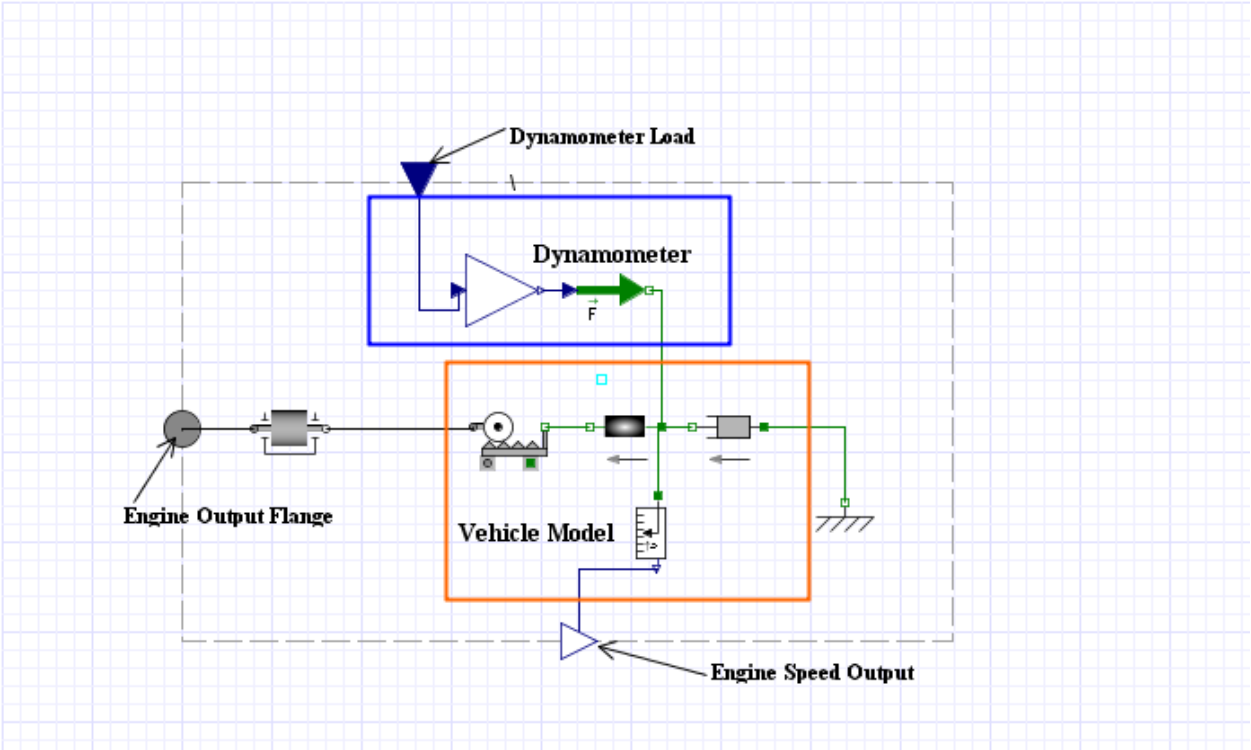

Figure 5.8 Powertrain and Vehicle Model in the MapleSim Model

Chapter 6

Validation and Results

An engine configuration similar to the one shown in Figure 5.1 is used to run the simulations. A set of throttle angle and mass flow data is used to find the throttle angle function and used in a "simulation" model, and another set of air mass flow data at angles different from the previous angle data is measured and used as an "experimental" model. The air mass flow in the simulation model is calculated by following equations:

$$\dot{m}_{thr}(\varphi, Pm/P0) = \dot{M}_{thr}\, g(\varphi)\, f\left(P_m / P_0\right) \tag{6.1}$$

where $\dot{M}_{thr}$=0.128 kg/s is the maximum air mass flow passing through a throttled and widely open throttle conditions. The pressure function is obtained by

$$f\left(P_m / P_0\right) = \begin{cases} 2\sqrt{\dfrac{P_m}{P_0} - \left(\dfrac{P_m}{P_0}\right)^2} & \text{for } P_m > \dfrac{P_o}{2} \\ 1 & \text{for } P_m \le \dfrac{P_o}{2} \end{cases} \tag{6.2}$$

The throttle angle function is defined by a third-degree cosine function.

$$g(\varphi) = -1.147 + 3.667\cos(\varphi) - 3.594\cos^2(\varphi) + 1.093\cos^3(\varphi) \tag{6.3}$$

The air mass flow for the experimental mass flow is obtained from a one-dimensional lookup table by changing the throttle angle valve gradually and measuring the air mass flow rate at the throttle upstream. Both the simulation and experimental models are then simultaneously run and results are compared.

The engine model has two inputs: a step signal for the driver and another one for the drivetrain load. Step signals enable the capture of both dynamic and steady-state conditions of a system. The input signals to the system can be considered as the ideal level of a variable, and can be as simple as a step signal for gas acceleration or brake deceleration pedals in a driver model, or more complicated signals such as drive-cycle data with much accelerating, decelerating and stopping. If a drive-cycle is used, the actual velocity at the wheels is computed and compared with the drive-cycle velocity, but if the engine is on a dynamometer, engine speed data can be compared with reference speed data. The engine speed can also be compared directly with the drive-cycle speed data if the transmission and final drive gear ratios are known in each instance of time.

A controller, such as a PID controller in this model, receives the input signal, compares it with the calculated value from the system, and outputs a signal comprised of the two. The controller's output in this model is a throttle valve angle varying from 7 degrees for completely closed to 90 degrees for the wide-open valve angles. The selected input variable for simulations are engine speed and drive train load actuating at t=60 s and t=100 s respectively, and all simulations are run for 120 s The speed step values are set at n=2000 rpm for the initial values of all simulations, and n=3000, 3500, 4000, and 5000 rpm for the offset values after the speed is ramped up. Running the experimental and simulation models simultaneously and depending on the load and speed data for each simulation, the controller projects a throttle angle signal profile for the simulation and another for the experimental model that differ from each other. The throttle air mass flow is then calculated from the throttle signal, and then other variables such as manifold pressure and engine power are obtained from it. The engine for the study is a four-stroke SI engine with 85 and 100 mm bore and stroke dimensions. The throttle valve pin and bore diameters are 8 and 64 mm, respectively.

As shown in Figure 6.1, at times t=0 s to t=60 s the engine speed is set to n=2000 rpm and the controller tries to adjust the throttle angle to about 12.2, and 9.8 degrees for the simulation and experimental models, respectively. Changing the engine speed abruptly to n=3000, 3500, 4000,

and 5000 rpm at t=60 s causes the controller to leave the valve in a completely open position for a few seconds. The time that the valve is completely open increases with the increase of the engine speed set point.

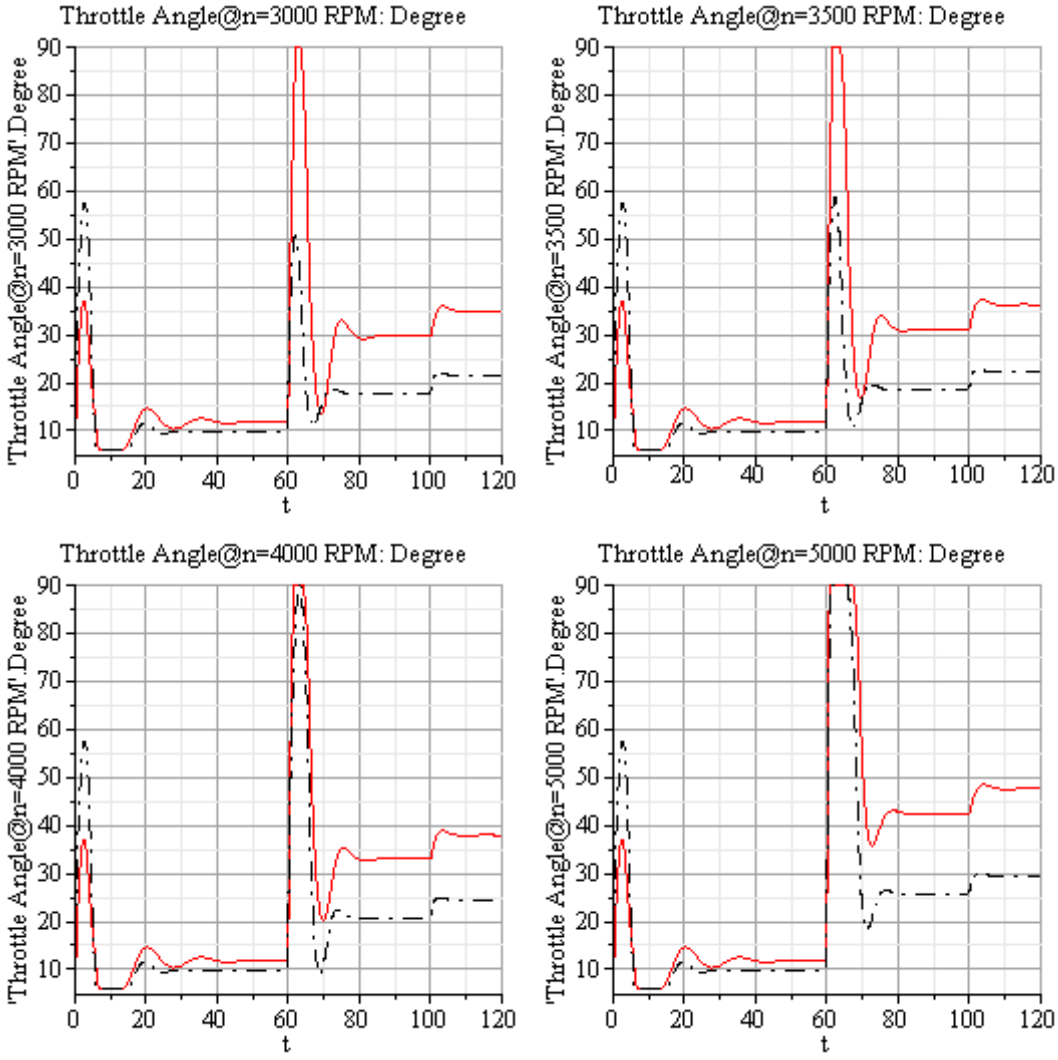

Figure 6.1 Results for the Throttle Angle

Simulation (Solid Lines) and Experimental (Dash-dot Lines)

After transition responses of the simulation and experimental models have died out, steady-state responses of the throttle angle signal appear as values offset from one another. These values are

then used to calculate the error percentages of the models. At t=100 s, the time that the dynamometer load is connected to the engine, the throttle angle is decreased to compensate for this effect by supplying more fuel power.

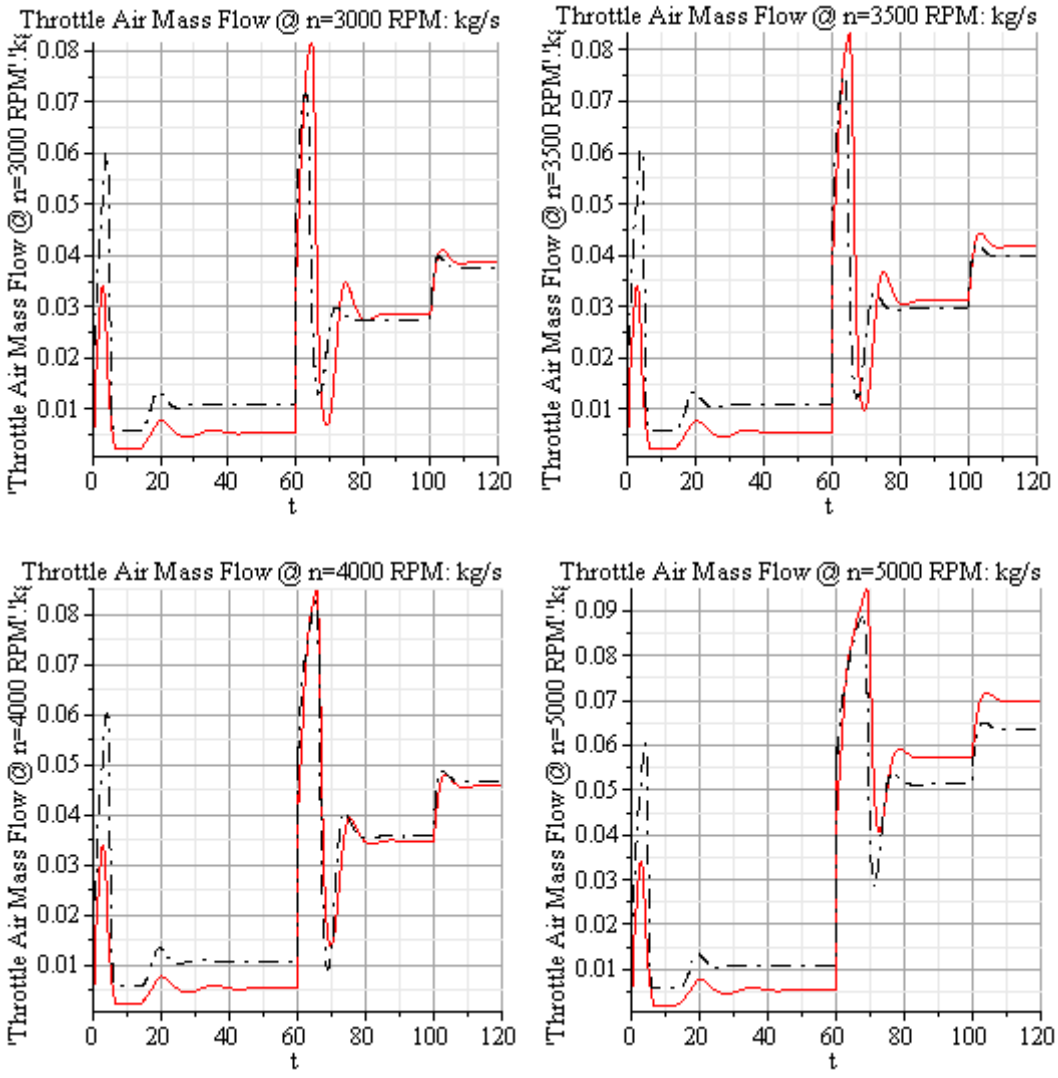

Figure 6.2 Throttle Air Mass Flow Results

Simulation (Solid Lines) and Experimental (Dash-dot Lines)

The throttle mass flow (Figure 6.2) and manifold pressure (Figure 6.3) have almost the same trends as the throttle angle, in that increasing the throttle angle increases the air mass flow rate.

At angles higher than 82 degrees and pressure lower than 52 kPa, both experimental and simulation throttle mass flows show constant values equal to the maximum air flow.

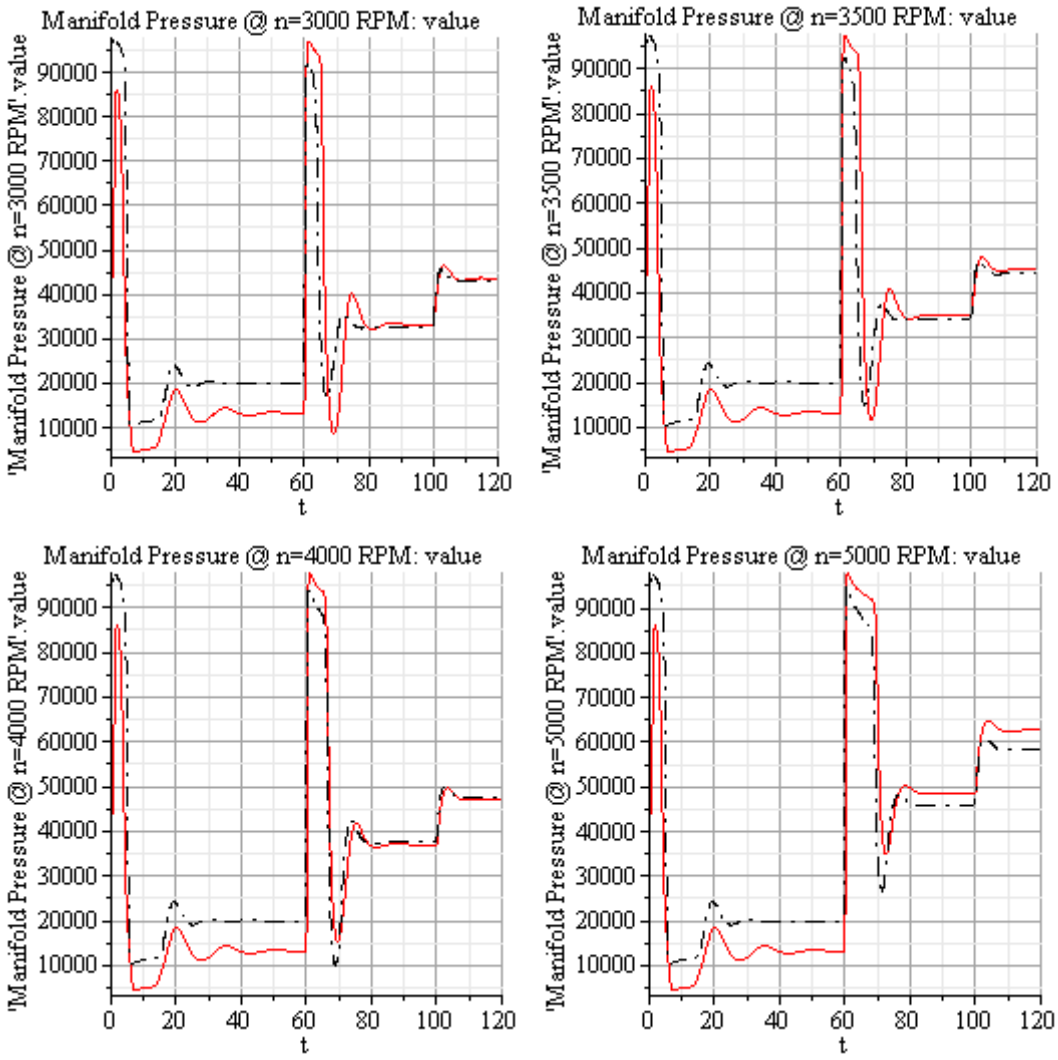

Figure 6.3 Manifold Pressure Results

Simulation (Solid Lines) and Experimental (Dash-dot Lines)

At the beginning of the simulation, that throttle angle is set at a completely closed position, and the air demand from the engine causes the manifold pressure to drop drastically, to about 10 kPa for both models. The manifold pressure is increased by increase of the engine speed and throttle valve angle.

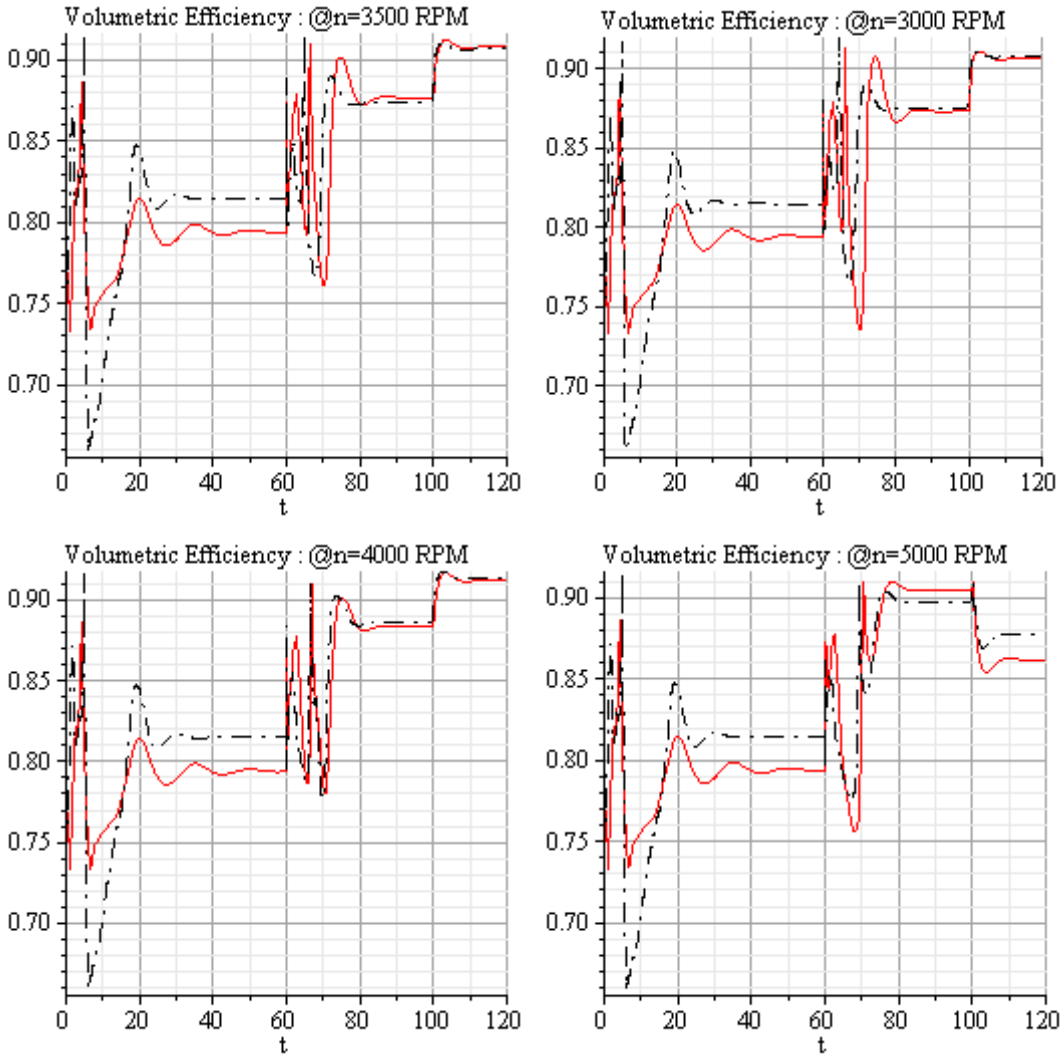

Figure 6.4 Volumetric Efficiency Results

Simulation (Solid Lines) and Experimental (Dash-dot Lines)

However, the volumetric efficiency, which is based on a 2D pressure-speed lookup table, shows different behaviour than the above variables (Figure 6.4). The higher values of the volumetric efficiency are obtained at n=3000 to n=4500, and at Pm= 30 kPa to Pm=50 kPa at t=0 to t=20 and at t=60 to t=80 s, which are the transition regions of the speed and manifold pressure. For any given speed and manifold pressure a value for volumetric efficiency is determined by the

table. Because the rate of speed and pressure changes is too high, the volumetric efficiency values show excessive fluctuations in this region.

Thermal efficiency is a function of spark angle, normalized fuel-air ratio, engine speed, and manifold pressure. Fixing the first two variables as constants, thermal efficiency becomes a function of only engine speed and manifold pressure. As shown in Figure 6.5, thermal efficiency shows to be less sensitive to engine speed. However, for engine speeds equal to or lower than 2000 rpm, thermal efficiency drops rapidly. Increasing the manifold pressure up to 65 kPa increases the thermal efficiency, but increasing the pressure to higher than 65 kPa has the reverse effect on thermal efficiency.

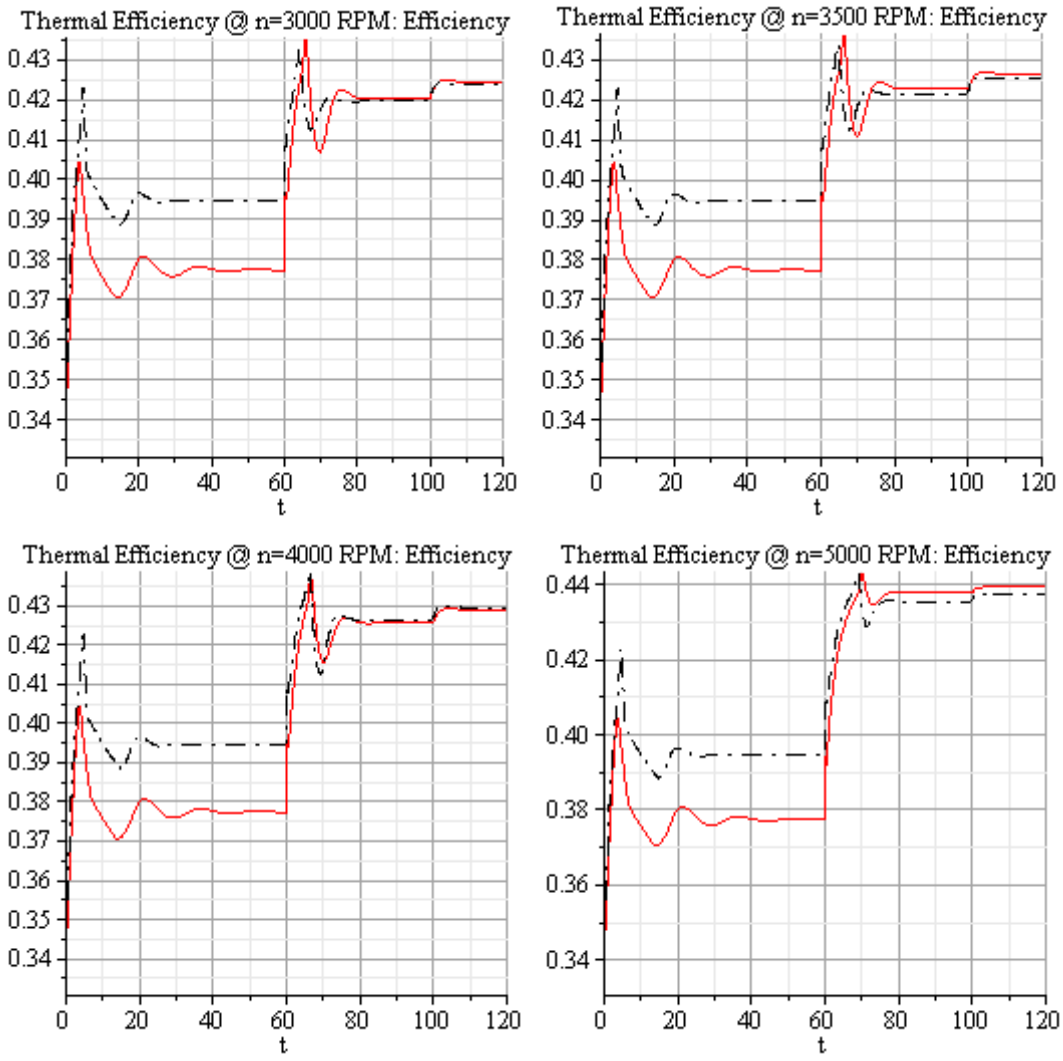

Figure 6.5 Thermal Efficiency Results

Simulation (Solid Lines) and Experimental (Dash-dot Lines)

The net power at the wheels, the power needed to overcome the vehicle resistances and to accelerate the vehicle, is obtained by subtracting the loss and load powers from the indicated power. The load power in this model is approximated by a polynomial function of the third-degree of the speed, and the loss power by a third degree of speed and linear function of manifold pressure. As shown in Figure 6.6, at times t=5.5 to 16.0, and t=64.5 to 69.5 s, if engine

speed is increased suddenly, the sum of the lost power and load power becomes greater than the indicated power, resulting in the net power becoming negative.

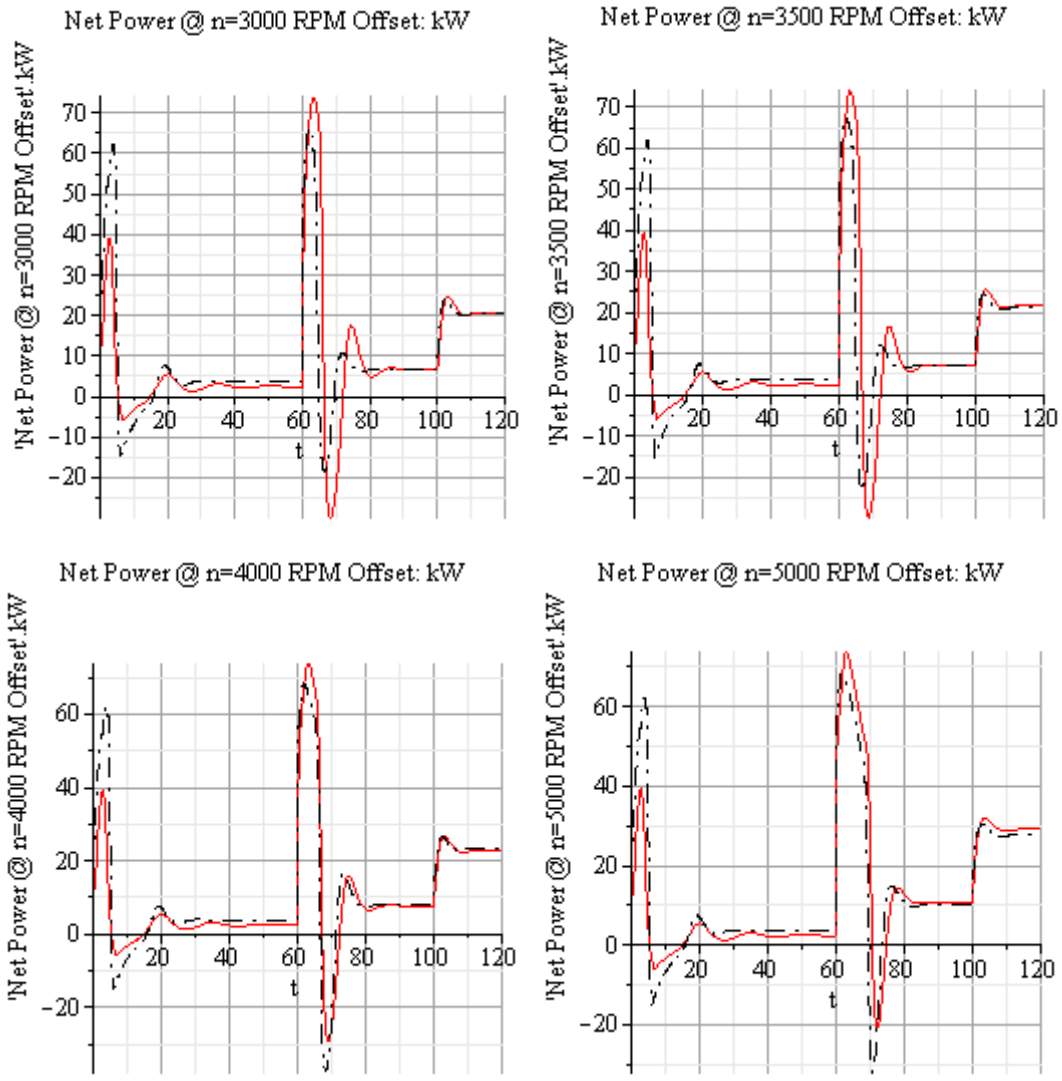

Figure 6.6 Net Power Results

Simulation (Solid Lines) and Experimental (Dash-dot Lines)

The error percentage for the engine variables are calculated from the following relation:

$$Error\,\% = \left(\frac{Simulation - Experimental}{Simulation} \right) \times 100 \tag{6.5}$$

The error percentage values for the throttle air mass flow, manifold pressure, volumetric efficiency, thermal efficiency, and net power are summarized in Table 6.1.

	Engine Speed (RPM)	Simulation	Experimental	Error %
Throttle Air Mass Flow (kg/s)	**2000**	0.006	0.011	-83.33
	3000	0.0388	0.0391	-0.77
	3500	0.0421	0.0401	4.75
	4000	0.0458	0.0468	-2.18
	5000	0.07	0.064	8.57
Volumetric Efficiency	**2000**	0.794	0.814	-2.52
	3000	0.905	0.906	-0.11
	3500	0.906	0.908	-0.22
	4000	0.911	0.914	-0.33
	5000	0.862	0.877	-1.74
Thermal Efficiency	**2000**	0.387	0.395	-2.07
	3000	0.425	0.423	0.47
	3500	0.425	0.426	-0.24
	4000	0.429	0.43	-0.23
	5000	0.44	0.437	0.68
Net Power (kW)	**2000**	2.532	3.611	-42.61
	3000	20.74	20.34	1.93
	3500	21.35	21.89	-2.53
	4000	22.4	22.84	-1.96
	5000	29.34	27.69	5.62
Manifold Pressure (kPa)	**2000**	13.13	20.02	-52.48
	3000	43.61	42.98	1.44
	3500	44.41	45.46	-2.36
	4000	47.31	47.82	-1.08
	5000	62.71	58.37	6.92

Table 6.1 Percentages of the Errors in the MVEM Simulation Model

Chapter 7

Conclusions and Future Works

The goal of this work was to create a new powertrain model using MapleSim software. The model should be able to capture the main events of the engine, and its components should be easily adjustable or replaceable for new engines. For this reason, a mean value engine is found to be a good starting model. The powertrain is a forward-looking strategy that receives command signals from a driver. The signal selected for the model is a gas-acceleration command, but it can be replaced by other signals, such as gas pedal displacement or drive-cycle time-velocity data. A PID is used to compare an input signal variable with the same variable calculated from the model equations.

Based on component complexity of the models, the simulation uses either analytical or experimental equations. Most of the components are defined in a parametric manner that can be easily changed to scale the model to an engine of interest. On the other hand, the model components can be modified by replacing the equations or sub-components with newer components. Another benefit of the new model is the Modelica language embedded in the MapleSim software that enables users to define physical and multi-domain models more easily than with other software. Using Modelica also facilitates replacement of causal with acausal sub-system components available in the software library.

The model consists of three main components, including the throttle body, the manifold, and the engine, and a dynamometer used to simulate the powertrain load. The throttle body is based on calculation of the air mass flow rate by the throttle valve opening angle and manifold pressure. The manifold model uses a lookup table for volumetric efficiency and the intake manifold block that calculates the manifold pressure from the ideal gas equation. The engine is based on the Hendricks et al. [25] parametric engine model that calculates the engine indicated, brake, loss,

and load powers from the air mass flow into the engine, and the manifold pressure, and the engine speed calculated from crankshaft dynamics.

7.1 Conclusions

The experimental air mass data is obtained from measuring of the air mass flow rate at throttle upstream while throttle angle is changed in one-degree increments. The experimental air mass data is then used to calculate other engine variables and to compare the simulation and experimental result simultaneously. Following conclusions can be obtained about the new engine model:

- The throttle air mass flow changes very quickly for angles between 12 to 82 degrees, and for higher degrees, it is almost a constant value. Comparing the experimental and simulation values shows a large error at lower throttle angles close to the completely closed throttle valve, but for higher angles, the errors are reasonable.

- The angle function, which is used in the model and fits the whole range of the data from 7 to 90 degrees, is a third-degree-cosine polynomial. This finding agrees with other similar models in the literature, but they usually use either a polynomial or cosine function, or a piecewise function for lower and higher throttle angles.

- The volumetric efficiency, which is based on a lookup table, shows fluctuations and higher error values for lower throttle angles and transition regions. The higher volumetric efficiencies are obtained for n=3000 to n=4500 RPM, and at Pm= 30 kPa to Pm=50 kPa regions.

- Lowering the engine speeds below 2000 rpm, the indicated thermal efficiency drops quickly, but increasing the engine speed above that point does not significantly affect the

thermal efficiency. Increasing the manifold pressure up to 65 kPa will increase thermal efficiency, but increasing the pressure more has a reverse effect on the thermal efficiency.

- Both pressure and engine speed have significant effects on the engine variables. Engine loss, and load parameters can best be described by experimental equations. Increasing the manifold pressure shows a linear increase of pumping loss, but the effect of increasing an engine speed can best be described by higher-degree polynomials.

7.2 Future Work

The MVEM model in this work is a basic engine that can be used for future research. The current model combines causal and acausal approaches. New gas connections should be defined and added to the software to enable inclusion of pressure, temperature, air mass flow, and heat power in a single connection, thus simplifying the model by reducing connecting lines between components. A more detailed model with gearbox, final drive, wheels, and vehicle features has already been created and will be used for future work. The gearbox and wheels in the new model are created from the Modelica components available in the MapleSim library; a controller is added to change the gear based on the engine and vehicle speeds. The vehicle speed is measured at the wheels by a speed sensor and compared with drive-cycle speed positioned in front of the PID controller. Finally, a model with a torque converter instead of gearbox and a variable-valve-timing system are being developed and will be implemented in the future.

Appendices

Appendix A: Modelica Language

Modelica is an equation-based language that enables the building of complicated models. In contrast to most of the programming languages that assign the value of the right side of an equation to the left side, both sides of equations in Modelica language have the same order of importance. Equations can be used as they appear, in a symbolic way without extra manipulating. For example, to calculate pressure from ideal gas law in conventional programming methods, the pressure equation should be arranged so:

$$P := \frac{mRT}{V}, \tag{A.1}$$

But in Modelica language, it can be written as implicit functions:

$$PV = mRT \tag{A.2}$$

In general, all components, packages, and connectors are called a class. The class has two parts: a declaration part for variables, parameters, and constant, and a part for equations. For example for the rotational spring model in Modelica is defined as

```
model Spring

  extends Modelica.Mechanics.Rotational.Interfaces.PartialCompliant;
  parameter SI.RotationalSpringConstant c (final min=0, start=10000)
  parameter SI.Angle phi_rel0=0

equation
```

tau = c(phi_rel - phi_rel0);*

end Spring;

Connectors are the smallest parts of the model and can be compared with pins in electrical domains or flanges in mechanical domains. Connections in Modelica can be defined as physical carriers like pipes, flanges, or electrical wires. In general, connections carry two types of potential and flow variables. In an electrical domain voltage is a potential variable, and current is flow variable; in a translational mechanical domain, position is a potential variable, and force is a flow variable; and in rotational mechanics, angle is potential, and torque is flow variable. In flow variables, the sum of flows into and out of the node equals to zero. In potential variables, values of the variables at connectors are equal. For example in an electrical domain voltage and current equations at a connector can be written as

$$i_1 + i_2 + i_3 + ... + i_n = 0 \qquad \text{(A.3)}$$

$$v_1 = v_2 = v_3 = ... = v_n \qquad \text{(A.4)}$$

An example for a mechanical domain is flange connector. Any mechanical components such as spring, and inertia, has two flanges: *flange_a* and *flange_b*, which are similar flanges, but one of them is input flange and the other is output flange. For example the flange_a codes in Modelica is defined as:

connector flange_a
Position s;
flow Force f;
end Flange;

A connection can carry different flow or potential variables. For example, a gas connection consists of mass flow rate and heat flow rate as flow variables, and pressure and temperature

as potential variables. Two pins or flanges of two different components can be joined together by a connection equation.

connect (flange_a, flange_b)

Simulation in Dymola is very easy. For example, components can be easily selected from the library to model a mass-spring-damper system. Dragging and dropping the components into the workspace and connecting them together leads to automatic generation of Modelica codes:

model MassSpringDamper

Modelica.Mechanics.Rotational.Components.Inertia	*inertia (J=0.01)*
Modelica.Mechanics.Rotational.Components.Spring	*spring (c=0.5)*
Modelica.Mechanics.Rotational.Components.Damper	*damper (d=0.3)*
Modelica.Mechanics.Rotational.Sources.Torque	*torque*
Modelica.Blocks.Sources.Step step	
Modelica.Mechanics.Rotational.Components.Fixed	*fixed*

equation

connect (torque.flange, inertia.flange_a)
connect (inertia.flange_b, spring.flange_a)
connect (spring.flange_b, damper.flange_a)
connect (step.y, torque.tau)
connect (fixed.flange, damper.flange_b)

end MassSpringDamper

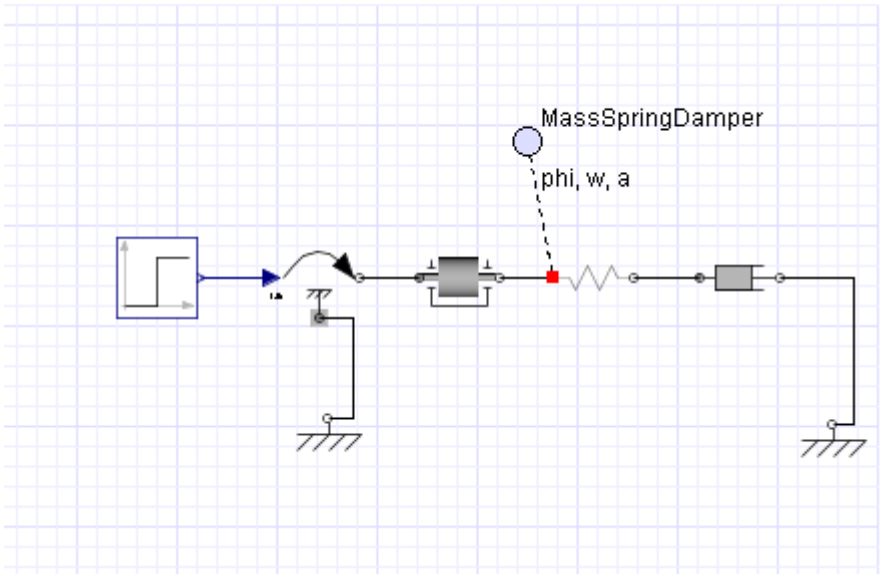

Figure A.1 Mass-spring-damper System in MapleSim

More information about Modelica can be found in [4, 42, 49, 63, 64, and 65].

Appendix B: Modelica Codes

During the process of creating of them model, Modelica codes are generated automatically in MapleSim and can be accessed by opening of "Component Folder" in MapleSim. Following codes define the MVEM component models and their connecting components in Modelica.

- **Throttle Area**

```
model ThrottleArea
  parameter Real phi0 = 0.14e0 "phi0";
  parameter Real d = 0.5e-2 "d";
  parameter Real Dt = 0.75e-1 "Dt";
  Real Athr;
  Real a;
  Real phi;
  Modelica.Blocks.Interfaces.RealInput inp annotation (extent=[-110, -10; -90, 10]);
  Modelica.Blocks.Interfaces.RealOutput out annotation (extent=[90, -10; 110, 10]);
equation
  a = d / Dt;
  Athr = (if phi < acos(a * cos(phi0)) then -d * Dt * sqrt(0.1e1 - a ^ 2) / 0.2e1 + d * Dt * sqrt(0.1e1 - a ^ 2 * cos(phi0) ^ 2 / cos(phi) ^ 2) / 0.2e1 + Dt ^ 2 * asin(sqrt(0.1e1 - a ^ 2)) / 0.2e1 - Dt ^ 2 * cos(phi) * asin(sqrt(0.1e1 - a ^ 2 * cos(phi0) ^ 2 / cos(phi) ^ 2)) / cos(phi0) / 0.2e1 else Dt ^ 2 * asin(sqrt(0.1e1 - a ^ 2)) / 0.2e1 - d * Dt * sqrt(0.1e1 - a ^ 2) / 0.2e1);
  inp = phi;
  out = Athr;
end ThrottleArea;
```

- **Throttle Air Mass Flow**

```
model ThrottleMassFlow
```

```
  parameter       Real     CDthr = 0.8e-1 "CDthr";
  parameter       Real     P0 = 100000 "P0";
  parameter       Real     T0 = 300 "T0";
  parameter        Real     R = 287 "R";
  parameter       Real     gam = 0.14e1 "gam";
  Real Athr;
  Real Pm;
  Real mdot;
    Modelica.Blocks.Interfaces.RealInput ManifoldPressure annotation (extent=[-110, 50; -90, 70]);
  Modelica.Blocks.Interfaces.RealOutput ThrottleMassFlow annotation (extent=[90, -9; 110, 11]);
  Modelica.Blocks.Interfaces.RealInput ThrottleArea annotation (extent=[-110, -9; -90, 11]);
equation
  mdot = (if (2 / (gam + 1)) ^ (gam / (gam - 1)) < Pm / P0 then CDthr * Athr * P0 * ((Pm / P0) ^ (1 /
gam)) * sqrt(0.2e1) * sqrt((gam / (gam - 1) * (1 - (Pm / P0) ^ ((gam - 1) / gam)))) * (R * T0) ^ (-
0.5000000000e0) else CDthr * Athr * P0 * sqrt(gam) * ((2 / (gam + 1)) ^ ((gam + 1) / (2 * gam - 2)))
* (R * T0) ^ (-0.5000000000e0));
  ManifoldPressure = Pm;
  ThrottleMassFlow = mdot;
  ThrottleArea = Athr;
end       ThrottleMassFlow;
```

- **Intake Manifold Pressure**

```
Model    IntakeManifold
  parameter       Real     Tm = 300 "Tm";
  parameter       Real     R = 287 "R";
  parameter       Real     Vm = 0.4e-2 "Vm";
  parameter       Real     S = 0.1e0 "S";
```

```
  parameter        Real     B = 0.85e-1 "B";
  parameter        Real     NEng = 2 "NEng";
  parameter        Real     Ncyl = 4 "Ncyl";
  Real    Pm (start = 95000, fixed=true);
  Real     etaV;
  Real    mdotIn;
  Real    mdotOut;
  Real    n;
  Modelica.Blocks.Interfaces.RealOutput Pressure annotation (extent=[90, 43; 110, 63]);
  Modelica.Blocks.Interfaces.RealInput EngineSpeed annotation (extent=[-110, 42; -90, 62]);
  Modelica.Blocks.Interfaces.RealInput MassIn annotation (extent=[-110, -19; -90, 1]);
  Modelica.Blocks.Interfaces.RealOutput MdoOut annotation (extent=[90, -36; 110, -16]);
  Modelica.Blocks.Interfaces.RealInput VolumetricEff annotation (extent=[-110, -67; -90, -47]);

Equation
der(Pm) = ((mdotIn - etaV * Ncyl * S * Modelica.Constants.pi * B ^ 2 * n * Pm / NEng / R / Tm /
0.240e3) * R * Tm / Vm);
  mdotOut = etaV * Ncyl * S * Modelica.Constants.pi * B ^ 2 * n * Pm / NEng / R / Tm / 0.240e3;
  Pressure = Pm;
  EngineSpeed = n;
  MassIn = mdotIn;
  MdoOut = mdotOut;
  VolumetricEff = etaV;
end       IntakeManifold;
```

- **Thermal Efficiency**

```
model           ThermalEfficiency
  parameter     Real     b1 = 0.558e0 "b1";
  parameter     Real     b2 = -0.392e0 "b2";
  parameter     Real     b3 = -0.360e0 "b3";
  parameter     Real     c1 = 0.9301e0 "c1";
  parameter     Real     c2 = 0.2154e0 "c2";
  parameter     Real     c3 = -0.1657e0 "c3";
  parameter     Real     d1 = -0.1299e1 "d1";
  parameter     Real     d2 = 0.3599e1 "d2";
  parameter     Real     d3 = -0.1332e1 "d3";
  parameter     Real     d4 = 0.205e-1 "d4";
  parameter     Real     d5 = 0.1714e1 "d5";
  parameter     Real     d6 = 0.754e0 "d6";
  Real Pm;
  Real etail;
  Real etain;
  Real etaip;
  Real etaitheta;
  Real etathermal;
  Real lambda;
  Real n;

  Modelica.Blocks.Interfaces.RealInput Pressure annotation (extent=[-110, 45; -90, 65]);
  Modelica.Blocks.Interfaces.RealOutput EtaThermal annotation (extent=[90, -10; 110, 10]);
  Modelica.Blocks.Interfaces.RealInput Speed annotation (extent=[-110, -10; -90, 10]);
  Modelica.Blocks.Interfaces.RealInput Lambda annotation (extent=[-110, -55; -90, -35]);
```

```
equation

  etain = b1 * (1 + b2 * n ^ b3);

  etaip = c1 + c2 * Pm + c3 * Pm ^ 2;

  etaitheta = 1;

  etail = (if lambda < 1 then d1 + d2 * lambda + d3 * lambda ^ 2 else if 1 <= lambda then d4 + d5 *
lambda + d6 * lambda ^ 2 else 0);

  etathermal = etain * etaip * etail * etaitheta;

  Pressure = Pm;

  EtaThermal = etathermal;

  Speed = n;

  Lambda = lambda;

End       ThermalEfficiency;
```

- **Engine Model**

```
Model    Engine

  parameter       Real      Hf = 46000 "Hf";

  parameter       Real     lambda = 1 "lambda";

  parameter       Real     Lth = 0.1467e2 "Lth";

  parameter        Real    lf1 = 0.1673e1 "lf1";

  parameter        Real    lf2 = 0.272e0 "lf2";

  parameter       Real     lf3 = 0.135e-1 "lf3";

  parameter       Real      lp1 = -0.969e0 "lp1";

  parameter       Real      lp2 = 0.206e0 "lp2";

  Real Pb;

  Real Pf;

  Real Pind;
```

```
  Real Pload;
  Real Ploss;
  Real Pm;
  Real Pnet;
  Real Pp;
  Real etai;
  Real mdot;
  Real mfdot;
  Real n;
   Modelica.Blocks.Interfaces.RealInput mdote annotation (extent=[-110, -25; -90, -5]);
  Modelica.Blocks.Interfaces.RealInput ManifoldPressure annotation (extent=[-110, 27; -90, 47]);
  Modelica.Blocks.Interfaces.RealOutput Pnet annotation (extent=[90, -29; 110, -9]);
  Modelica.Blocks.Interfaces.RealOutput Ploss annotation (extent=[90, -63; 110, -43]);
  Modelica.Blocks.Interfaces.RealInput LoadPower annotation (extent=[-110, -68; -90, -48]);
  Modelica.Blocks.Interfaces.RealOutput FuelMassFlow annotation (extent=[-10, -110; 10, -90]);
  Modelica.Blocks.Interfaces.RealInput Etai annotation (extent=[-110, 69; -90, 89]);
  Modelica.Blocks.Interfaces.RealInput EngineSpeed annotation (extent=[-110, -96; -90, -76]);
  Modelica.Blocks.Interfaces.RealOutput BrakePower annotation (extent=[90, 33; 110, 53]);
equation
  Pf = n * (lf1 + lf2 * n + lf3 * n ^ 2);
  Pp = n * (lp1 + lp2 * n) * Pm;
  Ploss = Pf + Pp;
  mfdot = mdot / lambda / Lth;
  Pind = Hf * etai * mfdot;
  Pnet = Pind - Ploss - Pload;
  Pb = Pind - Ploss;
  mdote = mdot;
```

```
  ManifoldPressure = Pm;
  Pnet = Pnet;
  Ploss = Ploss;
  LoadPower = Pload;
  FuelMassFlow = mfdot;
  Etai = etai;
  EngineSpeed = n;
  BrakePower = Pb;
End       Engine;
```

References

[1] Athans, M., The Role of Modern Control Theory for Automotive Engine Control, SAE Technical Papers, SAE 780853, 1978.

[2] Hendricks, E., Sorenson, S., Mean Value Engine Model for Control Studies, American Control Conference, 1990.

[3] Eriksson, L., VehProLib – Vehicle Propulsion Library, Library Development Issues, Proceedings of the 3rd International Modelica Conference, Linkoping, Nov 3-4, 2003.

[4] Modelica and Modelica Association, Available: http://www.modelica.org/, Retrieved May, 2010.

[5] MapleSim Applications, Available: http://www.maplesoft.com/Applications/maplesim/

[6] MapleSoft, Available: http://www.maplesoft.com/, Retrieved May, 2010.

[7] Powell, J. D., A review of IC Engine Models for Control System Design, IFAC 10th Triennial World Congress, Munich, 1987.

[8] Mencik, Z., and Blumberg, P. N., Representation of Engine Data by Multi-Variate Least-Squares Regression. SAE Technical Papers No. 780288. 1978.

[9] Prabhakar, R., Citron, S. J., and Goodson, R. E., Optimization of Automotive Engine Fuel Economy and Emissions, ASME 75-WA/Aut-19, 1975.

[10] Delosh, R. G., Brewer, K. J., Buch, L. H., Ferguson, T. F. W., Dynamic Computer Simulation of a Vehicle with Electronic Engine Control, SAE Paper No. 810447, 1981.

[11] Blumberg, P.N., Powertrain Simulation: A Tool for the Design and Evaluation of Engine Control Strategies in Vehicles. SAE Paper No. 760158, 1977.

[12] Baker, R., E., and Daby, E., E., Engine Mapping Methodology. SAE Paper No. 770077, 1977.

[13] Rishavy, E. A., Hamilton, S.C., Ayers, J. A., and Kean, M. A., Engine Control Optimization for Best Fuel Economy with Emission Constraints, SAE Paper No. 770075, 1977.

[14] Cassidy, J. F., A Computerized On-line Approach to Calculating Optimum Engine Calibrations. SAE Paper No. 770078, 1977.

[15] Auiler, E. J., Zbrozek, J. D., and Blumberg, P. N., Optimization of Automotive Engine Calibration for Better Fuel Economy Methods and Applications. SAE paper No. 770076, 1977.

[16] Dobner, D. J., A Mathematical Engine Model for Development of Dynamic Engine Control, SAE Paper No. 800054, 1980.

[17] Dobner, D. J., and Fruechte, R. D., An Engine Model for Dynamic Control Development, ASME WA$-11:15, 1983.

[18] Aquino, C. F., Transient AF Control Characteristics of the 5 Liter Central Fuel Injection Engine, SAE Paper No. 810494, 1981.

[19] Powell, B. K., A Dynamic Model for Automotive Engine Control, Proceeding of the 18th IEEE Conference on Decision and Control, pp. 120-126, 1979.

[20] Crossley, P. R., and Cook, J. A., A Nonlinear Engine Model for Drive Train System Development. In Proc. IEE Int. Conf., Control'91, 2:921–925, Conference publication 332, Edinburgh, UK, 1991.

[21] Yuen, W.W., Servati, H., A Mathematical Engine Model Including the Effect of Engine Emissions, SAE Papers No. 840036, 1984.

[22] Harington, D. L., and Bolt, J., A., Analysis and Digital Simulation of Carburetor Metering, SAE Paper 700082.1970.

[23] Moskwa, J. J., Automotive Engine Modeling for Real Time Control, Ph.D. Dissertation, Massachusetts Institute of Technology, 1988.

[24] Hendricks, E., Sorenson, S. C., Mean Value Modelling of Spark Ignition Engines, SAE 900616, 1990.

[25] Hendricks, E., Chevalier, A., Jensen, M., and Sorenson, S. C., Modelling of the Intake Filling Dynamics, SAE 960037, 1996.

[26] Wipke, K. B., Cuddy, M. R., and Bruch, S. D., Advisor 2.1: A User-Friendly Advanced Powertrain Simulation Using a Combined Backward/forward Approach, National Renewable Energy Lab Report, NREL/JA-540-268339, August 1999.

[27] Wipke, K. B., Cuddy, M. R., and Bruch, S. D., Advisor 2.0: A Second Generation Advanced Vehicle Simulator for System Analysis, National Renewable Energy Lab Report, NREL/JA-540-25928, March 1999.

[28] Markel, T., Brooker, A., Hendricks, T., Johnson, V., Kelly, K., Karmer, B., O'Keefe, M., Sprike, S., and Wipke, k., Advisor: A System Analysis Tool for Advanced Vehicle Modeling, Journal of Power Science 110 (2002) 255-266.

[29] Rousseau, A., PSAT Overview, Argonne National Laboratory, 2005.

[30] Rousseau, A., Sharer, P., Pagerit, S., PSAT documentation, 2005.

[31] Rousseau, A., Pagerit, S., Monnet, G., and An, F., The New PNGV System Analysis Tool kit PSAT V4.1 –Evolution and Improvement, SAE Technical Paper Series 2001-01-2536, August 2001

[32] Rousseau, A., Sharer, P., and Besnier, F., Feasibility and Reusable Vehicle Modeling: Application to Hybrid Vehicle, SAE 2004-01-1618

[33] Guzzella, L., and Sciarretta, A., Vehicle Propulsion Systems, Springer, 2005.

[34] Guzzella, L., Amstutz, A., The QSS Toolbox Manual, Swiss Federal Institute of Technology Zurich; Measurement and Control Laboratory, 2005.

[35] Matlab and Simulink for Technical Computations, The Mathworks, Available: http://www.mathworks.com/, Retrieved May, 2010

[36] Simulink - Simulation and Model-Based Design, The Mathworks, Available: http://www.mathworks.com/products/simulink/, Retrieved May, 2010.

[37] SimDriveline 1.5.4, Model and Simulate Mechanical Driveline Systems, Available:

http://www.mathworks.com/products/simdrive/, Retrieved May, 2010.

[38] SimDriveline 1 User's Guide, Matlab/Simulink, Available:

http://www.mathworks.com/access/helpdesk/help/pdf_doc/physmod/drive/drive.pdf, Retrieved May, 2010.

[39] Butts, K., Bernard, P., Liefeld, T., and Quinn, S., Engine Timing Model with Closed Loop Control, Available: http://www.mathworks.com/products/simulink/demos.html?file=/products/demos/shipping/simulink/sldemo_enginewc.html, Retrieved June, 2010.

[40] Mathworks-SimDriveline 1.5.4, Full Car Model, Available: http://www.mathworks.com/access/helpdesk/help/toolbox/physmod/drive/a1068571102.html, Retrieved June, 2010.

[41] Mathworks-SimDriveline 1.5.4, Complete Vehicle Demo, Available: http://www.mathworks.com/products/simdrive/demos.html?file=/products/demos/shipping/drive/drive_vehicle.html, Retrieved June, 2010.

[42] Dymola- Dynamic Model Laboratory, Demo Version, ver. 7.4, Available:

http://www.3ds.com/products/catia/portfolio/dymola , Retrieved June, 2010.

[43] Batteh, J., Tiller, M., and Newman, C., Simulation of Engine Systems in Modelica, Proceeding of the 3rd International Modelica Conference Linkoping, pp. 139-148.

[44] Woschni, G. A universally applicable equation for the instantaneous heat transfer coefficient in the internal combustion engine. SAE Technical Paper, 670931, 1967.

[45] Hohenberg, G. F., Advanced approaches for heat transfer calculations. SAE Technical Paper, 790825, 1979.

[46] Heywood, J. B., Internal Combustion Engine Fundamentals, McGraw-Hill series in mechanical engineering, McGraw-Hill, 1988.

[47] Eriksson, L., VehProLib – Vehicle Propulsion Library, Library development issues, Proceedings of the 3rd international Modelica Conference, Linkoping, Nov 3-4, 2003.

[48] Schlegel, C., Bross, M., Beater, P., HIL-Simulation of the Hydraulics and Mechanics of an Automatic Gearbox, 2nd International Modelica Conference Proceedings, March 2002, pp. 7-75.

[49] Tiller, M. M., Introduction to Physical Modeling with Modelica, Kluwer Academic Publishers, 2001.

[50] Blair, G. P., Callender, E., Mackey, D. O., Maps of Discharge Coefficients for Valves Ports and Throttles, SAE Papers No. 2001-01-1798/4219, 2001.

[51] Cho, D., Hedrick, J. K., Automotive Powertrain Modeling for Control, ASME, Journal of Dynamics Systems, Measurement, and Control, Vol. 111/569, Dec. 1989.

[52] Hendricks, E., Engler, D., Fam, M., A Generic Mean Value Engine Model for Spark Ignition Engines, 41st Simulation Conference, Denmark Technological University, Lyngby, Denmark, June 2000.

[53] Cho, D., Hedrick, J. K., Automotive Powertrain Modeling for Control, ASME, Journal of Dynamics Systems, Measurement, and Control, Vol. 111/569, Dec. 1989.

[54] Cook, J. A., and Powell, B. K., Nonlinear low frequency phenomenological Engine Modeling and Analysis, American Control Conference, Minneapolis, Minnesota, June 1987.

[55] Moran, J. M., Shapiro, H. N., Fundamentals of Engineering Thermodynamics, Fifth Ed., John Wiley & Sons Inc., 2006.

[56] Hendricks, E., Isothermal vs. Adiabatic Mean Value SI Engine Models, IFAC Advances in Automotive Control, Karlsruhe, Germany, 2001.

[57] Taylor, C. F., The Internal Combustion Engine in Theory and Practice, Vol. 1: Thermodynamics, fluid flow, Performance, The MIT Press, 1985.

[58] Hendricks, E., Engine Modelling for Control Applications: A Critical Survey. Meccanica 32: 387-396, 1997.

[59] Chang, R. T., A Modelling Study of the Influence of Spark-Ignition Engine Parameters on Engine Thermal Efficiency and Performance, MASc. Thesis, Massachusetts Institute of Technology, 1986.

[60] Nitschke, R. G., The Effects of Spark-Ignition Engine Design Parameters on Performance and Economy: A Modelling Study, MASc. Thesis, Massachusetts Institute of Technology,1987.

[61] Poulos, S. G., The effect of combustion chamber geometry on S.I. engine combustion rates : a modeling study, MASc. Thesis, MIT, 1982.

[62] Gillespie, T. D., Fundamentals of Vehicle Dynamics, SAE Inc., 1992.

[63] Fritzson, P.A., Principles of Object-Oriented Modeling and Simulation with Modelica 2.1, IEEE Press, Wiley Interscience, A John Wiley & Sons, Inc. Publication, 2004.

[64] Fritzson, P.A., Introduction to Object-Oriented Modeling and Simulation with Open Modelica, 2006.

[65] Modelica Association, Modelica™ - A Unified Object-Oriented Language for Physical Systems Modeling, Tutorial, Version 1.4, Dec 2000, Available: http://www.modelica.org/documents/ModelicaTutorial14.pdf, Retrieved July 2010.